MAREK MOSZYŃSKI

STATISTICAL ANALYSIS FOR DIGITAL PROCESSING OF PELAGIC FISH ECHOES

GDAŃSK UNIVERSITY OF TECHNOLOGY - 2005

CONTENTS

LIST OF SYMBOLS AND ACRONYMS

Symbols

α – acoustic absorption coefficient or combination constant in HK integral
α_1 – alongship split-beam angle
α_2 – athwordship split-beam angle
α_{ap} – phase aperture in split-beam system
γ – parameter in beam pattern approximation or ratio of gas specific heats
$\gamma_{\max}$ – maximum angle in bent cylinder
δ – dumping factor or attanuation parameter or Dirac delta function
ε – geometric constant in Helmholtz equation
ε_n – Neumann number
η – electroacoustic efficiency of transmitter or phase shift
η_n – n-partial wave phase shift
θ – azimuthal angle of measurement position
θ_{3dB} – half power beam angle
$\theta_{\max}$ – maximum acquisition angle
θ_w – beam width
κ – compressibility of a medium or matrix condition number
λ – acoustic wavelength or regularization parameter
μ – shear rigidity complex modulus
ρ – density of the water
ρ_V – fish volume density
σ – acoustic cross section or Poisson ratio
σ_{bs} – acoustic backscattering cross section
σ_{sp} – spherical cross section
σ_s – total scattering cross section
σ_e – extiction cross section
σ_a – absorption cross section
σ_{ag} – aggregate backscattering cross section
τ – echo sounder pulse duration
φ – elevation angle of measurement position
χ – tilt angle of the object
χ_0 – fish swimbladder tilt angle
ψ – wavelet function
ω – angular frequency
ω_0 – carrier angular frequency
Γ – resolvent of integral equation
Δ – generalized finite increment
$\Delta\theta$ – angular resolution or separation
$\Delta\phi$ – phase difference
Δr – depth layer
Δt – time period
ΔV – spatial resolution
Ψ – equivalent integrated beam width

Ω – solid angle
∇ – gradient operator
∇^2 – Laplacian operator
a – radius of spherical or cylindrical object
a_{ec} – equivalent cylinder radius
b – intensity domain transducer beam pattern
b_{20} – constant in mean target strength regression
b_n – narrow beam pattern in dual beam system
b_w – wide beam pattern in dual beam system
c – sound velocity in water
c_1 – sound velocity in an object for compressional waves
c_2 – shear wave velocity in an object
d – circular transducer diameter
d_λ – diameter in wavelengths
d_n – circular transducer diameter of narrow channel in dual beam system
d_w – circular transducer diameter of wide channel in dual beam system
e – echo amplitude or normalized echo amplitude
e_n – narrow beam echo amplitude in dual beam system
$e_{\min}$ – minimum echo signal
e_w – wide beam echo amplitude in dual beam system
f – signal frequency or generalized function
f_0 – carrier frequency
f_∞ – form function of spherical objects
f_R – resonant frequency
g – acceleration of gravity
h_n – spherical Hankel function
i – index number
j – imaginary number
j_n – spherical Bessel function
l_{bs} – acoustic backscattering length
$l_{bs}^{(fb)}$ – acoustic backscattering length of fish body
$l_{bs}^{(sb)}$ – acoustic backscattering length of fish swimbladder
l_{ec} – equivalent cylinder length
k – wave number
ka – wave number radius product
k_x – hydroacoustic system constant
k_V – volume scattering system constant
m – coefficient in mean target strength regression
n – number of targets per unit volume or noise error
$\mathbf{n}$ – normal vector
n_c – critical fish density for echo counting
p – acoustic pressure
p_0 – reference pressure as used in underwater acoustics
p_1 – pressure at 1 m from source
p_θ – fish angular position PDF
p_a – ambient pressure
p_b – beam pattern PDF
p_e – echo amplitude PDF
$p_{l_{bs}}$ – backscattering length PDF
p_{scat} – scattered acoustic pressure

p_B – logarithmic beam pattern PDF
$p_{B_f|TS_0}$ – conditional fish directivity pattern PDF
p_E – echo level PDF
p_{TS} – target strength PDF
r – distance of the measurement position from the target
r_1 – reference distance 1 m
r_c – radius of curvature of bent cylinder
s – sounding pulse waveform
s_a – area backscattering coefficient
s_x – transducer receiving sensitivity
s_A – nautical area backscattering coefficient
s_V – volume backscattering coefficient
t – time variable
u – particle displacement
v – particle velocity
X – generalized variable
Y – generalized variable
Z – distance along the propagation path of a plane wave or depth
A – transducer aperture or generalized amplitude
B – logarithmic two-way beam pattern of tranducer or boundary
B_f – logarithmic fish directivity pattern
B_n – logarithmic one-way beam pattern of narrow beam tranducer
B_w – logarithmic one-way beam pattern of wide beam tranducer
C_F – Fresnel cosine integral
D – directivity pattern function in pressure domain
D_r – receiving directivity pattern function in pressure domain
D_t – transmitting directivity pattern function in pressure domain
DI – transducer directivity index
E – normalized echo level, expectation operator or bulk modulus of elasticity
E_e – echo energy
$E_{\min}$ – minimum echo level
EL – echo level (echo intensity level)
F – generalized cumulative distribution function (CDF)
F_B – beam pattern CDF
F_{TS} – target strength CDF
G – receiver gain or frequency response function of receiver
G_k – free-space Green function in three dimensions
G_A – analog receiver gain
G_{ADC} – analog-to-digital conversion gain
H – Heaviside step function
H_n – cylindrical Henkel function of the first kind n order
I – intensity of a plane wave
$\mathbf{I}$ – identity matrix
I_0 – reference intensity as used in underwater acoustics
I_1 – intensity at 1m from source
I_{bs} – intensity of backscattered wave
I_{inc} – intensity of the incident wave at the target
I_{scat} – intensity of scattered wave at the measurement position
J – transducer spherical reciprocity parameter
J_n – cylindrical Bessel function of the first kind n order

K – kernel of integral equation or complete elliptic integral of first kind
$\mathbf{K}$ – integral equation kernel matrix
K_d – dual beam logarithmic drop-off coefficient
K_n – narrow channel logarithmic dual beam system constant
K_w – wide channel logarithmic dual beam system constant
K_x – logarithmic constant of hydroacoustic system
K_D – dual beam relative drop-off constant
K_V – logarithmic constant for volume scattering
L – length of the object
M – Mellin transform operator
N – number of fish echos in a trace
N_n – cylindrical Neumann function of the first kind n order
P – pressure amplitude
P_e – sonar transmitter electric power
P_n – Legendre polynomial
P_s – total scattered power of acoustic wave
R – reflection coefficient
R_{fb} – reflection coefficient in the fish-swimbladder interface
R_{wf} – reflection coefficient in the water-fish body interface
R_P – transducer paralell resistance
RS – echo sounder receive sensitivity
RS_n – narrow channel dual beam system receive sensitivity
RS_w – wide channel dual beam system receive sensitivity
S – water salinity, surface of the object or spectrum of transmitting pulse
S_a – area backscattering strength
S_x – open circuit voltage response
S_A – nautical area backscattering strength
S_F – Fresnel sine integral
S_V – mean volume backscattering strength
SL – echo sounder source level
T – temperature or transmission coefficient or period of vibration
T_x – transducer transmit voltage response
TL – two-way transmisson loss
TL_V – two-way transmisson loss for volume reverberation
TS – target strength
TS_0 – maximum target strength
TS_U – uncompensated target strength
V – volume occupied by a scattering medium (reverberation volume)
V_{RMS} – voltage amplitude on transducer terminals
VR – transducer receive voltage response
Z – acoustic impedance of the medium
Z_1 – acoustic impedance of the object for compressional waves

Acronyms

AEMS – Adaptive Expectation Maximization Smoothing
ATSR – Along Track Scanning Radiometers
AVHRR – Advanced Very High Resolution Radiometers
BEM – Boundary Element Method

CT	– Computerized Tomography
CDF	– Cumulative Density Function
CZCS	– Coastal Zone Color Scanners
DMT	– Discrete Mellin Transform
DSL	– Deep Scattering Layer
DWT	– Discrete Wavelet Transform
EM	– Expectation Maximization
EMS	– Expectation Maximization Smoothing
ETM	– Enhanced Thematic Mapper
FAO	– Food and Agriculture Organization
GSI	– Gonadosomatic Index
HK	– Helmholtz-Kirchhoff Integral
ICES	– International Council for the Exploration of the Sea
KRM	– Kirchhoff-Ray-Mode Model
MER	– Maximum Entropy Regularization
MSY	– Maximum Sustainable Yield
NMEA	– National Marine Electronics Association
NMFS	– National Marine Fisheries Service
NOAA	– National Oceanic and Atmospheric Organization
PCX	– Phase Contrast X-rays
PDF	– Probability Density Function
RCS	– Radar Cross Section
RSL	– Reduced Scattering Length
RTS	– Reduced Target Strength
SAM	– Swept Area Method
SAR	– Synthetic Aperture Radar
SAS	– Synthetic Aperture Sonar
SLR	– Side Looking Radar
SVD	– Singular Value Decomposition
TVG	– Time-Varied Gain
VPA	– Virtual Population Analysis
VWD	– Vaguellete-Wavelet Decomposition
VRML	– Virtual Reality Modeling Language
WGFAST	– Working Group on Fisheries Acoustics and Technology
WSVD	– Windowed Singular Value Decomposition
WVD	– Wavelet-Vaguellete Decomposition

Chapter 1

INTRODUCTION

Sonar has for a long time been a tool used to study the ocean. Among its many applications, sonar is employed to help remotely classify distributions of biological organisms such as pelagic fish populations and plankton. Species, location, size distribution and behavior are among the important properties of the marine organisms. Knowledge of those properties aids in fish supply management and ecological study [149].

The amount of discussion about so-called sustainable fisheries is increasing worldwide. The crisis in a lot of big fisheries, e.g. salmon fisheries along the Pacific coast of the USA and Canada and cod fishery on the Grand Banks, must lead to different management regimes [22]. Moreover, natural phenomena have also taken their toll on the marine fisheries environment. El Niño – a disruption of the ocean and atmosphere in the tropical Pacific – has ravaged both Chilean and Peruvian fisheries. Similarly, some fishers in the North West Atlantic blame warmer waters and pollution for the scarcity and erratic migration patterns of coldwater fish like cod. But it is inadequate fisheries management and policies that are mostly to blame [134]. The FAO reported in 2000 [28] that, globally, an estimated 25% of the fish stocks are under or moderately exploited, 50% of stocks are fully exploited, 15% are over exploited and about 10% have been depleted or are recovering from depletion. As a result of international cooperation a number of conventions are signed to prevent further overfishing of marine resources. In particular, the countries of the Baltic Sea commit themselves to take all appropriate measures to counter and prevent pollution to control the environment of the Baltic Sea in a sustainable way. The Convention on the Protection of the Marine Environment of the Baltic Sea Area (Helsinki Convention), originally signed in 1974 and later updated in 1992 is administered by the Helsinki Comission (HELCOM).

In fishery research, acoustical techniques have been increasingly important over the years [85]. Following the pioneering work of Sund [155], acoustical technology has had a major impact on fishing. With sonar it is possible to search a substantial volume of water at great speed. Alternative sampling methods as trawl fishing are very slow by comparison [80].

During the last few decades sonar systems has been significantly improved. Apart from single-beam systems, the dual-beam and split-beam systems became the typical systems used in fishery research. Improvements of spatial resolution generally simplify the interpretation of data because the sonar displays more clearly the shape of the objects. However, in the case of measurement of the fish, obtaining anatomical features requires a physically large aperture or a parametric source to produce the narrow beams.

Most *in-situ* measurements performed during acoustic surveys uses medium reso-

lution systems where the individual fish are resolved but individual features are not. Thus, all components of the fish contribute to the total echo. Quantitatively, the echo signal depends on the acoustic reflecting properties of the individual fish, the density of fish and their position in the sonar beam.

1.1. Introduction into acoustic methods of fish population estimation

The technique of acoustic survey may be used to estimate the fish abundance in appropriate circumstances. There is an extensive literature on this topic, for example [9, 69, 85]. The method depends upon measuring the fish echoes and estimating the quantity of fish that would be expected to produce such echoes. However, the acoustic survey is useful only when the particular fish are conveniently located in the water column. They must not be too close to the seabed or the sea surface. In these regions, the fish echoes are obscured by the much stronger return from the water boundaries. Fortunately, many important species spend at least part of the time in midwater. These pelagic fish include shoaling species such as the herring (family *Clupeidae*) and the mackerels (*Scombridae*).

Accurate fish target strength *TS* (which is a measure of fish scattering properties) information is an essential element of acoustic surveys of fish populations [38]. Methods of *TS* estimation using dual-beam and split-beam techniques enable direct measurements of fish *in situ* [26, 40] and theoretically provide the best estimate of *TS* to scale integrator outputs [87, 128]. However, several potential biases limit the use of *in situ TS*. Bias can be attributed to the acoustic measurements themselves, in particular to the resolution of single targets [132, 140], or as a result of transducer motion [50]. The complex nature of fish behaviour can lead to variations in tilt-angle distribution and *TS* [32] as a consequence of vertical migration and the avoidance of a boat or towed body [72, 111, 118]. The physiological state of the fish [113] can also affect the TS. Furthermore, interpretation of the species and size composition necessary for unbiased *TS* estimation depends on representative biological sampling [86]. However, fishing gears are selective [81] and it is often difficult to sample fish at the exact time and location at which they were ensonified. The most realistic solution to these problems has been to conduct *in situ TS* experiments under optimal or well-measured conditions [129, 160].

1.2. The objectives of the dissertation

In fishery acoustics, it is common to study the fish abundance by using hydroacoustic systems and compare the data with trawl caches made before and after the survey. When the system is not equipped with trawling facilities, the researchers use regression relations determined experimentally for conversion of acoustical measures obtained from the surveys to the ones that has physical meaning.

For several decades, many fishery acousticians used a well-known relation, which states that fish mean target strength is proportional to logarithmic value of fish length with linear coefficient equal to 20. The theoretical justification was that target strength should be proportional to cross-sectional area, and that area should scale as

the square of fish linear dimensions.

One of the objectives of the dissertation is to show that this is misinterpretation. The reason of obtaining such proportionality lies rather in the set of following facts. Firstly, the acoustic models shows that, for example, for swimbladdered fish the theoretical consideration should give proportionality scaled by 30 for maximum value of target strength. Secondly, the data from surveys measuring fish in their natural conditions contains echoes backscattered from fish randomly oriented in space. Finally, as the fish observation has stochastic properties and the scale for mean value of target strength to length regression is influenced rather by randomness of fish orientation than by geometrical cross section area.

Thus, the only reasonable way of treating fish data is by means of statistical processing. Such processing when combined with adequate models of fish scattering properties can be used to estimate not only fish target strength, but also the fish length distribution with no need to use trawl catches.

1.3. Chapters overview

After this introductory chapter the scattering from underwater objects are described. In particular, the aspects related to the theory of scattering by a sphere and a cylinder, which are used in modeling of scattering properties of a fish are considered. To measure reflecting properties of the fish, terms like backscattering cross section, backscattering length and target strength are defined, which are commonly used for monostatic systems used in fisheries. Some experimentally obtained formulae for target strength to length relationship are presented along with acoustic models of the fish.

It is shown in chapter 3, that among the methods used in these days for remote classification of fish populations the only reasonable ones are in situ acoustic methods. The hydroacoustic systems used in fisheries until 1980ties equipped with classical single beam systems enabled fish abundance estimation using so called echo integration approach. The unknown fish position in the transducer beam push forward the development of specialized system for fishery application like dual- beam systems and split-beam systems. Nevertheless, as the fish echoes were resolved, the fish target strength estimates could be calculated from single-beam systems by statistical removal of unknown fish position, which were regarded at that time as a very modern method. The detailed analysis of echo formation process presented in the chapter and formulated in the form of stochastic process enables solving the problem of fish target strength estimation by applying the concept of beam pattern probability density function (PDF) as a kernel function of integral equations. The effective solution of such equations leads to application of inverse techniques.

Hence, in chapter 4 the inverse methods as applied to fish target strength estimation are presented. It is well known that in most practical cases found in physics, the inverse approach results in numerically ill conditioned and unstable solution. Therefore, exact methods of solution simply fail. However, as it was shown in the chapter the modern methods based on regularization and iterative approaches give quite reliable solutions, which are particularly useful for probability density estimates.

Chapter 5 presents, transducer beam pattern PDF, fish directivity pattern PDF and the ways of their determination. Both PDFs represent kernel functions of integral equation required for solving the inverse problem. The former is used in fish target strength estimation, the latter – in fish length estimation.

Chapter 6 contains examples of data acquired in acoustic surveys and the results of their statistical processing using methods presented in the previous chapters.

The last chapter is slightly different from the main stream of the book. It introduces the modern Information Technology techniques in the field of fishery acoustics. The results of signal processing and specialized algorithms as used by the author enable 3D visualization of fish echo data.

Chapter 2

SCATTERING OF SOUND FROM UNDERWATER OBJECTS

Fairly good acoustic wave propagation conditions in the sea due to relatively small attenuation facilitate penetration of sea environment and its acoustic visualization. Hydroacoustic systems utilize the scattering effect of acoustic waves on inhomogeneities of water column for extracting information on properties of the sea environment and underwater objects including seafloor and sea surface.

Propagation of sound in the water depends on mechanical properties of the medium, in particular on its inertia and its elasticity. The forces – generated as a result of particle acceleration coming from the reaction of the medium – produce tension and the energy related to the forces is composed of kinetic energy of the movement and potential energy represented by inner tensions. The propagation of this disturbance leads to the generation of longitudinal elastic wave in the medium. This mechanism is one of the oldest questions of natural philosophy [75].

2.1. Wave equation

In acoustics, the propagation of the disturbance is described by use of wave-equation, which relates changes in time and space of acoustic field described by pressure in the medium p, speed of acoustic particle v and density of the medium ρ. Wave equation along with boundary conditions and initial conditions represents mathematical model of sound propagation. The model is simple when the water is modeled as idealized liquid medium homogeneous in space, isotropic and lossless. Wave equation for such a fluid can be derived from conservation laws and the equation of state, which are scalar and vector partial differential equations. Mathematically, wave equation in ideal medium at rest can be written as homogeneous equation [8, 138]:

$$\nabla^2 p - \frac{1}{c^2}\frac{\partial^2 p}{\partial t^2} = 0 \tag{2.1}$$

where p is acoustic pressure, $c = (E/\rho)^{1/2} = (\rho\kappa)^{-1/2}$ is the speed of wave propagation in the medium, E is bulk modulus of elasticity, κ is compressibility of the medium and ρ is density of the medium. Two important solutions are worth mentioning:

$$p = f(\mathbf{n}\cdot\mathbf{r}/c \pm t) \tag{2.2}$$

$$p = \frac{f(r/c - t)}{r} \tag{2.3}$$

where f is arbitrary smooth functions and unit vector $\mathbf{n}$ ($|\mathbf{n}| = 1$) is normal to those planes where the argument of the function f is constant. Plane waves described by Eq. (2.2) propagate along $\mathbf{n}$ at the speed c without changing their shape or amplitude. In case of spherical wave described by Eq. (2.3) with spherical symmetry, the sound pressure and other characteristics of the sound field are constant at spheres $r = const$ at fixed moments of time [8].

For an oscillating source, the wave contains the areas with higher density than at initial state and the areas with lower density. These areas propagate from the source of sound with the constant velocity c, determined by properties of the medium. As far as the homogeneous medium is concerned, the pressure maxima represents concentric spherical surface surrounding wave source. As to the sources vibrating harmonically, the spherical surfaces are equally spaced with the distance equal to wavelength in the water λ. The waves, which propagate with a spherical symmetry are called spherical waves and are described by time-space spherical wave equations.

Sufficiently far from the source and in small areas spherical wave front can be approximated by a plane. Then the spherical wave equation can be simplified into the case describing plane wave [164]. In most cases, in fishery acoustics, the plane wave approximation enables simple description of dependence between physical parameters of the medium and the parameters of acoustic wave.

In scattering problems, the solution depends mainly on boundary conditions. In two classical cases of the so called soft scatterer, where excess pressure p at the surface is equal to zero (Dirchlet boundary condition) and for hard (rigid) scatterer, where boundary is not affected by the wave and normal component of particle velocity v is zero (Neumann boundary condition) the solution can be found analytically only for simple geometrical shapes. In general case of an interface between two fluids at rest two boundary conditions have to be satisfied: (1) equality of normal components of particle velocities at both sides of the interface (kinematic condition) and 2) equality of the forces acting upon each part of the interface from both sides (dynamic condition) [8].

The dependence of acoustic pressure p on particle velocity v, coming from Newton second law, enables expressing characteristic acoustic impedance of medium for plane wave: $Z = \rho c$, which represents synthetic characterization of acoustic medium [164]. At the same time, mean power density of acoustic wave is proportional to mean value of the product of pressure and particle velocity $<vp>$ and is named acoustic intensity of the wave. It can be expressed as: $I = <p^2>/Z$, [164], where $<>$ denotes a time average.

For harmonic waves $p(z,t) = A\sin(\omega t - kz)$, where A is a pressure amplitude, and $k = 2\pi/\lambda$ is a wave number, its intensity $I(z)$ in space oscillates with angular frequency equal to $\omega = 2\pi f$, between values 0 and A^2/Z.

2.2. Helmholtz-Kirchhoff integral

The surface Helmholtz integral equation is a common approach for the problem of the acoustic scattering by obstacles. The reason is that this approach has the advantages of reducing the dimensionality of the problem by one and transforming

an infinite domain to finite boundaries in which the far-field radiation condition is satisfied automatically [168].

For harmonic waves, the time factor described using complex notation as $e^{-j\omega t}$ enables transforming wave equation into the so called Helmholtz differential equation:

$$(\nabla^2 + k^2)p = 0 \tag{2.4}$$

The equivalent boundary integral formulation can be obtained by using Green's theory [138], which is valid for acoustic medium B' exterior to a finite body B with surface S and represents total pressure p as a sum of incident pressure p_{inc} and scattered pressure described by integral over surface S:

$$\varepsilon p(P) = p_{inc}(P) + \int_S \left(p(Q)\frac{\partial G_k(P,Q)}{\partial n_Q} - G_k(P,Q)\frac{\partial p(Q)}{\partial n_Q} \right) dS_Q \tag{2.5}$$

where the free-space Green's function G_k for Helmholtz equation in three dimensions is given by $G_k(P,Q) = e^{jkr}/4\pi r$, where r is the distance between field point P and the point Q on the surface S, and n_Q is the outward directed normal at Q. The value of geometric constant ε depends on the position of $P$and is defined by the solid angle Ω [66]:

$$\varepsilon = 1 - \frac{\Omega}{4\pi} = 1 + \int_S \frac{\partial G_0}{\partial n_Q} dS_Q = \begin{cases} 0, \, for \, P \in B \\ 1, \, for \, P \in B' \\ \frac{1}{2}, \, for \, P \in S \end{cases} \tag{2.6}$$

Boundary relation of Eq. (2.5) fails to yield unique solution at certain characteristic frequencies. Non-uniqueness is a pure mathematical problem arising from the breakdown of boundary integral representation rather than from the nature of the physical problem [169]. To avert the problem two approaches can be used, namely combined Helmholtz integral equation formulation proposed by Schenk [133] or composite outward normal derivative overlap relation proposed by Burton and Miller [11], which is used in boundary element modeling of fish swimbladder scattering.

The so called Helmholtz-Kirchhoff integral for scattered field is derived immediately from Eq. (2.5) and using simplified notation can be expressed as:

$$p_{scat} = \frac{1}{4\pi} \int_S \left[p\frac{\partial}{\partial n}\left(\frac{e^{jkr}}{r}\right) - \frac{e^{jkr}}{r}\frac{\partial p}{\partial n} \right] dS \tag{2.7}$$

The solution is still difficult and requires further approximations. The Kirchhoff approximation assumes that the reflection and transmission coefficients R and T that would be derived for the reflection and transmission of an infinite plane wave at an infinite plane interface can be used at every point of a rough surface interface [89]. Furthermore, when they are slowly varying over the surface they can be replaced by mean value that gives:

$$p_{scat} = \frac{R}{4\pi} \int_S \frac{\partial}{\partial n}\left(p\frac{e^{jkr}}{r}\right) dS \tag{2.8}$$

As an example of Kirchhoff approximation shows that for rigid sphere ($|R| = 1$, $\partial p/\partial n = 0$ on the surface) the total pressure is assumed to be twice the incident

pressure ($p = 2p_i$) on the illuminated side of the sphere and is assumed to be zero ($p = 0$) on its shadowed side, which neglects diffraction effects.

The Kirchhoff approximation is often called the geometrical optics approximation because the ray description is assumed to represent the reflected waves at the point where the ray strikes the plane interface [89]. It is often used for solving scattering problems for rather higher frequencies at near vertical incidence angles and is the background method for Kirchhoff-Ray-Mode technique used in fish scattering modeling.

2.3. Scattering from geometrical objects

The marine acousticians are interested in spheres and cylinders since scattering from these simple models have been well studied. The results of their research are applicable to many forms of marine organisms [89]. General approach to solving wave equation for these cases makes use of matching the incident wave and the scattering wave at the boundary of the body. Special approximations and simplifications can be made when one considers small or large objects compared to the wavelength. The small objects are best treated with the integral equation method and produce scattering proportional to f^4, which is the Rayleigh scattering. Scattering from objects that are large compared to wavelength (with large radius of curvature of the surface) represents the so called geometric scattering and can be treated with ray tracing approach.

2.3.1. Scattering from sphere

Let us assume a situation with a sphere of radius r consisting of solid isotropic material and supporting both compressional and shear waves having velocities $c_1$and c_2 respectively, confined in water with different density ρ or compressibility κ ($Z = \sqrt{\rho/\kappa}$) and the wave number is $k = \omega/c$, where $\omega = 2\pi f$ is the angular frequency of the incident field. Since we have a homogeneous object in a homogeneous medium, the material properties are constant except for discontinuity at the object border. Hence, the homogeneous wave equation is satisfied in the region outside the object and in the region inside the object. The symmetry suggests the use of spherical coordinates which gives wave equation in medium as follows [138]:

$$\frac{1}{r^2}\frac{\partial}{\partial r}\left(r^2\frac{\partial p}{\partial r}\right) + \frac{1}{r^2\sin\theta}\frac{\partial}{\partial\theta}\left(\sin\theta\frac{\partial p}{\partial\theta}\right) + \frac{1}{r^2\sin\theta}\frac{\partial^2 p}{\partial\varphi^2} - \frac{1}{c^2}\frac{\partial^2 p}{\partial t^2} = 0 \tag{2.9}$$

The equation is solved by separation of functions dependent on the space variables r, θ, ϕ and combining boundary conditions for compressional and shear waves inside sphere [29]. For incident plane wave with amplitude A expanded in series representation of Legendre polynomials P_n for direction θ and spherical harmonics j_n for distance r:

$$p_{inc} = Ae^{jk(r\cos\theta - ct)} = Ae^{-j\omega t}\sum_{n=0}^{\infty}(-j)^n(2n+1)P_n(\cos\theta)j_n(kr) \tag{2.10}$$

scattered pressure is:

$$p_{scat} = -Ae^{-j\omega t}\sum_{n=0}^{\infty}(-j)^{n+1}(2n+1)\sin\eta_n e^{-j\eta_n}P_n(\cos\theta)h_n(kr) \tag{2.11}$$

where h_n is spherical Hankel function of second kind and angle η_n for n'th partial wave is defined by [63]:

$$\tan\eta_n = -\frac{j_n(x)F_n - j_n'(x)}{n_n(x)F_n - n_n'(x)} \tag{2.12}$$

with

$$F_n = \frac{\rho}{\rho_1}\frac{x_2^2}{2}\frac{\frac{x_1 j_n'(x_1)}{x_1 j_n'(x_1) - j_n(x_1)} - \frac{2n(n+1)j_n(x_2)}{(n^2+n-2)j_n(x_2)+x_2^2 j_n''(x_2)}}{\frac{x_1^2\{[\sigma/(1-2\sigma]j_n(x_1) - j_n''(x_1)\}}{x_1 j_n'(x_1) - j_n(x_1)} - \frac{2n(n+1)[j_n(x_2) - x_2 j_n'(x_2)]}{(n^2+n-2)j_n(x_2)+x_2^2 j_n''(x_2)}} \tag{2.13}$$

where $\sigma = 1 - 0.5/(1-(c_2/c_1)^2)$ is a Poisson ration and $x = ka$, $x_1 = cx/c_1$, $x_2 = cx/c_2$. The other formulations without derivatives of spherical functions can be found, for example, in [58]. Certain limiting cases are of interest. If $F_n \to 0$, the solution would then apply to scattering by a rigid immovable sphere (hard sphere). If $F_n \to \infty$ the solution for scattering by a free-surface is obtained. Note as an example, that for hard sphere, the $n = 0$ partial wave, which is usually referred to as the s-wave (spherically symmetric scattering) yields $\tan\eta_0 = (\sin ka/ka)/(- - \cos ka/ka)$. After simplification it follows that $\eta_0 = --ka$, what means that actual radial wave function is phase shifted as referenced to incident wave by ka.

The far-field condition ($kr \gg 1$) enables exponential approximation of spherical harmonics and gives

$$p_{scat} = -Ae^{j(kr-\omega t)}\frac{j}{kr}\sum_{n=0}^{\infty}(-j)^n(2n+1)\sin\eta_n e^{-j\eta_n}P_n(\cos\theta) \tag{2.14}$$

The total scattering cross section σ_s, which is the total scattered power divided by the incident intensity $I_{inc} = A^2/\rho c$, can then be calculated by integration in all directions θ and ϕ over sphere surface and results in:

$$\sigma_s = \pi a^2\frac{4}{(ka)^2}\sum_{n=0}^{\infty}(2n+1)\sin^2\eta_n \tag{2.15}$$

When the sphere's diameter is much larger than the wavelength ($a \gg \lambda$) and perfectly rigid than all partial waves up to $n_{\max} = ka$ contribute significantly to the scattering cross section. Thus, it is legitimate to replace $\sin^2\eta_n$ by with the average

value 1/2. Hence, the total scattering cross section approaches, in this limited case, the value equals twice the physical cross section of the sphere:

$$\sigma_s = 2\pi a^2 \tag{2.16}$$

and is independent of the wavelength. The scattered wave is composed of the two parts: one, which is scattered from the front of the sphere, and the other shadow-making wave that cancels out the incident wave behind the sphere. Note however, that using geometric optics (Kirchhoff approximation) when diffraction effects are neglected, the value of scattering cross section is equal to the first part only and is also equal to physical cross section of the sphere [164, 89]. This value is often used as a reference for scattering from objects and enables describing angular scattering properties of acoustic objects as the product of geometrical cross section and a function of the form:

$$\sigma_s(\theta) = \pi a^2 \left| f_\infty(ka, \theta) \right|^2 = \pi a^2 \left| \frac{2}{jka} \sum_{n=0}^{\infty} (2n+1) \sin \eta_n e^{-j\eta_n} P_n(\cos\theta) \right|^2 \tag{2.17}$$

For practical purposes the form function of actually four parameters which describe properties of the sphere and surrounding medium [82] in the backscattered direction (towards the wave source where $\theta = \pi$ with $P_n(\cos\pi) = (-1)^n$) are used:

$$f_\infty \left(ka, \frac{c_1}{c}, \frac{c_2}{c}, \frac{\rho_1}{\rho} \right) = \frac{2}{jka} \sum_{n=0}^{\infty} (-1)^n (2n+1) \sin \eta_n e^{-j\eta_n} \tag{2.18}$$

where complex function f_∞ proportional to backscattered pressure is called far field form function for the object insonified by a monochromatic plane wave.

Sample form functions for spherical objects like gas air bubble, fluid filled sphere, rigid sphere and tungsten carbide sphere are shown in Figs. 2.1 – 2.4. Gas-filled spherical or spheroid bubbles were used in early swimbladder bearing fish models, whereas fluid-filled spheres were used to model scattering by zooplankton. In these models, the shape of the animal was ignored.

The results obtained for elastic sphere has also practical application when calibrating acoustical equipment using calibration spheres as the form function dependency on frequency of such spheres (Fig. 2.4) requires careful selection of material and its size to assure nearly flat frequency response (without drop downs coming from Lamb waves interferences [89]) at operating frequency band. Practically, the standard calibration spheres are made of copper [35] and tungsten carbide [45]. Most promising material is tungsten carbide, which is extremely hard (9.5 on Mohs hardness scale) and commercially available in the form of precision ball bearings. The frequency dependence of its form function follows that of ideally hard sphere up to a wavenumber-radius product of about six [13] and can be observed comparing Fig. 2.3 and Fig. 2.4.

Another note is related to any real sonar echo, which contains a spectrum of frequencies, so it is necessary to express the scattering properties in terms of an appropriate cross section averaged over system bandwidth. Following the definition of Foote [35], the effective scattering cross section is:

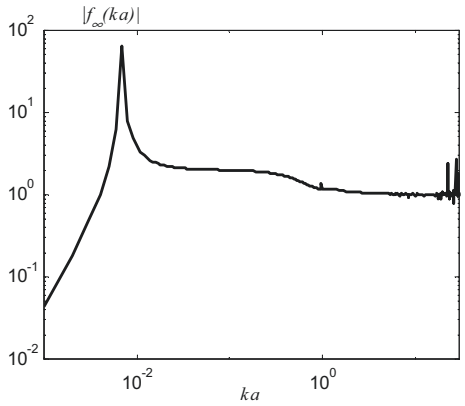

Fig. 2.1. Form function $|f_\infty(ka)|$ for spherical air bubble (c_1=0.22c, $c_2 \to 0$, $\rho_1 = 0.00129\rho$) confined in water with $c = 1450$ m/s, $\rho = 1000$ kg/m^3

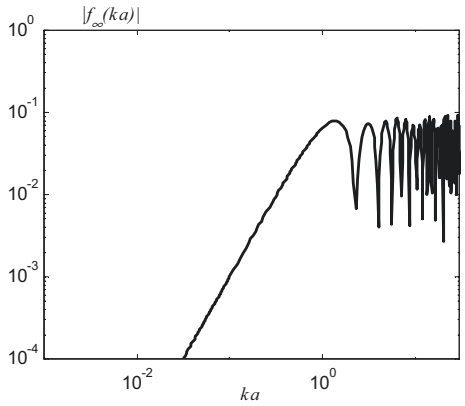

Fig. 2.2. Form function $|f_\infty(ka)|$ for fluid-filled sphere ($c_1 = 1.02c$, $c_2 \to 0$, $\rho_1 = 1.06\rho$) confined in water with c = 1450 m/s, $\rho = 1000$ kg/m^3

$$\sigma_s = \pi a^2 \frac{\int_0^\infty |S(\omega) f_\infty(\omega) G(\omega)|^2 \, d\omega}{\int_0^\infty |S(\omega) G(\omega)|^2 \, d\omega} \tag{2.19}$$

where $S(w)$ is the spectrum of the transmitted pulse and $G(w)$ is the frequency response function of the receiver.

2.3.2. Scattering from cylinder

When taking into consideration the scattering from infinite cylinder, the same approach of expressing incident plane wave into series representation can be used.

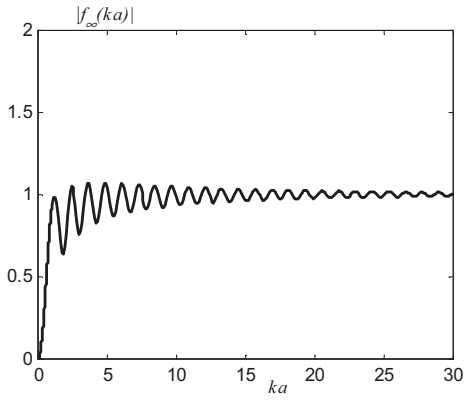

Fig. 2.3. Form function $|f_\infty(ka)|$ for rigid sphere (c_1,$c_2 \to \infty$ and $c_1/c_2 = 2^{1/2}$) confined in water with $c = 1450$ m/s, $\rho = 1000$ kg/m^3

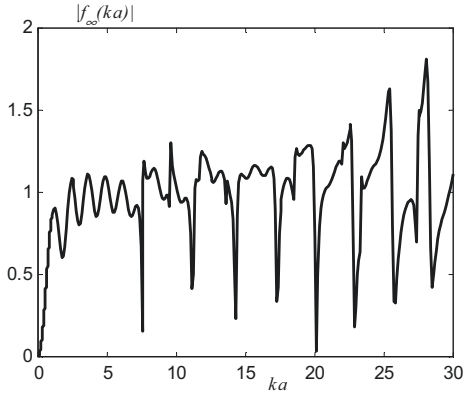

Fig. 2.4. Form function $|f_\infty(ka)|$ for tangsten carbide sphere ($c_1 = 6853$ m/s, $c_2 = 4171$ m/s, $\rho_1 = 14900$ kg/m^3) confined in water with $c = 1450$ m/s, $\rho = 1000$ kg/m^3

However, due to axial symmetry, the incident plane wave can be reexpressed as the sum of cylindrical waves (solution of the wave equation in cylindrical coordinates) with radial and azimuthal dependence:

$$p_{inc} = Ae^{j(kz-\omega t)} = Ae^{-j\omega t} \sum_{n=0}^{\infty} \varepsilon_n j^n \cos(n\theta) J_n(kr) \tag{2.20}$$

where ε_n is the Neumann number ($\varepsilon_0 = 1$, $\varepsilon_{n>0} = 2$).

The sound pressure scattered by infinite cylinder is

$$p_{scat} = -Ae^{-j\omega t} \sum_{n=0}^{\infty} \varepsilon_n j^n \sin \eta_n e^{-j\eta_n} \cos(n\theta) H_n(kr) \tag{2.21}$$

where H_n is the Hankel function of the first kind and the η_n constant is expressed using the same expressions as for sphere Eq. (2.12) and Eq. (2.13) except the spherical Bessel and Neumann functions j_n and n_n are replaced by cylindrical Bessel J_n and cylindrical Neumann N_n functions.

The far-field condition ($kr \gg 1$) enables now exponential approximation of cylindrical functions and results in

$$p_{scat} = -Ae^{j(kr-\omega t)} \sqrt{\frac{2}{\pi kr}} e^{-j\pi/4} \sum_{n=0}^{\infty} \varepsilon_n \sin \eta_n e^{-j\eta_n} \cos n\theta \tag{2.22}$$

Practically, many marine organisms could be treated as a finite cylinder of length L and radius a tilted (as referenced to horizontal plane) by angle χ and for this case the backscattered sound pressure can be approximated as shown by Stanton [145]:

$$p_{scat}(L) \approx -jA \frac{e^{j(kr-\omega t)}}{r} \frac{L}{\pi} \frac{\sin(kL \sin \chi)}{kL \sin \chi} \sum_{n=0}^{\infty} \varepsilon_n \sin \eta_n e^{-j\eta_n} \cos n\theta \tag{2.23}$$

This equation is the basis for numerous approximations of scattering properties based on replacing infinite summation with other functions representing high-pass filter like functions [145, 146, 147, 148].

2.4. Fish acoustic scattering properties

Pelagic fish represents one of more complicated and variable underwater targets taking into account large differences in species, diversified morphology, changeable orientation in space and variable behavior in time. In particular, the last property, which depends on the history of the vertical migration of a fish, its current depth and fish avoidance phenomena (due to ship noise, trawling tools and acoustic field) makes the problem of determination of fish acoustic scattering properties rather difficult.

The mutual reaction of fish and acoustic sounding pulse for relatively large fish (larger than wavelength) is very complicated as the fish generates perturbation field with the virtual sources located inside its body. Partly absorption of the wave energy and partly scattering enables defining fish directivity pattern. As typically *in situ* measurements use vertical echo sounders, the most interesting is dorsal aspect of the pattern [151]. Most of fish species has swimbladder tilted when referred to horizontal position and they even swim with a slight tilt angle. This results in deviation of the main lobe of its directivity pattern referred to vertical position as shown for example in Foote's measurements in Fig. 2.5 [36].

The most important source of variability in scattering properties of fish is existence of its swimbladder, which although represents several percent of its volume but is responsible for over 90 percent of energy reflection. It results from high impedance difference between gas filled swimbladder and the water. Swimbladder is used by the

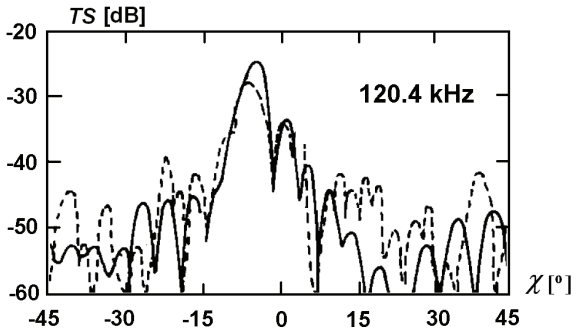

Fig. 2.5. Target strength TS as a function of tilt angle χ for a 31.5 cm pollock [36]

fish for keeping its buoyancy and the changes in its volume may result in changes in scattering level.

Using geometric approximations there are several experiments found in literature for modeling backscattering phenomena of fish swimbladder and fish body. The shape of swimbladder was modeled by ellipsoid, prolate ellipsoid or cylinder [89]. Foote has calculated numerically Helmholtz-Kirchhoff integral using Kirchhoff approximation for such models [36]. The comparison between numerical results and the measurements on actual fish has shown high correlation coefficient.

The mutual reactions of swimbladder and internal structure of fish body along with the variability in changes of the positions of scattering sources due to alternations in the shape of the fish body during swimming results in complicated acoustic response of the fish. Consequently, the *in situ* patterns are much more complicated then those observed in analysis using geometrical models. Hence, the statistical properties of fish echo amplitude are considered, and still its variability is observed due to high variability of relative fish length and its tilt angle [89].

2.4.1. Target strength and scattering cross section

Acoustic properties of underwater objects including fish are described by target strength *TS*, or scattering cross section σ, which measures reflection of acoustic wave in logarithmic and absolute domain [164]. Although target strength definition is unambiguous, the usage of scattering cross section can be used in twofold ways. First quantity – total scattering cross section σ_s is a measure of scattering in all directions and has application in bistatic systems. Second quantity – backscattering cross section $\sigma_{bs}$is, just like target strength, a measure of backscattering properties and is used in monostatic systems, which are used typically in fishery acoustics.

Total scattering cross section is defined as total power P_s scattered in all directions by a target divided by intensity of incident wave I_{inc} measured 1 meter from the center of a target in direction of the source:

$$\sigma_s = \frac{P_s}{I_{inc|r=1m}} \quad [\mathrm{m}^2] \tag{2.24}$$

Whereas, backscattering cross section as a measure of scattering in a source direction is defined as a intensity I_{bs} backscattered by a target in a source direction at 1 meter distance from the target divided by a intensity of incident wave I_{inc}:

$$\sigma_{bs} = r_1^2 \frac{I_{bs}}{I_{inc\,|r_1=1m}} \quad [\mathrm{m}^2] \tag{2.25}$$

For a target scattering in an isotropic way the total scattering cross section is related to backscattering cross section by a simple equation:

$$\sigma_s = \frac{P_s}{I_{inc|r_1=1m}} = \frac{4\pi\ r_1^2 I_{scat}}{I_{inc}} = 4\pi\,\sigma_{bs} \tag{2.26}$$

Target strength, as a logarithmic measure of backscattering can be defined as:

$$TS = 10\log\frac{\sigma_{bs}}{r_1^2} \tag{2.27}$$

what for isotropically scattering targets gives:

$$TS = 10\log\frac{\sigma_s}{4\pi r_1^2} \tag{2.28}$$

It is worth noting that formal inclusion of reference distance in above equations are very often removed by many authors. This leads to informal logarithmic transformation of variables that have dimension. In this case some authors introduce formal description of logarithmic decibel scale referenced to the dimension i.e. [83].

Backscattering cross section σ_{bs} is directly proportional to acoustic wave intensity Ior pressure squared p^2 and expressed in m^2. Hence, the term proportional to acoustic pressure p or received voltage is called backscattering length l_{bs} as it is expressed in meters. All three quantities can be defined in one equation by relation:

$$TS = 10\log\sigma_{bs} = 20\log|l_{bs}| \tag{2.29}$$

Backscattering length l_{bs} is a complex function and it has a sense of acoustic fish length [89].

Note also that scattering cross section is known in radar as the radar cross section (RCS), and expressions for simple shapes are prevalent in the radar literature. These expression can be translated into sonar TS by dividing them by 4π [166].

2.4.2. Fish target strength

The dependence of fish target strength (or fish backscattering cross section) on fish length has been defined experimentally by comparison of the results coming from acoustic surveys to catch samples for a certain fish species. This dependence is valid in the range where geometric scattering is observed i.e. for relatively large fish ($L/\lambda \gg 1$) or for rather higher operated frequencies. In this range the total backscattering cross section σ_s of a sphere with a radius a is approximately equal to its geometric cross section, which means that $\sigma_s = \pi a^2$ and backscattering cross section is equal to $\sigma_{bs} = a^2/4$. In logarithmic domain it is equivalent to the value of target strength equal $TS = 20\log(a/2)$.

In general, the mean target strength dependence on fish length L is linear in logarithmic scale and can be expressed as:

$$\overline{TS} = m \log \frac{L}{L_0} + b_m \tag{2.30}$$

where m is proportionality coefficient, L_0 is the reference length and the value of b_m has two components: one which is constant and one with weak frequency dependency $m_L \log(L/\lambda)$ which is often negligible [36]. Typically $m = 20$ and then the value of b_m is called b_{20} parameter:

$$\overline{TS} = 20 \log \frac{L}{L_0} + b_{20} \tag{2.31}$$

The sample regressions curves for actual data are shown in Fig. 2.6. The theoretical justification was that the target strength should be proportional to cross-section area, and that the area should scale as the square of linear dimension (scaling proportional to L^2) rather than to volume (scaling proportional L^3).

The empirical formula given by Love in 1971 for the fish observed in its dorsal aspect is found to be classical expression in fishery acoustics [76, 89]:

$$\overline{TS} = 18.9 \ \log L + 1.1 \log \lambda \ - \ 23.8 \qquad [\text{dB}] \tag{2.32}$$

where fish fork length L and wavelength λ are expressed in meters. The transformation to absolute domain gives an equivalent expression for backscattering cross-section:

$$\frac{\bar{\sigma}_{bs}}{\lambda^2} = 0.0042 \left(\frac{L}{\lambda} \right)^{1.89} \tag{2.33}$$

Eq. (2.32) and Eq. (2.33) are the results of linear regression analysis done for a large number of measurements and represent approximation enabling only estimation of mean target strength from catch histograms.

Well known are also equations presented by Foote [42] and Traynor [161]. However, the variance of estimates obtained from such equations is sometimes very large (even up to 10 dB) restricts its usage only as a very rough first estimate [151]. Foote also gives the following approximate equations for physoclists and physostomes as measured *in situ* at 38 kHz [19]:

$$\begin{aligned} \overline{TS} &= 20 \log L - 27.5 \quad (physoclists) \\ \overline{TS} &= 20 \log L - 31.9 \quad (physostomes) \end{aligned} \tag{2.34}$$

where fish length L is expressed in meters. For nonswimbladdered fish, backscattering cross section σ_{bs} may very roughly be assumed to be 5 – 10% of the corresponding value of σ_{bs} for physoclists [34].

The mean value of TS according to the National Marine Fisheries Service (NMFS) regression model fit is:

$$\overline{TS} = 20 \log L - 26 \tag{2.35}$$

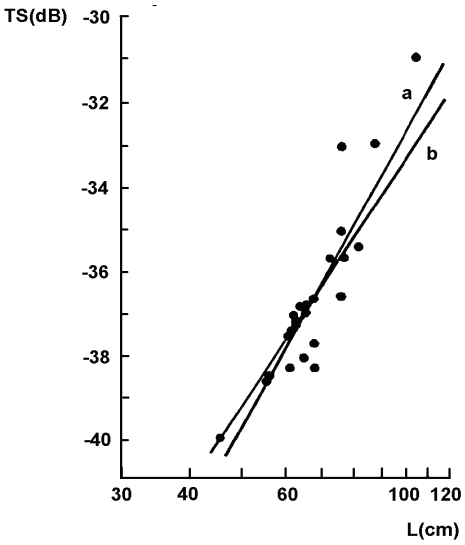

Fig. 2.6. A sample regression curves of target strength for hoki fish [21]: a – Eq. (2.31), b – Eq. (2.32)

with $L_0 = 1$ m which means that the mean backscattering length is roughly equal to one twentieth of the fish fork length ($l_{bs} = L/20$). Practically, the fish length is expressed in cm and then:

$$\overline{TS} = 20 \log L[\text{cm}] - 66 \tag{2.36}$$

In the fishery literature, there is a large amount of papers showing different equations introduced for different species. When not forced through $m = 20$, L regression has values between 18 – 30 [87] or even 5 – 30 [38]. Similarly, b_{20} is also tabulated for different species [78, 87] and ranges at 30 kHz from –25.3 (–65.3 re 1 cm) for blue whiting to –39.3 (—79.3 re 1 cm) for mackerel.

Recently, for some commercial species an expanded target strength relations have been derived from *in situ* observation. For example, Ona [114] using multiple linear regression analysis, gives relation for herring:

$$\overline{TS} = 20 \log L[\text{cm}] - 65.4 - 2.3 \log(1 + z/10) + 0.24(GSI) \tag{2.37}$$

with z representing fish depth and GSI (gonadosomatic index) representing size of gonads [%]. The depth or a rather pressure dependence is found to be in agreement with the Boyle's law [56].

It should be noted that by the nonlinear (logarithmic) transform $TS = 10 \log \sigma_{bs}$ the mean value of a target strength is not in general equal to the estimate obtained as a logarithmically transformed mean value of backscattering cross section, what could be written as:

$$\overline{TS} \neq 10 \log \bar{\sigma}_{bs} \tag{2.38}$$

Although it is common in fishery acoustics to denote $\overline{TS}$ for the quantity representing logarithmic value of mean backscattering cross section ($10 \log \bar{\sigma}_{bs}$).

2.5. Fish scattering models

A simple scattering model of a fish has been developed by Clay and Heist [16]. During high-resolution laboratory measurements, it appeared that the peak value in fish echo profile corresponds to the swimbladder and head, and low level returns are from the skeleton. Additionally, when the fish was moving and flexing the echo was fluctuating from ping to ping. So, as the echo from medium-resolution sonar ping is composed of the echoes from individual parts of the fish the interferences from moving fish can be modeled as composed of a concentrated component and distributed component. They use two-parameter Rice probability density function (PDF) to describe such fluctuations as an analogy between scattering process and Rice's signal theory [149]. Clay and Heist PDF models were partly proved by experimental data, and presented by other authors, i.e. [67]. The second parameter γ can be interpreted as the ratio of concentrated component σ_c to distributed component σ_d ($\gamma = \sigma_c/\sigma_d$) and it depends on the fish behavior and morphology and also on the fish length to wave length (L/λ) ratio. When γ is small, the Rayleigh distribution is obtained, when γ is large, it results in the Gaussian distribution. These two limiting cases apply respectively to large and small fish.

Beside Clay and Heist's stochastic model, more accurate model was formulated by Foote [36] using Kirchhoff approximation and morphology of the swimbladder. Stanton [148] described scattering from finite bent cylinder, which approximates the shapes of the zooplankton and fish. Clay and Horne [17] applied the ray-mode model using actual cod morphology (KRM model). Foote and Francis [43, 48] formulated Helmholtz equation in the context of boundary element method (BEM) and implemented the method for digitized morphology of swimbladder. These recent models are improvements in the modeling of fish backscatter because they facilitate more realistic approximation of the fish body and swimbladder morphology.

Models and measures of acoustic scattering by zooplankton, fish and their swimbladders are continuously evolving. Zooplankton have been modeled as fluid-filled spheres and bent fluid-filled cylinders. Early swimbladder models were based on gas-filled spherical or spheroid bubbles, and gas-filled cylinders. The fish body was first modeled as a gas-filled sphere that ignored the shape of the animal. Arrays of point scatterers have also been used to model the fish body form. More anatomically correct models use fluid-filled cylinders for zooplankton, or a combination of gas- and fluid-filled cylinders for fish. Empirical scattering models of fish and zooplankton are derived using echo measurements and known lengths of caged, tethered, or free ranging organisms. Statistical models of fish backscatter assume a theoretical or tabulate empirical probability density function (PDF) of scattering amplitudes within an insonified beam. Simple geometric shapes (e.g. sphere) regularly used in acoustic modeling efforts do not realistically represent fish body and swimbladder anatomy.

They are only used in resonant region of fish scattering.

2.5.1. Resonant frequency model

Scattering from an individual fish may be significantly increased by the acoustic response of the swimbladder. This gas-filled internal organ is found in many species and may have several functions including hearing and buoyancy. A swimbladder is similar to an air bubble within a fish. The primary scattering mechanism is considered to be a swimbladder vibrating in the volume pulsating mode (monopole) when ensonified at the appropriate resonance frequency. It is now generally accepted that resonance scattering by swimbladdered-bearing fish is the major cause of volume reverberation in the ocean at frequencies up to at least 10 kHz [30]. Since the monopole resonance characteristics of fish swimbladders and air bubbles in water are physically similar, "bubblelike" models have been a popular method for describing resonance scattering from swimbladder bearing fish. One clear difference between bubbles and swimbladders is in their shapes as the swimbladders are usually elongated. However, the assumption has been made in swimbladder scattering models that, since the acoustic wavelength at the monopole resonance is much grater than the dimensions of the object the detailed shape of the swimbladder is relatively unimportant.

The basic model for swimbladdered fish at or near resonance has been given by Andreeva [4]. In the model the fish is treated as spherical air bubble in an infinite elastic medium (i.e. with the properties of fish flesh). The modal solution for scattering from the sphere represented by Eq. (2.18) and exemplified in Fig. 2.1 gives the resonant shape of form function for ka close to 0.01 ($ka \ll 1$). For practical usage the backscattering cross section near resonance can be approximated by:

$$\sigma_{bs} = \frac{a^2}{\left(\frac{f_R^2}{f^2} - 1\right)^2 + \delta^2} \tag{2.39}$$

where a is the equivalent spherical radius of the swimbladder and δ is the damping factor. The resonant frequency is given by:

$$f_R = \frac{1}{2\pi a}\sqrt{\frac{3\gamma p_a + 4Re\{\mu\}}{\rho}} \tag{2.40}$$

where $\gamma = 1.4$ is ratio of gas specific heats, ρ is density of a medium, $p_a = 1.013{\cdot}10^5 + \rho g z$ is ambient static pressure at the depth z ($g = 9.81$ m/s is acceleration of gravity) and $\mu = 3{\cdot}10^5(1 + 0.3j)$ N/m^2 is a complex shear rigidity modulus.

The geometry of a bubble in the model was extended to the ellipsoidal shape by Weston [3] and prolate spheroidal shape by Furusawa [49]. Additionally, Love [77] considered fish flesh as a viscous rather than an elastic medium and Feuillade combined both models surrounding air bubble by viscous and elastic shell [30]. The good overview of resonant models can be found in [30, 156].

At resonance, the damping factor δ determines the peak value of the acoustic cross section $\sigma_{bs}(f_R) = a^2/\delta^2$, which is much larger than the geometrical cross section. It is the following sum:

$$\delta = \delta_r + \delta_t + \delta_v \tag{2.41}$$

of the reradiation (scattering) term $\delta_r = ka$, the dumping constant due to thermal conductivity $\delta_t = d/b$ (d,b – real and imaginary part of complex adiabatic ratio γ) and viscous term $\delta_v = \mathrm{Im}\{\mu\}\mathrm{v}(\rho\pi^2 f^2 a^2)$ [89].

The air bubble models were developed in acoustical oceanography where they are extensively used, especially in the cases, when the nonlinear effects can be observed in a dense subsurface layers [119]. Their usage in fish target strength estimation are of minor importance as the operated frequencies of systems used in fish acoustic surveys are typically above 10 kHz, where scattering properties of the fish are within geometric region and due to an elongated shape of a swimbladder they demonstrate directional properties. However, some simplified semi-heuristic models (i.e. [78]) use a resonant model to describe low frequency scattering and the classical formula of Love for high frequency scattering. They assume that a swimbladder could be represented by air-bubble with radius a, that may be related to the fish length L by $a \approx 0.04L$. In the Rayleigh scattering region σ_{bs} is determined by:

$$\sigma_{bs} = \frac{4\pi^2 V_{sb}^2}{\lambda^4} \tag{2.42}$$

where V_{sb} represents the volume of swimbladder.

2.5.2. Tilted cylinder model of swimbladdered fish

For modeling purposes, the equivalent parameters of fish swimbladder were derived from a simple model, which approximates fish swimbladder to a finite cylinder as proposed by Haslett [59]. The swimbladder is first approximated by a combination of a hemisphere, a short cylinder, and a cone of fixed dimensions relative to the fish fork length. Then this shape is modified to a cylinder maintaining their geometrical cross section. The model is shown in Fig. 2.7.

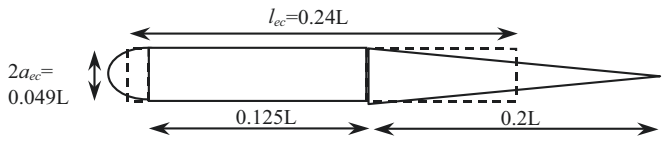

Fig. 2.7. A simple approximation of a fish swimbladder to a cylinder as proposed by Haslett [59]; L – fish fork length

According to [89], the scattering properties of swimbladdered fish can be modelled using the theory of scattering from gas-filled cylinder. The amplitude of acoustic backscattering length of a gas-filled cylinder in water may be evaluated from Helmholtz-Kirchhoff integral and is given by:

$$|l_{bs}(\chi)| = l_{bs0} \frac{\sin\left(kl_{ec}\sin(\chi+\chi_0)\right)}{kl_{ec}\sin(\chi+\chi_0)} \sqrt{\cos(\chi+\chi_0)} \tag{2.43}$$

where

$$l_{bs0} = l_{ec}\sqrt{\frac{a_{ec}}{2\lambda}} \tag{2.44}$$

is fish maximum backscattering length, a_{ec} and l_{ec} are the radius and length of the equivalent swimbladder as a cylinder, $k = 2\pi/\lambda$ is wave number, χ is fish angular orientation and χ_0 is a tilt angle of the swimbladder. The $\sin(x)/x$ dependence determines angular properties of fish pattern as the *cosine* dependence is rather week. Eq. (2.44) is equivalent to relation describing maximum scattering cross section of a swimbladdered fish in a dorsal aspect expressed as the product of wavelength and both equivalent parameters of the cylinder $\sigma_{bs0} = ka_{ec}l_{ec}^2$.

Thus, the two parameters approximation of fish swimbladder by equivalent cylinder length l_{ec} and equivalent cylinder radius a_{ec} allows estimating maximum fish target strength using finite cylinder model. As an example when using $l_{ec} \approx L/4$ and $a_{ec} \approx L/40$ approximations as in Haslett model,one can define approximate dependence of maximum value of fish target strength TS_0 on fish length L as [108]:

$$TS_0 = 20\log(L^{3/2}/4\sqrt{80\lambda}) = 30\log L[\text{m}] + 10\log f[\text{kHz}] - 33 \tag{2.45}$$

in which an approximated value of sound speed $c = 1500$ m/s was used when converting wavelength λ to operating frequency f. It eventually enables recovering L distribution from TS_0 distribution in statistical processing. Different values in relations between equivalent parameters and the fish length may result in introducing bias in fish length estimate.

Although the model lacks versatility [21] its simplicity enables statistical modeling of probability distribution function of scattering from single fish of length L having random body orientation.

2.5.3. Finite bent cylinder model

The finite bent cylinder model introduced by Stanton (1989) [148] computes scattering length l_s of the fish as a finite uniformly bent cylinder:

$$l_s = \pi\frac{L_{arc}}{\gamma_{\max}}\int_0^{\gamma_{\max}}\sum_{n=0}^{N}\frac{-\varepsilon_n}{1+jC_n}\cos(n\theta)e^{2jkr_c(1-\cos\gamma)}d\gamma \tag{2.46}$$

with $\theta = \pi$ for backscatter, where $C_n = \frac{ZJ_n'(k_1a)N_n(ka) - -Z_1J_n(k_1a)N_n'(ka)}{ZJ_n'(k_1a)J_n(ka) - -Z_1J_n(k_1a)J_n'(ka)}$ and Z_1 and Z are acoustic impedances of cylinder and surrounding water, respectively. The fish body and swimbladder are converted to finite uniformly bent cylinder of total arc length $L_{arc} = 2\gamma_{\max}r_c$, where radius of curvature r_c and maximum angle $\gamma_{\max}$ ($2\gamma_{\max}$ subtends entire arc) describe cylinder deformation.

2.5.4. Low-resolution acoustic model

Foote (1985) [36] and Foote and Traynor (1988) [46] used the Helmholtz-Kirchhoff integral to develop an accurate and elaborate method to estimate backscattered sound

from fish. Their approach was simplified by Clay (1991) [15] who incorporated Stanton's finite bent cylinder equation and fluid- or gas-filled cylinders into model fish backscatter. Clay's low resolution acoustic model [15] modifies finite bent cylinder model described by Eq. (2.46) by moving the summation of modal components out of integral and inserting an empirical roughness attenuation parameter δ obtained by modeling irregularities of fish body by Gaussian distribution:

$$l_{bs} = -\frac{j}{\pi} \sum_{n=0}^{N} \frac{\varepsilon_n}{1 + jC_n} (-1)^n e^{-\delta(ka)^2} \int_0^L e^{2kz(x)} dx \tag{2.47}$$

where x denotes the along-cylinder axis, $z(x)$ denotes the perpendicular distance the cylinder is deformed and L is the length of the cylinder as projected to the x axis. The $z(x)$ function, which influence phase shift is simplified to a parabolic function $z(x) = \alpha x^2$. The phase shift integral can be evaluated using change of variables and computing Fresnel integrals $C_F(x) = \int_0^x \cos(\pi\xi^2/(2)d\xi$ and $S_F(x) = \int_0^x \sin(\pi\xi^2/(2)d\xi$ what reads:

$$l_{bs} = -\frac{j}{\pi} \sum_{n=0}^{N} \frac{\varepsilon_n}{1 + jC_n} (-1)^n e^{-\delta(ka)^2} \sqrt{\frac{\pi}{4k\alpha}} [C_F(x) + jS_F(x)] \tag{2.48}$$

where $x = (4k\alpha/\pi)^{1/2} L$.

In the calculation of l_{bs} only several first modal components are typically used (low modes) hence the name of the model.

2.5.5. Kirchhoff-Ray-Mode model

The Kirchhoff-Ray-Mode model represents the culmination of several backscatter modeling efforts. Clay and Horne (1994) [17] combined previous approaches to model backscatter by representing the fish body as a contiguous set of fluid-filled cylinders that surround a set of gas-filled cylinders representing the swimbladder. Using radiographs, lateral and dorsal silhouettes of the fish body and swimbladder are traced, scanned, and digitized. A sample model of a fish body or swimbladder is shown in Fig. 2.8. Normal resolution of the cylinders is 1 mm.

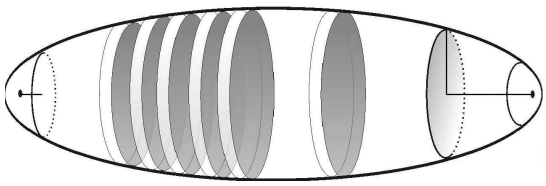

Fig. 2.8. Three-dimensional representation of a fish body or swimbladder with 1 mm cylinders [51]

Backscatter from each cylinder is estimated using a low mode cylinder solution and a Kirchhoff-ray approximation ($ka > 0.2$). Backscattering cross-sections from

each finite cylinder are summed over the whole swimbladder $l_{bs}^{(sb)}$ or body $l_{bs}^{(fb)}$ and then added coherently [17]:

$$l_{bs} = l_{bs}^{(sb)} + l_{bs}^{(fb)} \tag{2.49}$$

Swimbladder backscattering length $l_{bs(sb)}$ is calculated from its cylindrically modeled N parts as:

$$l_{bs}^{(sb)} = -j\frac{R_{fs}(1-R_{wf}^2)}{2\sqrt{\pi}} \sum_{i=0}^{N} A_{sb}\sqrt{k_{fb}a_i + 1}e^{-j(2k_{fb}a_i+\varphi_{sb})}\Delta l_i \tag{2.50}$$

with $A_{sb} = ka_i/(ka_i + 0.083)$, $\varphi_{sb} = ka_i/(ka_i + 40) - 1.05$, $R_{fs} = (Z_{sb} - Z_{fb})/(Z_{sb} + Z_{fb})$, $R_{wf} = (Z_{fb} - Z)/(Z_{fb} + Z)$, a_i are radiuses of cylindrical parts of fish swimbladder. Similarly, fish body backscattering length $l_{bs}^{(fb)}$ is calculated as:

$$l_{bs}^{(fb)} = -j\frac{R_{wf}}{2\sqrt{\pi}} \sum_{i=0}^{N-1} \sqrt{k_{fb}a_i}\left[e^{-j2ka_{U,i}} - (1-R_{wf}^2)e^{-j(2ka_{U,i}-2k_{fb}(a_{U,i}-a_{L,i})+\varphi_{fb})}\right]\Delta l_i \tag{2.51}$$

with $\varphi_{fb} = \pi k_{fb}a_{U,i}/2(k_{fb}a_{U,i} + 0.4)$. The substripts *wf* and *fs* denote the water-fish and fish-swimbladder interfaces, $a_{U,i}$ and $a_{L,i}$ are radiuses of upper and lower body parts and Δl_i is incremental distance between the elements. The amplitude A_{sb} and phases φ_{sb} and φ_{fb} are empirical adjustments for small *ka*.

Actually, the model calculates backscatter normalized to fish length L as so-called reduced scattering length *RSL*, which is used for elongated objects:

$$RSL = \frac{|l_{bs}|}{L} \tag{2.52}$$

The concept of using reduced scattering length is analogous to the introduced earlier form function f_∞ of spherical objects defined as backscattering amplitude normalized to geometrical cross section πa^2. Logarithmic equivalent of the reduced scattering length is called reduced target strength and is defined by:

$$RTS = 20\log RSL = 20\log|l_{bs}| - 20\log L \tag{2.53}$$

The more familiar target strength *TS* is obtained than as:

$$TS = RTS + 20\log L \tag{2.54}$$

For any digitized fish, the KRM model may estimate backscatter as a function of a fish length, wavelength (i.e. speed of sound in water/acoustic frequency), and fish tilt. Results from the model can be reported for the swimbladder, body, or the whole fish to show the contribution of the body parts to the total backscatter. Model results can be combined to summarize backscatter characteristics of a single fish. A backscatter response surface represents reduced scattering length as a function of fish aspect θ and a ratio of fish length L to acoustic wavelength λ as shown for Atlantic cod in Fig. 2.9. The dependence of echo amplitude on aspect angle is low at low L/λ

values. As fish length or acoustic frequency increases, the influence of fish aspect on echo amplitude increases. Since maximum backscatter occurs when the top surface of the swimbladder is parallel to the transducer and corresponding incident wave front, maximum backscatter occurs at 85 degrees with the fish tilted slightly head down. The influence of fish aspect increases as L/λ increases. The response surface becomes quasi-symmetrical as θ deviates positive or negative from 85°. Along the fish length to acoustic wavelength axis, if fish length is kept constant, then higher L/λ values correspond to higher acoustic frequencies. Keeping frequency constant illustrates the effect of changes in the fish length. The periodic peaks and valleys along the maximum backscatter ridge correspond to constructive and destructive interference between the swimbladder and body.

Component backscatter plots and backscatter response surfaces can be modeled for any species. Tilt angles, lengths, and frequencies are chosen to reflect the species and behavior of interest. The model has been expanded to include backscatter calculations as a function of fish roll. This is important as fisheries sonars are insonifying fish aggregations at angles other than 90 degrees incidence (i.e. looking downward).

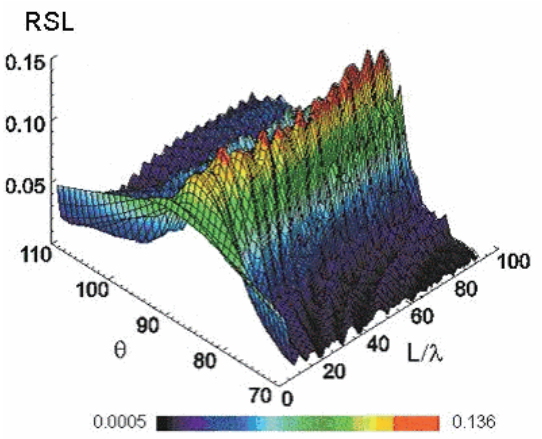

Fig. 2.9. Backscatter response surface for an Atlantic cod obtained by KRM model

2.5.6. Boundary-element model

The boundary-element model uses boundary-element method (BEM) for modeling scattering by swimbladder-bearing fish. The method was introduced by Foote and Francis [43] as the one, which includes the effects of diffraction. All of the high-frequency models cited so far neglect this effect. In addition to treating diffraction, the BEM enables using general conditions on the swimbladder boundary surface with explicit representation of the internal fluid. Thus, the BEM can also be used to study pressure-dependent effects, which are otherwise precluded by the standard Kirchhoff-approximation model.

To develop the acoustic boundary-element method, the wave equation for the pressure p is reduced to the Helmholtz form by assuming the harmonic time dependence

and rewritten in integral form, in which the pressure at every point is expressed in terms of the acoustic pressure and normal displacement u on the scattering surface S. This surface is subdivided into elements, and the pressure and displacement distributions on S are represented by discrete values, p_i and u_i, respectively, at each node i associated with these elements. For each element the standard Helmholtz equation Eq. (2.5), which suffers from singularities at certain critical frequencies, is transformed to so-called composite boundary integral equation, which is a linear combination of Helmholtz integral equation and its normal gradient as proposed by Burton and Miller [11, 167]:

$$\begin{aligned} &\varepsilon\left[p(P)+\alpha\tfrac{\partial p(P)}{\partial n_P}\right]= \\ &=\int_S\left(p(Q)\tfrac{\partial G_k}{\partial n_Q}-G_k\tfrac{\partial p(Q)}{\partial n_Q}\right)dS_Q+\alpha\int_S\left(p(Q)\tfrac{\partial^2 G_k}{\partial n_P\partial n_Q}-\tfrac{\partial G_k}{\partial n_Q}\tfrac{\partial p(Q)}{\partial n_Q}\right)dS_Q \end{aligned} \tag{2.55}$$

where α is combination factor which is a complex constant. The resulting equation can be written using gradient formulation expressed in matrix form for exterior pressure [47]:

$$\mathbf{Ap}=\mathbf{Bu}-\mathbf{p}_{inc}-\alpha\frac{\partial\mathbf{p}_{inc}}{\partial n} \tag{2.56}$$

and for interior pressure:

$$\mathbf{A}_1\mathbf{p}=\mathbf{B}_1\mathbf{u} \tag{2.57}$$

The coefficients of the matrices $\mathbf{A}$ and $\mathbf{B}$ which are dependent on local distances $\boldsymbol{r}_i$ taken at global node i, are assembled from local matrices pertaining to each element of the mesh [43]. Matrices $\mathbf{A}_1$ and $\mathbf{B}_1$ resemble the respective matrices $\mathbf{A}$ and $\mathbf{B}$, but use the properties of the internal gas rather than those of the external fluid. The details and definitions of these parameters are in [48]. As pressure and normal displacement are continuous across water-gas interface the simultaneous solution is derived directly:

$$\mathbf{u}=(\mathbf{B}-\mathbf{A}\mathbf{A}_1^{-1}\mathbf{B}_1)^{-1}(\mathbf{p}_{inc}-\alpha\frac{\partial\mathbf{p}_{inc}}{\partial n}) \tag{2.58}$$

and

$$\mathbf{p}=\mathbf{A}_1^{-1}\mathbf{B}_1\mathbf{u} \tag{2.59}$$

The scattered pressure at any exterior point $\mathbf{r}$ is obtained from the standard integral equation:

$$p_{scat}(\mathbf{r})=\mathbf{a}(\mathbf{r})\mathbf{p}-\mathbf{b}(\mathbf{r})\mathbf{u} \tag{2.60}$$

where coefficients of vectors $\mathbf{a}$ and $\mathbf{b}$ are calculated similarly to coefficients of matrices $\mathbf{A}$ and $\mathbf{B}$ replacing local distances $\mathbf{r}_i$ by the position vector $\mathbf{r}$ [43]. The target strength is finally calculated as the amplitude of backscattered length $|l_{bs}|$ at finite range r referenced to the unit distance $r_0 = 1$ m:

$$TS = 10 \log \frac{|l_{bs}|^2}{r_0^2} = 20 \log \frac{r\,|p_{scat}(\mathbf{r})|}{r_0\,|p_{inc}|} \tag{2.61}$$

The elements used in the method are quadrilaterals and triangles of the quadratic isoparametric type, in which both the geometric and acoustic quantities are interpolated from the nodal values using quadratic shape functions, the nodes being suited at the vertices and midsides [170]. As the general guide, good representation of the acoustic variables is obtained if the lengths of the sides of the elements are less than one-third of a wavelength. The accuracy of geometrical representation depends on the degree of undulation of the surface, but it should be noted that the quadratic interpolation allows the elements to be curved.

The detailed examples of calculation using BEM are presented in [43] and [48] on discrete mesh of an actual fish swimbladder as shown in Fig. 2.10 and Fig. 2.11. The mesh is typically obtained through quantitative use of various radiograph technologies – traditional X-rays, phase contrast X-rays (PCX) and computerized tomography (CT) scans [125]. The obtained results highlight its applicability especially at lower frequencies as the diffraction is addressed in a fundamental manner.

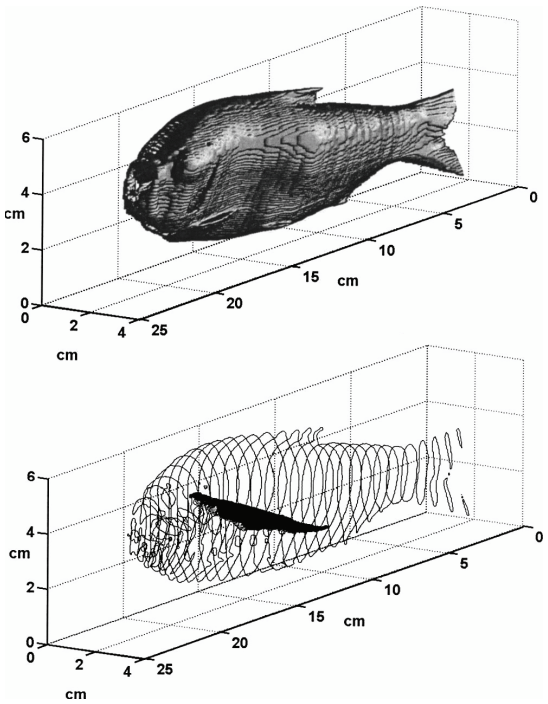

Fig. 2.10. Three-dimensional digital model generated from computerized tomography (CT) scan imagery [125], required for BEM method

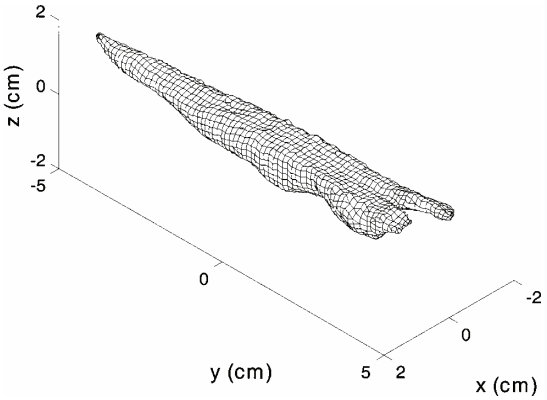

Fig. 2.11. Boundary element mesh of the 108 mm pollack swimbladder [48]

Chapter 3

FISH TARGET STRENGTH ESTIMATION

Remote sensing of the sea state and the existence of marine living resources, in particular of pelagic fish population, not only plays a central role in such fields like environmental protection, biology of the sea or oceanography, but also pushes forward the development of dedicated information systems based on digital signal processing of acoustic echoes. Moreover, the remote sensing and estimation of fish abundance represents one of the main streams in functioning of such international institutions as the Food and Agriculture Organization (FAO) or the International Council for the Exploration of the Sea (ICES).

The principal aim of remote sensing of fish population is delivering the data for optimal exploitation of marine living resources. As the size of living resources is limited but renewable, it may be treated as the search for such a level of exploration, which in a long-term situation will ensure the maximization of the catches without changes in biological equilibrium. In fisheries economics it was described by the concept of Maximum Sustainable Yield (MSY) introduced by Gordon in 1954 in his famous article [55]. Because of the complexity of ecosystems and the problems with defining a MSY, in 1999 the EU fisheries management replaced it with the Precautionary Principle [22]. The concept includes the following points: (1) stock specific reference points, (2) restriction of fishing because of declining stocks, (3) reconstruction programmes for overused stocks. These directions were recommended to the EU-commission by ICES.

Methods used in population estimation of marine living resources can be divided into three groups: biostatistic-trawl methods, remote sensing or teledetection methods and hydroacoustic methods.

Biostatistic-trawl methods, although historically first methods in this group, represent rather invasive technique done *in situ*. They use catch samples for estimation of some parameters of fish population like for example length distribution. Since the main thread in the book is related to acoustic methods, let us just list two most popular viz.: virtual population analysis (VPA) [90] and swept area method (SAM) [57].

In the last three decades, introduction of the satellite technology and its application in remote sensing has open new possibilities in detection of fish populations. When compared with conventional methods remote sensing has many advantages: noninvasiveness, simultaneous large area coverage and high acquisition speed. It makes use of passive and active techniques like microwave and infrared radiometry, photogrametry, radar techniques, laser spectrometry etc.

In fishery applications, the passive methods are used in measurement of chlorophyll concentration. Concentration of chlorophyll is related through photosynthesis

with a primitive productivity in a sea, which gives direct measure of plankton resources, and through this, it determines fish resources. Such measurement uses color scanners, which utilize spectrum properties of the reflectance. So-called Coastal Zone Color Scanners (CZCS) installed in the NIMBUS-7 satellite delivers also additional information such as distribution of temperature and salinity and oxygen contents in the oceans.

The radiometric measurements of temperature using Advanced Very High Resolution radiometers (AVHRR) represent the second passive method, complementary to color scanners method. The radiometers of this type were installed in the NOAA-X satellite series and deliver thematic maps of selected ocean regions. The usage of this technique enables estimation of fish distribution in the course of evolution. In the last decades, the new generations of scanning radiometers so called Along Track Scanning Radiometers (ATSR) were installed in ERS and TOPEX satellites. They facilitated acquisition of integrated data for monitoring fish resources. The Enhanced Thematic Mapper (ETM+) scanner, which works on the LANDSAT satellite, delivers up to seven images of the same area in the different spectrum ranges. The spectral analysis of this data shows thematic layers with information on phytoplankton contents, temperature distribution, etc.

The active methods use mainly radiolocation techniques such as Side Looking Radar (SLR), Synthetic Aperture Radar (SAR), altimeters, lidars and dispersion meters. First two techniques were successfully applied to indirect detection of pelagic fish populations by observation of the sea state. However, it is worth noting that satellite teledetection methods with their recognised advantages have also many disadvantages such as low time-spatial resolution, low precision, problematic calibration and the only sea surface observation.

As a consequence, from the above mentioned population estimation methods, mainly hydroacoustic methods are commonly applied for monitoring of sea living resources due to their many advantages [151], which will be described in this chapter in detail.

3.1. Analysis and the model of hydroacoustic fish echo

The model of location of a fish population in a water column assumed here covers with a certain restrictions to all actual fish concentration, viz.: single fish, fish in scattering layers and pelagic fish. In the first case, the echoes from the fish treated as single distinguishable targets represent non-overlapping single echoes. Whereas in the last two cases, the single echoes overlap as a result of scattering interferences from neighbouring fish. The resultant reverberation represents the sum of scattered waves from the fishes treated as a targets. What is more important, pelagic fishes may have different degree of concentration, which influences characteristics of echo signals received in the hydroacoustic system. Typically, fish are organized in the so-called schools, with a relatively medium density as compared to higher density concentration observed in shoals or even in very dense swarms [144], in which the multiple scattering and excess attenuation may be observed [151].

Target discrimination is determined by spatial resolution of the hydroacoustic

system. It is often assumed that targets are resolvable if in spatial resolution cell only one target is present [151]. The spatial resolution cell ΔV is proportional to the product of spatial length of sounding pulse $\Delta r = c\tau/2$ and angular resolution $\Delta\theta$, which is often assumed to be equal to transducer beam width (or its equivalent integrated beam width).

The echo analysis will be performed for the general case of multiple (even overlapped) echoes from fish schools and fish scattering layers as a biomass of a large amount of pelagic fish represents this type of aggregation.

It is assumed, that in the first approximation, for fish populations in the sea the point scattering model of the first order is valid. It means that the observed echo is the result of superposition of individual echoes from randomly located scattering targets. The echoes originate independently from the presence of other targets. It means that the multiple scattering effects are neglected [151]. This assumption is valid when the concentration of targets and its spatial location in the direction of signal propagation is not high, what can be expressed by critical density of the scatterers [144].

As almost all sonar systems used in fisheries operate in the monostatic geometry, let us further assume that the transmitter and receiver are located in the same place in the vertical configuration. Hence, we are interested only in backscattering phenomena.

3.1.1. The model of the echo formation process

Let us assume that the transmitter generates narrow band sounding pulse $s(t)$ with a rectangular envelope $A(t)$ with a time duration τ, and angular frequency ω_0 matched to the resonance frequency of the transducer:

$$s(t) = A(t)\cos\omega_0 t \tag{3.1}$$

Foote [42] showed that in the fish echo formation process backscattered pressures sum up linearly, and resulting echo scattered from randomly located fishes is the sum of individual echoes [89]:

$$p_s(t) = \sum_{i=1}^{n(t)} p_{s,i}(t) \tag{3.2}$$

where $n(t)$ is the number of echoes received by transducer in the acquisition time gate up to current time t and

$$p_{s,i}(t) = p_0(t - 2r_i/c)r_0\, l_{bs,i}\, b^2(\theta_i, \varphi_i)\frac{10^{-\alpha r_i/10}}{r_i^2} \tag{3.3}$$

is the pressure scattered by i^{th} target, $p_0(\cdot)$ is the on-axis pressure amplitude generated by transmitting signal $s(t)$ at reference distance $r_0 = 1$ m from the source, $l_{bs,i}$ is the backscattering length of the i^{th} target and $b^2(\theta_i,\varphi_i)$ is the value of transducer beam pattern for i^{th} target located in spherical coordinates r_i, θ_i, φ_i.

It is also assumed that the fish relative position changes in contiguous transmissions so that for high operating frequencies used in echo sounders the signal phase changes are large enough [144]. As a result, the phases of overlapping fish echoes which

constitute the level of echo from clouds of scatters are uncorrelated with a uniform distribution $p_\varphi(\varphi) = \frac{1}{2\pi}$ in the range of (0,2π).

Thus assuming linearity phenomena and neglecting Doppler shift generated by frequency changes due to relative fish and transducer movement, the echo signal $e(t)$ can be defined as a convolution of transmitted signal $s(t)$ with impulse response representing clouds of targets in the hydroacoustic channel $k(t)$:

$$e(t) = \int_0^t s(\tau)k(t-\tau)d\tau \tag{3.4}$$

For the assumed point scattering model of the first order, the impulse response of such clouds can be modeled as a sum of weighted delta Diraca pulses [89]:

$$k(t) = \sum_{i=1}^{N} \underline{w}_i \delta\left(t - \underline{\tau}_i\right) \tag{3.5}$$

where $\underline{w}_i$ is a random variable representing the weight amplitude of i^{th} target response proportional to backscattering length of the target l_{bs}, $\underline{\tau}_i$ is the random variable representing delay of the echo obtained from i^{th} target ($\underline{\tau}_i = 2r_i/c$) and n is the number of targets. Consequently, the echo signal can be described as the following sum:

$$e(t) = \sum_{i=1}^{n} \underline{A}_i s\left(t - \underline{\tau}_i\right) \tag{3.6}$$

where $\underline{A}_i = \underline{w}_i A(t-\underline{\tau}_i) = \underline{A}(t-\underline{\tau}_i) l_{bs,i} b^2(\theta_i, \varphi_i) 10^{-0.2\alpha r_i}/r_i^2$ is the total amplitude of i^{th} echo.

The distribution of random variable $\underline{\tau}$ representing echo delays are related directly to the already considered phase distribution, whereas the statistical properties of peak echo amplitude random variable $\underline{A}_i$ are the subject of a considerable amount of scientific research. Theoretically, using statistical signal theory the echo envelope may have the Rayleigh distribution. It has been observed [26] that for fish echoes the Rayleigh distribution may occur only for relative fish size $L/\lambda \gg 25$ and due to fish movement the distribution may evolve through Rice distribution [16] to normal distribution. For overlapping echoes, the extremal distribution can be defined [144]. The detailed examples of theoretical distributions of backscattering length, backscattering cross section and target strength can be found in [151, 156].

It is worth noting that in a general case beside useful information in signal $e(t)$ the two additive components are present: noise and reverberation. However, in most cases in fishery acoustics the echo signal to noise level is of high value and reverberation level in case of vertical sounding is negligible. Worth noting is also the fact that echoes from very high dense scattering layers have also the characteristics of reverberation as they represent superposition of sounding pulse echoes scattered on elementary targets.

3.1.2. Echo counting

Using quite realistic assumptions, the fish population in the sea may be treated as a set of independent elementary scattering targets, randomly distributed in a water

column. For that purpose, Ehrenberg [24] defined a nonhomogenious Poisson process as an integer-valued counting process $n(s)$ with the intensity $v(s)$ governed by the following probability law:

$$P(k = n(s)) = \frac{\left(\int_S v(s)ds\right)^k}{k!} e^{-\int_S v(s)ds} \tag{3.7}$$

where $v(s)$ is nonnegative function with bounded integral. If the intensity function $v(s)$ is constant in its domain, the process describes the uniformly distributed targets and is called homogeneous Poisson process. The density of fish targets may be then interpreted as an average frequency of its appearance in the unit volume. The probability of appearance of n targets in volume V may be described by Poisson distribution [151].

$$P(k = n) = \frac{(\rho_V V)^k}{k!} e^{-\rho_V V} \tag{3.8}$$

where n is random variable representing the number of targets and $\rho_V V = E\{n\}$ has a sense of a mean value of the number of targets.

When the fish targets are sparsely distributed so that only a small proportion of the echoes overlap, it is possible to identify and count the echoes from individual fish [80]. Hence, the count gives an estimate of the number density of fish in the acoustic beam [39]:

$$\rho_V = \frac{\overline{n}}{V} \tag{3.9}$$

where $\overline{n}$ is an average number of echoes obtained in the sampled volume V per sounding.

To calculate the fish count n, the echo counter must include some means of selecting the echoes associated with an individual fish, by rejecting echoes that result from two or more fish being detected concurrently. For the transmitted pulse of duration τ the echo duration will rather be longer than τ. Single-fish echoes might be identified by cross correlating the received signal and the transmitted pulse waveform. Any portions of received signal that begins and ends at a preset threshold level, within which the signal is always above it, may be considered to be an echo from one or more targets. One criterion would be to reject echoes whose duration is above some limit i.e. $t > 1.5\tau$ [80]. This would eliminate echoes from multiple targets separated by more than one pulse length in a range. Other criteria are necessary to eliminate echoes from multiple targets at nearly the same range. Algorithms may take account of the echo rise time or fluctuation of the echo envelope, the factors that should remain within well-defined limits for single-fish echoes.

The general theory of acoustic sampling volume V was defined by Foote [39]. According to his definition for directional scatters with backscattering cross section σ_{bs} and minimum signal threshold level e_{min}, acoustic sampling volume is:

$$V = \iint H(k_x b^2 \sigma_{bs} - e_{\min}) dF dV \tag{3.10}$$

where $H(\cdot)$ is Heaviside step function defined by $H(x) = 0, \frac{1}{2}, 1$ as $x < 0$, $x = 0$, $x > 0$, respectively, k_x is system constant and the integration is also performed over the range of orientations determining the sampled values of σ_{bs} according to the cumulative distribution F. However, practically the reverberation volume V is calculated as a difference of cones (more precise calculation).

$$V = \frac{1}{3}\Psi\left[\left(r + \frac{c\tau}{4}\right)^3 - \left(r - \frac{c\tau}{4}\right)^3\right] \tag{3.11}$$

or cylinders (less precise) [156]:

$$V = r^2\Psi\frac{c\tau}{2} \tag{3.12}$$

where Ψ is an equivalent beam width and will be described later in this chapter. As the cylinder difference gives simple formula and the errors introduced are negligible, it is often used in practice.

The echo amplitude has different statistical properties according to whether or not the echoes overlap. Statistical estimator may be used to determine whether conditions are suitable for echo counting or to estimate the fish density directly from statistical models of echo formation i.e. [142, 143, 144]. The critical density at depth r as defined by Stanton [144] is:

$$n_c = \frac{1}{r^2\Delta\theta^2\frac{c\tau}{2}} \tag{3.13}$$

where $\Delta\theta$ is angular separation between the first nulls of the beam pattern.

3.1.3. Echo integration

As it was shown, the elementary fish echoes have random characteristics of phase shifts and time of arrivals to the receiver. Therefore, they cannot be defined in a deterministic way but rather their properties can be extracted by analysis of their pressure amplitude squared. This approach is called in fishery acoustics echo integration [89, 151] as the integration of pressure (or voltage) squared waveform in the time period $\Delta t = t_2 - t_1$ has a sense of averaging of this variable in the depth layer $\Delta r = r_2 - r_1 = c\Delta t/2$.

Moreover, if the phase shift is distributed randomly (which gives noncoherent scattering) then squaring operation is required before integration. That is why further analysis is performed using averaged pressure squared (or intensity) of the echo. The integrated in time period Δt pressure squared can be expressed as:

$$\langle p^2\rangle_{\Delta t} = \int_{t_1}^{t_2} |p_s(t)|^2\, dt \tag{3.14}$$

which gives:

$$\left\langle p^2 \right\rangle_{\Delta t} = \sum_i \int_{t_1}^{t_2} |p_i(t)|^2 \, dt + \sum_i \sum_j \int_{t_1}^{t_2} p_i(t) p_j(t) dt \tag{3.15}$$

As it is easily seen the first sum contains only positive values whereas the second one contains the products of pressures scattered by two targets located in the ranges r_i and r_j from the transducer. The cross products can be positive or negative and this results in fluctuations of the integral. However, the first sum is much larger than the second one, which additionally decreases in contiguous pings. Therefore, the fluctuations due to cross products can be neglected when increasing the number of targets and echoes [89].

As it was shown by Ehrenberg [27] an expected value of echo integration $E\left\{\left\langle p^2 \right\rangle_{\Delta t}\right\}$ is proportional to mean fish density ρ_V in the sounding volume V defined in the period (t_1, t_2):

$$E\left\{\left\langle p^2 \right\rangle_{\Delta t}\right\} = \frac{1}{2} E\{e^2\} \Delta t \rho_V V_{(t_1,t_2)} \tag{3.16}$$

where $\rho_V V = E\{n\}$ is the expected value of a number of fish in the volume $V_{(t1,t2)}$ and$e = k_x b(\theta_i,\varphi_i) l_{bs}$ is random variable representing echo amplitude (k_x is system constant). As the echo integration is performed on voltage waveform $e(t)$ rather than on pressure $p(t)$ so the voltage squared amplitude e^2 is used. The voltage can be used due to assumption of linear electro-acoustic conversion with the conversion coefficient equal to received sensitivity s_x of the transducer ($e = s_x p$). The factor $E\{e^2\}\Delta t/2$ can be treated as the expected value of echo energy from a single fish, which (assuming independence of random variables $\underline{b}$ and $\underline{l}_{bs)}$ can be described by:

$$E_e = \frac{1}{2} E\{e^2\} \Delta t = k_x^2 \, E\{b^2(\theta, \phi)\} \, E\{\sigma_{BS}\} \tag{3.17}$$

If the value of energy E_e is known or can be measured – which requires estimation of the expected values of $\underline{b}$ and $\underline{l}_{bs}$ – the output of integration can be scaled to be the estimate of acoustic number of fish in the volume V:

$$\hat{n} = \frac{E\left\{\left\langle p^2 \right\rangle_{\Delta t}\right\}}{\frac{1}{2} E\{e^2\} \Delta t} \tag{3.18}$$

where $E\{\hat{n}\} \equiv \rho_V V_{(t_1,t_2)} = E\{n\}$ means that scaled properly output of echo integrator enables obtaining unbiased estimation of a fish number $\hat{n}$ in the sounding volume V or fish density $\rho_V = n/V$ [89, 151].

3.1.4. Scattering analysis for fish schools

Let us assume again monostatic geometry of hydroacoustic system for backscattering measurement and uniform distribution of fish in the layer $\Delta r = r_2 - r_1$ with a density ρ_0 large enough to achieve echoes from multiple targets. Let us assume also that the echo sounder is calibrated acoustically so that its source level SL and receiver sensitivity RS is known. The intensity of echo acquired from fish targets

included in elementary volume $dV = r^2 c\tau/2 d\Omega$ in the range r from the transducer can be expressed as:

$$dI_{bs} = I_1 r_1^2 \frac{10^{-0.2\alpha r}}{r^4} b^2(\theta,\varphi) s_V r^2 \frac{c\tau}{2r_1} d\Omega \tag{3.19}$$

where $I_1 = 10^{0.1SL}$ is on-axis intensity of transmitting signal observed in the reference distance $r_1 = 1$ m, $10^{-0.2\alpha r}/r^4$ is a two-way transmission loss due to spreading of spherical wave and attenuation, $b^2(\theta,\varphi)$ is intensity domain transmit-receive directivity pattern of the echo sounder's transducer, $d\Omega = \sin\varphi d\theta d\varphi$ is the elementary solid angle, τ is the sounding pulse length, $c$is sound velocity in the sea water and s_V is the volume backscattering coefficient.

Total echo intensity received from hypothetical fish layer with a thickness equal to spatial pulse length $c\tau/2$ and reverberation volume equal to $V = r^2 \Psi c\tau/2$ are obtained by the integration of elementary intensity and results in:

$$I_{bs} = \int_V dI_{bs} = I_1 r_1^2 \frac{10^{-0.2\alpha\tau}}{r^2} \Psi(\theta_r) \frac{c\tau}{2r_1} s_V \tag{3.20}$$

where $\Psi(\theta_r) = \int_0^{2\pi} \int_0^{\theta_r} b^2(\theta,\varphi) \sin\theta d\theta d\varphi$ is integrated beam pattern function replacing beam pattern function $b^2(\theta,\varphi)$ for multiple targets [151].

The voltage squared of echo envelope e^2 observed on the echo sounder output is:

$$e^2 = s_x^2 I_1 r_1^2 \frac{10^{-0.2\alpha\tau}}{r^2} \Psi(\theta_r) \frac{c\tau}{2r_1} s_v \tag{3.21}$$

where $s_x = 10^{0.05RS}$ is receiver sensitivity of transducer expressed in V/μPa.

Integrated beam pattern $\Psi(\theta_r)$ can be calculated for any transducer aperture and treated as a constant value Ψ , often called an equivalent beam width for volume reverberation [164] or equivalent solid angle of transducer [162]. Thus all variables except s_V, are constants, which makes the relation between e^2 and $s_V$proportional for every reverberation volume $V = r^2 \Psi c\tau/2r_1$ [164]. Proportionality factor k_V equal to:

$$k_V = I_1 s_x^2 \Psi \frac{c\tau}{2r_1} \tag{3.22}$$

is called echo sounder constant for volume reverberation. In logarithmic domain the echo level obtained on the output of echo sounder E[164]:

$$EL = SL + RS + S_V - 2TL_V + 10\log\Psi + 10\log\frac{c\tau}{2r_1} \tag{3.23}$$

where $EL = 20\log(e/e_1)$ is an echo level referenced to $e_1 = 1$ V, the two-way transmission loss for volume reverberation is expressed as $2TL_V = 20\log(r/r_1) + 2\alpha r$ and $S_V = 10\log s_V$ is the volume backscattering strength [dB]. The logarithmic constant K_V is defined by:

$$K_V = 10\log k_V = SL + RS + 10\log\Psi + 10\log\frac{c\tau}{2r_1} \tag{3.24}$$

which is actually different from the echo sounder constant $SL + RS$ by $10\log\Psi c\tau/2r_1$.

Volume backscattering strength S_V – similarly to echo level EL – has a sense of random variable. In fishery acoustics practical meaning has its mean values or rather the mean value of its absolute equivalent s_v in the sounding layer $\Delta r = r_2 - r_1$ and after certain number of pings m. Averaging is done by echo integration expressed here in a discrete version:

$$\langle e^2 \rangle_{\Delta r} = \sum_{i=1}^{n} \sum_{j=1}^{m} e_{i,j}^2 \tag{3.25}$$

where n is a number of samples, e^2 is voltage integrated in the depth interval Δr and m is a number of transmissions in which the integration was performed [151].

The mean value of volume backscattering strength is related to the mean value of spatial fish density by the following formulae [164]:

$$\bar{s}_V = \bar{n}_V \bar{\sigma}_{bs} \tag{3.26}$$

where $\bar{n}_V = \rho_V$ is a mean number of fish in unit volume and $\bar{\sigma}_{bs}$ is a fish mean backscattering cross section.

As the mean value of backscattering volume coefficient s_v is proportional to equivalent fish density so it can be treated as its relative estimate. Moreover, if the value of mean backscattering cross section σ_{bs} is known the output of echo integration is proportional to the mean fish density in the sounding volume V:

$$\langle e^2 \rangle_{\Delta r} \equiv \overline{e^2} = k_V \bar{\sigma}_{bs} \bar{n}_V \tag{3.27}$$

and can be treated as the absolute acoustic estimates of mean density $\rho_0$of fish population. Hence, the crucial problem of fishery acoustics is estimation of fish backscattering cross section or its logarithmic equivalent target strength.

3.2. Overview of fish target strength estimation methods

Fish target strength estimation methods can be classified into three principal groups [87]: (1) theoretical methods, (2) *ex situ* measurements of dead or alive fish under controlled conditions and (3) *in situ* measurements of free swimming fish in their natural habitat. Due to many facts explained in the following section, theoretical methods and *ex situ* methods have been practically push out by *in situ* methods, which as it is thought, are the only reliable methods for the estimation of fish population.

3.2.1. Ex situ fish target strength estimation methods

To avoid the greatest hazard of in situ measurements, which is not knowing precisely what the target is, *ex situ* techniques have been developed and pursued since the beginning of the fish target strength studies [19]. They can be split in two separate categories, namely tethered fish measurements and caged fish measurements.

By tethering, anesthetized and sometimes swimming fish are suspended in the known position of the transducer beam. Since beam value b is known, measurement of echo amplitude e allows backscattering cross section σ_{bs} to be determined immediately from sonar equation [164]. A significant aim of these has been description of the orientation dependence of target strength. Combination of such measurements with information on orientation may specify the effective cross section or target strength for application to fish in the wild [109]. The examples of such experiments can be found in [92].

Measurement of swimming fish confined to a cage has been a popular method of determining target strength. This may depend on the spatial distribution of fish in the cage if the transducer beam is narrow, but the echo integration method can be applied in any case. The caged fish experiments are described in many papers. The examples of extensive experiments could be found in [23] and literature review in [37].

The results of single fish target strength measurements in controlled conditions, [87] and its indirect estimation using echo integration [151] and also the results of theoretical calculations using different approaches, have shown that TS estimates obtained from theoretical and *ex situ* methods are not reliable and in most cases are not in agreement with those obtained in *in situ* methods. It seems that the reason for this lies in the fact that the value of fish target strength depends on the number of parameters such as vertical migration, body orientation, fish behavior and acquisition time-spatial context. In particular, due to fish vertical migration, the most important role is played by the dynamics of TS changes. As it is known, most of pelagic fishes keep its swimming state adapting pressure in the swimbladder to actual depth. As a result, a fish removed from its natural environment (catched) and put again into the water for controlled measurements, must adapt to new conditions. The changes of fish TS related to the adaptation process may reach up to $2-4$ dB, which means 50% of uncertainty in the estimates obtained *ex situ*, as it very rarely is able to reconstruct its acoustic reflecting properties after new insertion in a water. Transforming those changes into estimation of fish population biomass results in the error on a level of 50%, which is obviously hard to accept. Moreover, the caged fishes have usually different tilt angle than free swimming ones, and additionally they are acoustically observed nearly on the same depth, what may change its target strength up to $2-$ 3dB in relation to its natural conditions.

3.2.2. In situ fish target strength estimation methods

The intensity of echo received from single target located at (r,θ,φ) could be expressed as [89]:

$$I_{bs} = k_x \frac{10^{-0.2\alpha\, r}}{r^4} b^2(\theta\,,\varphi)\sigma_{bs} \tag{3.28}$$

where k_x is a system constant, $10^{-0.2\alpha r}/r^4$ is a two-way transmission loss and $b^2(\theta,\phi)$ is a transmit-receive transducer's beam pattern function. Eq. (3.28) could be expressed equivalently in logarithmic domain as an echo level EL on an echo sounder output:

$$EL = SL + RS + TS - 2TL + B \tag{3.29}$$

where $B = 10\log b^2$ is the value of a logarithmic two-way beam pattern function and $2TL = 40\log(r/r_1) + 2\alpha r$ is a two-way transmission loss. The logarithmic system constant is defined by:

$$K_x = 10 \log k_x = SL + RS \tag{3.30}$$

As it may be observed, to estimate σ_{bs} or *TS,* from received echoes it is required to know system constant, transmission loss and the values of beam pattern function B for each target. Two first components are deterministic. The first one is determined during acoustic calibration of the system (measurement of K_x). The second one is compensated by time-varied gain correction $40\log r/r_1 + 2\alpha r$ [164]. The validity of this correction, especially in short distances, is discussed in [79] and [107]. The third component related to unknown angular fish location in the beam – and equal to the value $B(\theta,\varphi)$ in fish direction (θ,φ) – is random and far more difficult in elimination. The removal of the effect, or more precisely beam pattern compensation, could be achieved directly by appropriate calculations for every single target, or indirectly by processing done on the set of echoes from many fish. These two approaches to elimination of beam pattern influence represent two categories in *in situ* target strength estimation methods.

Direct *TS* estimation methods are in general more complex and expensive than indirect methods, as they require special beam configuration and multichannel receiver [151].

Indirect methods could use the same single-beam echo sounder, which is used in routine acoustic surveys aimed for echo integration, but they require the knowledge of beam pattern function of the echosunder, and they typically assume *implicite* uniform distribution of fish in a water column, what may not always be fulfilled.

3.3. Direct fish target strength estimation methods

There are three methods classified as direct *in situ* estimation methods, in which the effect of random fish position in the beam is removed for a single echo, namely: dual beam method, split beam method and quasi-ideal beam method. The methods differ in the technique of extracting the information used for removal of beam pattern effect. In the first and third case, they use amplitude information, and in second case, the phase information is used. All three methods require special beam configuration and sufficient processing power for calculations.

The common requirement for all methods presented here is the need for extraction of echoes from individual fish as overlapping echoes introduce errors in estimates. The extraction is performed using several conditions like (1) echo amplitude should be much larger then detection threshold to eliminate effects of noise and reverberations, (2) time duration of echo signal should be not longer than $1.5 - 1.8$ of sounding pulse duration τ and not shorter than 0.8τ, and additionally (3) correlation coefficient between the shape of sounding pulse and the received echo should be larger than certain value set up during processing.

As only the first two methods were implemented as commercially sold systems, they will be presented in the following sections. However, there are new concepts in fisheries acoustics related to application of multibeam sonar systems [52, 53, 141], Doppler sonar systems [159], broadband measurement systems [125] and broadband echo sounders [137]. They are still at an early stage.

3.3.1. Dual-beam method

Dual beam method was introduced by John Ehrenberg [26], and then developed by other researchers [161] before being finally commercialized by an American company Biosonics Inc. in its system based on digital signal processing technology. It was named ESP as an acronym for echo signal processor. The method uses the transducer with two beams, narrow and wide positioned concentrically. The sounding signal is transmitted only by narrow transducer, and the echoes are received simultaneously by both channels. Hence, due to unambiguous dependence of both beam patterns on common angle θ, the measurement of voltage squared amplitudes, enables: estimating the angle, from which the echo signal is acquired, and estimating fish backscattering cross section $\sigma_{bs.}$

Let us assume, that the fish with an unknown backscattering cross section σ_{bs} is located in a distance r from the transducer's beam in direction (θ_i,ϕ_i). According to Eq. (3.28) and assuming time varied gain compensation we have expressions for squares of echo amplitudes on the channel outputs as follows:

$$e_n^2 = k_n b_n^2(\theta_i, \varphi_i)\sigma_{bs} \tag{3.31}$$

and

$$e_w^2 = k_w b_n(\theta_i, \varphi_i) b_w(\theta_i, \varphi_i)\sigma_{bs} \tag{3.32}$$

where $e_{n,w}$ are time-varied gain corrected echo amplitudes, $k_{n,w} = 10^{0.1(SL+RS_{n,w})}$ are echo sounder constants in narrow and wide channel σ_{bs} is backscattering cross section, $b(\theta_i,\phi_i)$ is the value of beam pattern for angles θ_i,φ_i and indices n i w refers to narrow and wide beam. In the first of the above equations, it was assumed that the transmitter and receiver beam pattern functions are equal.

In the first early method [26], it was assumed that the wide beam pattern does not change significantly in a working range of narrow beam ($b_w = 1$). Therefore, the approximate relation for backscattering cross section is expressed as:

$$\sigma_{bs} \cong \frac{e_w^4 k_n}{e_n^2 k_w^2} \tag{3.33}$$

However, the results obtained by using this approximation, have shown that the error coming from omitting the decrease of wide beam pattern (which increases as square of distance from the axis) might be quite large. This error could be removed by adding correction factor:

$$\sigma_{bs} = \frac{e_w^4 k_n}{e_n^2 k_w^2} k_d(\theta) \tag{3.34}$$

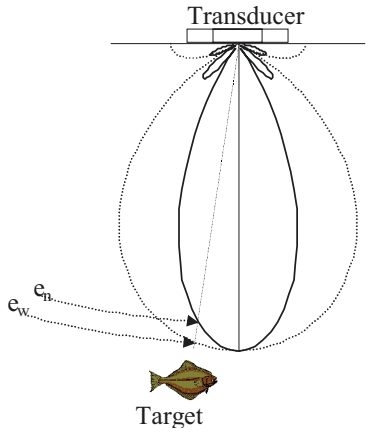

Fig. 3.1. The principle of dual beam technique

where $k_d(\theta) = 1/b_w^2(\theta)$is wide beam drop-off function.

Actually, as the term fish target strength TS is more often used in acoustic monitoring of fish abundance, then the term back scattering cross section σ_{bs}, the dual-beam algorithm is often presented in logarithmic domain [151]:

$$E_n = TS + 2B_n + K_n \tag{3.35}$$

$$E_w = TS + B_n + B_w + K_w \tag{3.36}$$

with the solution:

$$TS = 2E_w - E_n + K_{n,w} + K_d \tag{3.37}$$

where $E_n = 20\log e_n/e_1$ is voltage level in narrow beam channel, $E_w = 20\log e_w/e_1$ is voltage level in a wide beam channel, $K_{n,w} = K_n - 2K_w = 10\log\left(k_n/k_w^2\right)$is dual-beam echo sounder constant, $K_d = -2B_w$ is logarithmic drop-off function of wide beam $B_w = 10\log b_w(\theta)$.

It appears that in logarithmic domain by introducing relative coefficient defined as:

$$K_D = \frac{B_n}{B_n - B_w} \tag{3.38}$$

the solution of Eq. (3.35) and Eq. (3.36) may be expressed as follows:

$$TS = E_n - K_n + 2K_D\left[(E_w - E_n) - (K_w - K_n)\right] \tag{3.39}$$

This equation is particularly useful as K_D has approximately constant value for transducers used in dual beam systems and therefore it may be called dual beam drop-off constant. To evaluate the value of K_D for circular transducers let us use

exponential approximation of beam pattern function for circular piston valid for small values of Bessel function arguments:

$$b_{n,w}(\theta) = \left[\frac{2J_1(x_{n,w})}{x_{n,w}}\right]^2 \approx e^{-\frac{1}{4}x_{n,w}(\theta)^2} \tag{3.40}$$

where $x_{n,w} = \pi(d_{n,w}/\lambda)\sin(\theta)$ and d_n, d_w are diameters of transducers. Now, using the definition of dual beam drop-off constant (Eq. 38) we have:

$$K_D = \frac{10\log b_n}{10\log b_n - 10\log b_w} = \frac{\left(\frac{d_n}{\lambda}\right)^2}{\left(\frac{d_n}{\lambda}\right)^2 - \left(\frac{d_w}{\lambda}\right)^2} \tag{3.41}$$

and using approximation for 3 dB angle for circular transducer $d/\lambda = 30/\theta_{3dB}$ we have eventually:

$$K_D = \frac{\theta_{3dB,w}^2}{\theta_{3dB,w}^2 - \theta_{3dB,n}^2} \tag{3.42}$$

As an example let us check the value of K_D for dual-beam systems having circular transducers with 3 dB angles 6° and 14°. Inserting these values into Eq. (3.42) gives $K_D = 14^2/(14^2-6^2) = 1.225$. For wider beam the K_D is obviously smaller i.e. 6°/15° system has $K_D = 1.19$.

Dual beam method in its basic version has some limitation due to bias observed in target strength estimates. The bias is introduced, as the detection conditions for targets located off-axis are worse than for the same sized targets located on-axis. Consequently, acquired off-axis echoes originate only from a larger fish [161]. In modified version of dual-beam method the bias is compensated by the control of sounding volume. Introduced angular threshold $\theta_{\max}$ restricts the detection echoes to such angles in which most of the fish from those directions are detectable. The threshold is defined by the ratio of amplitudes squared in both channels equal to the ratio of the values of its beam patterns [153]:

$$\frac{e_n^2}{e_w^2} = \frac{b_n(\theta)}{b_w(\theta)}_{\theta=\theta_{\max}} \tag{3.43}$$

However, although the bias in σ_{bs} estimates is reduced, it results in reduction of sampling volume, which reduces also the number of received echoes. Thus the number of samples in the set is reduced increasing the variance of estimates. So, the method should be used very carefully to ensure minimum of root-mean-square error [151]. As it was shown by simulation [161] the optimal threshold is obtained by setting angular threshold $\theta_{\max}$ equal to 3 dB beam angle θ_{3dB}.

3.3.2. Split-beam method

Split beam method has been worked out and commercialized by Norwegian company Simrad in the EY series of echo sounders. The method makes use of special configuration of echo sounder's transducer. Its elements are split electronically into four quadrants, which in transmitting mode work in parallel in full beam regime with

the same amplitude and phase [87]. The receiver part contains four channels, which in receiving mode acquires the echoes from single targets by every quadrant separately. At each of the four transducer elements (i = 1,2,3,4) the reflected pressure waveform $p_{bs,i}(t)$ can be expressed as:

$$p_{bs,i}(t) = r_1^2 \frac{10^{-0.1\alpha(r+r_i)}}{r r_i} \frac{l_{bs}}{r_1} p_1\left(t - (r+r_i)/c\right) e^{-j(\omega t - k(r+r_i))} \tag{3.44}$$

where $p_1(t)$ is transmitted pressure observed at 1m from transducer, r is the range from the transducer origin when transmitting to the target and r_i are ranges from transducer quadrants to the target.

The calculation makes use of the electronic phases $k(r+r_i)$ or more precisely phase differences between two alongship halves $\Delta\phi_1$ and two athwordship halves $\Delta\phi_2$. These phase differences reflect the time of arrival differences due to path differences $a_{1,2}$ ($\Delta\phi_{1,2} = ka_{1,2}$) for along and across directions which represent split beam coordinates. When the differences are within one wavelength λ than without ambiguity:

$$\frac{a_{1,2}}{\lambda} = \frac{\Delta\phi_{1,2}}{2\pi} \tag{3.45}$$

When the effective separation $d_{1,2}$ between the two transducer halves are known, then, due to formal relation $a_{1,2} = d_{1,2}\sin\varphi_{1,2}$ for plane wave it allows us to make calculation of split beam angles as:

$$\alpha_{1,2} = \arcsin\left(\frac{\lambda}{2\pi d_{1,2}}\Delta\phi_{1,2}\right). \tag{3.46}$$

The distance $d_{1,2}$ between halves are often given by the manufactures in the form of the so called phase aperture α_{ap} calculated for operated frequency as:

$$\sin\alpha_{ap} = \frac{\lambda/2}{d_{1,2}} \tag{3.47}$$

Using small angles approximation the split beam angles can be calculated then as:

$$\alpha_{1,2} \approx \alpha_{ap}\frac{\Delta\phi_{1,2}}{\pi} \tag{3.48}$$

Thus, the mechanical angles $\alpha_{1,2}$ are proportional to electronically obtained and normalized phase differences and are in the range not larger than phase aperture.

The target location in the beam in spherical coordinates are obtained immediately by coordinate transformation [42]:

$$\theta = \arccos(1 + \tan^2\alpha_1 + \tan^2\alpha_2)^{-1/2} \tag{3.49}$$

$$\varphi = \arctan(\tan a_1/\tan\alpha_2) \tag{3.50}$$

The split beam method gives all the three coordinates (r,θ,φ) of an individual animal, provided that it is separated from other scatterers by a radial distance greater than the range resolution $c\tau/2$ [87] and the echo exceeds the detection threshold.

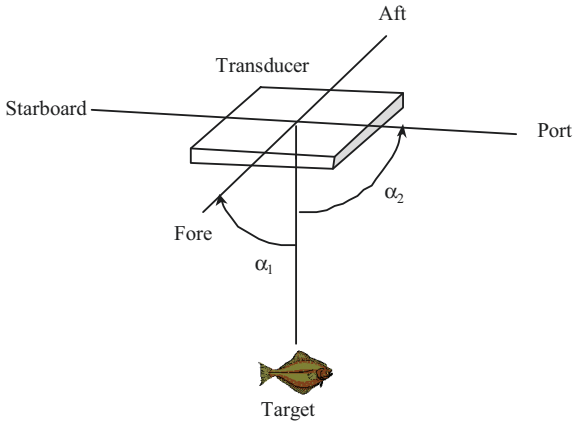

Fig. 3.2. The principle of split beam technique

From both angles the value of beam pattern $b^2(\theta,\varphi)$ can be calculated and used for compensation of each target echo to obtain compensated target strength values:

$$TS = TS_U - B\left(\theta(\alpha_1,\alpha_2),\varphi(\alpha_1,\alpha_2)\right) \tag{3.51}$$

where TS_U is called in fishery acoustics jargon uncompensated target strength, which in fact is the acquired voltage divided by system constant and expressed in logarithmic form. This name reflects unknown location of the target in the transducer's beam as it would be its target strength if the target has been located on-axis of transducer.

The split beam method seems to be better suited for fishery research as its estimates is thought to give less error [161] than dual beam estimates. Additionally, due to absolute target localization in the three-dimensional space, it makes fish tracking algorithm far more feasible [112].

3.4. Indirect target strength estimation methods

The main advantage of indirect estimation methods is its low hardware requirements as the data obtained from classical single beam echo sounder can be used for that purpose. However, they require far greater computational power as data processing is done for many echoes, statistically. Additionally, it is often necessary to assume distribution of fish in a sampling volume and the method uses beam pattern of transducer in a non-deterministic way, which is unique in underwater acoustics.

The indirect methods can be divided into two groups: parametric and nonparametric. The former estimates some parameters of assumed probability distribution function (PDF), the latter tries to estimate the whole PDF.

The parametric methods were introduced by Petersen and Clay [121], who used Rayleigh distribution for backscattering length PDF estimate. The proposed technique matches unknown parameters of assumed distribution as long as theoretically obtained echo PDF agrees with the measured echo histogram. The parametric ap-

proach represents forward technique of solving the estimation problem, whereas non-parametric one can be solved by inverse techniques and it will be presented in detail.

Historically, different methods were used to achieve the goal. In the following sections three most important approaches as applied to fish data are presented followed by modern formulation as introduced in [154].

3.4.1. Craig-Forbes method

The statistical method for elimination of influence of beam pattern introduced by Craig and Forbes [18] was thought as a pioneer method in the fishery acoustics at that moment. It transforms the histogram of the echo level measured on the output of the echo sounder into histogram of target strength using histogram of a beam pattern as shown in Fig. 3.1. Histogram of beam pattern is obtained from beam pattern function by a division into finite number of layers in three-dimensional space (cross sections) defined by the same value of this function. For discrete values obtained from histograms it result in a set of linear equations:

$$\begin{aligned} n_0 &= A_0 N_0 \\ n_1 &= A_0 N_1 + A_1 N_0 \\ n_2 &= A_0 N_2 + A_1 N_1 + A_2 N_0 \\ &\dots \quad \dots\dots\dots\dots\dots\dots\dots\dots \\ n_{k-1} &= A_0 N_{k-1} + A_1 N_{k-2} + \dots + A_{k-1} N_0 \end{aligned} \tag{3.52}$$

where n_i is the number of echoes in i^{th} level, N_i is the number of fish of i^{th} class and A_i is the surface of i^{th} beam cross section. It can be interpreted as an assumption that the highest echo levels n_0 are acquired from the large fish N_0 located on-axis A_0. The next echo level n_1 come from the slightly smaller group of fish N_1 located on-axis A_0 and from large fish N_0 located slightly off-axis A_1, etc. The solution can be achieved iteratively by back substitution:

$$\begin{aligned} N_0 &= n_0/A_0 \\ N_1 &= (n_1 - A_1 N_0)/A_0 \\ &\vdots \\ N_{k-1} &= (n_{k-1} - \sum_{i=0}^{k-2} A_{k-1-i} N_i)/A_0 \end{aligned} \tag{3.53}$$

This way of solution is similar to polynomial division and leads to large cumulative errors. In a matrix notation it can be written as $\mathbf{n} = \mathbf{A}\,\mathbf{N}$:

$$\begin{bmatrix} n_0 \\ n_1 \\ n_2 \\ \vdots \\ n_{k-1} \end{bmatrix} = \begin{bmatrix} A_0 & 0 & 0 & \cdots & 0 \\ A_1 & A_0 & 0 & \cdots & 0 \\ A_2 & A_1 & A_0 & \cdots & 0 \\ \vdots & \vdots & \vdots & \ddots & 0 \\ A_{k-1} & A_{k-2} & A_{k-3} & \cdots & A_0 \end{bmatrix} \begin{bmatrix} N_0 \\ N_1 \\ N_2 \\ \vdots \\ N_{k-1} \end{bmatrix} \tag{3.54}$$

where $\mathbf{A}$ is left-lower triangular matrix and can be solved by matrix inversion:

$$\mathbf{N} = \mathbf{A}^{-1}\mathbf{n} \tag{3.55}$$

The solution obtained by inverse operation performed on a matrix $\mathbf{A}$ are practically non reliable and not stable [124] as the inverse matrix $\mathbf{A}^{-1}$ very often does not exist.

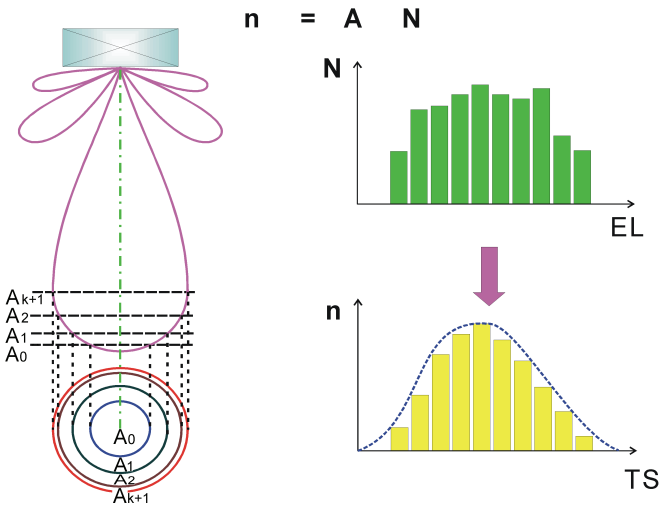

Fig. 3.3. The illustration of Craig and Forbes method

3.4.2. Ehrenberg method

Ehrenberg [26] proposed an alternative approach by solution of integral equation for echo intensity. In his method it was assumed that the echo intensity $I$from the fish is a result of two random variables $\underline{A}$ and $\underline{B}$, where $\underline{A} = k_x\sigma_{bs}$ and $\underline{B} = b^2(\theta,\varphi)$. It allows us to solve integral equation as Volterra equation with unknown PDF of $p_A(a)$ of random variable $\underline{A}$:

$$p_I(i) = C \int_0^{A_{MAX}} \frac{1}{a} p_A(a) p_B\left(\frac{i}{a}\right) da, \quad i \geq A_T \tag{3.56}$$

where C is normalization constant dependant on amplitude threshold A_T. The estimate $\hat{p}_A(a)$ is obtained by numerical solution using polynomial approximation of the unknown function $p_A(a)$:

$$p_A(a) = \frac{1}{C} \sum_{j=1}^{n} \alpha_j a^j \tag{3.57}$$

where polynomial coefficients α_j are calculated by the least square method from following equation:

$$\hat{p}_I(i) = \sum_{j=0} \alpha_j \int_o^{A_{MAX}} a^{j-1} p_B\left(\frac{i}{a}\right) da \tag{3.58}$$

The weak point of the method is still its ill-conditioning for higher polynomial degrees.

Robinson [127] modified Ehrenberg's method by division of estimate range on intervals and then performing approximation by the use of polynomials of the third degree, with a condition of equality of estimated function and its first derivative on interval borders. All coefficients are calculated using the same least square error approach, which nevertheless is the problem, as the determinants in equations for actual data appeared to be very small.

3.4.3. Deconvolution method

Clay [14] as a first formulated Craig and Forbes method in deconvolution terminology. Using substitution of variables $E = Ce^{-y}$ and $B = e^{-x}$ he transformed Fredholm integral into convolution integral:

$$p_E(E) = \int_{-\infty}^{\infty} p_B(E - TS) p_{TS}(TS) dTS \tag{3.59}$$

where p_E is PDF of echo level, p_B is PDF of beam pattern and p_{TS} is PDF of target strength. He performed numerical deconvolution by applying Z-transform [123] what is in fact equivalent to a division of polynomials. The method resulted in large errors especially for multimodal distributions and small echo amplitudes [89].

The Clay's method along with the Rice distribution matched *a'posteriori* to backscattering length PDF, has been used also by Rudstam [130] for fish density and size estimation. However, he obtained artifacts, as many modes of PDF function can't be treated as many groups of fish.

3.4.4. Single beam integral equation formulation

All nonparametric methods assumes that acquired echoes from fish can be treated as stochastic process and echo intensity and pressure can be written as product of random variables:

$$\underline{I}_{bs} = k_x \frac{10^{-0.2ar}}{r^4} \underline{b}^2 \frac{\underline{\sigma}_{bs}}{r_1^2} \tag{3.60}$$

$$\underline{p}_{bs} = \sqrt{k_x Z_0} \frac{10^{-0.1ar}}{r^2} \underline{b} \frac{\underline{l}_{bs}}{r_1} \tag{3.61}$$

The echo amplitude can be written formally assuming $p_{bs} = (k_x Z_0)^{1/2}(10^{-0.1\alpha r}/r^2)/r_1 e$ as a pure product of two random variables:

$$\underline{e} = \underline{l}_{bs} \underline{b} \tag{3.62}$$

where e has a sense of normalized echo amplitude. Normalization means here the removal of range and source sound pressure dependaces [121].

Hence, the estimation of mean value of backscattering length or even its PDF requires the knowledge of beam pattern PDF.

As it is known [120], the PDF of the product of random variables $\underline{z} = \underline{x}\,\underline{y}$ can be calculated from equation:

$$p_z(z) = \int_{-\infty}^{\infty} p_y(z/x)p_x(x)dx/x \tag{3.63}$$

which for unknown PDF $p_x(x)$ has a sense of solution of Fredholm integral equation and is called Mellin convolution integral [123]. Using introduced notation for echo amplitude it can be written as:

$$p_e(z) = \int_{0}^{\infty} p_b(z/x)p_{l_{bs}}(x)dx/x \tag{3.64}$$

where integration interval is limited to positive values of backscattering cross section. In the fishery acoustics, Eq. (3.64) is known as the single beam integral equation [62, 154]. Note also that when operated on squares of these variables ($\underline{e}^2 = \underline{b}^2\underline{\sigma}_{bs}$) we obtain equivalent formulae in intensity domain:

$$p_{e^2}(z) = \int_{0}^{\infty} p_{b^2}(z/x)p_{\sigma_{bs}}(x)dx/x \tag{3.65}$$

Moreover, using logarithmic variables Eq. (3.62) can be expressed as a sum of random variables:

$$\underline{E} = \underline{B} + \underline{TS} \tag{3.66}$$

where $E = 20\log e$ is random variable representing echo level in [dB] and $B = 20\log b$ is random variable representing logarithmic beam pattern function expressed also in [dB].

The PDF of a sum of the two independent random variables $\underline{z} = \underline{x} + \underline{y}$ is a convolution of PDF's components [120]:

$$p_z(z) = \int_{-\infty}^{\infty} p_x(x)p_y(z-x)dx \tag{3.67}$$

and using acoustic variables from logarithmic domain $\underline{E}$, $\underline{B}$ and $\underline{TS}$, it results in equivalent integral:

$$p_E(z) = \int_{-\infty}^{\infty} p_B(z-x)p_{TS}(x)dx \tag{3.68}$$

The solution of presented integral equations leads to estimate of PDF functions $p_{l_{bs}}(l_{bs})$, $p_{\sigma_{bs}}(\sigma_{bs})$ or $p_{TS}(TS)$. In the equations the kernel of integral is represented by beam pattern PDF and its knowledge is required for estimation of the unknown PDFs. The modern methods using inverse techniques as applied to fish data are the subject of the next chapter.

Chapter 4

INVERSE TECHNIQUES APPLIED TO FISH TARGET STRENGTH ESTIMATION

Inverse techniques have found their application in many fields of science, physics in particular [54], and especially in those related to different aspects of tomography. In underwater acoustics, they are mainly used in ocean acoustical tomography, where the speed of sound along ray paths is reconstructed from the pattern of sound pressure time of arrivals [157].

It was shown in previous chapter that the problem of reconstructing the distribution of fish target strength from observed echo amplitude distribution leads to different kinds of integral equations. The solution of integral equation represents the problem often encountered in mathematical physics. Generally, there are two types of integral equations, namely Fredholm integral equations and Volterra integral equations.

The Fredholm integral equations introduced by Ivar Fredholm, are more general one, and give rise to a Fredholm operator [64]. From the point of view of functional analysis, it therefore has a well-understood abstract eigenvalue theory. In this case, that is supported by a computational theory, including the Fredholm determinants. An inhomogeneous Fredholm equation of the first kind is written:

$$z(t) = \int_a^b K(x,t)f(x)dx \tag{4.1}$$

and the problem is, given the continuous kernel function $K(t,s)$, and the function $z(t)$, to find the function $f(x)$. An inhomogeneous Fredholm equation of the second kind is essentially a form of the eigenvalue problem for the above equation:

$$z(t) = \lambda \int_a^b K(x,t)f(x)dx + f(t) \tag{4.2}$$

The kernel K is a compact operator to show that it relies on equicontinuity. It therefore has a spectral theory that can be understood in terms of a discrete spectrum of eigenvalues that tend to zero [122].

Fredholm equations are based on definite integrals. If the integration limits are variable, then the corresponding integral equations are Volterra equations [165]. An inhomogeneous Volterra equation of the second kind, corresponding to Eq. (4.2), has the form:

$$z(t) = \lambda \int_a^x K(x,t)f(x)dx + f(t) \tag{4.3}$$

If $z(t)$ =0, then one has a homogeneous Volterra equation of the second kind. By contrast, a Volterra equation of the first kind has the form:

$$z(t) = \int_a^x K(x,t)f(x)dx \tag{4.4}$$

where $z(t)$ is known and $f(x)$ is the unknown function. A Volterra integral equation may be viewed as a Fredholm equation whose kernel vanishes for $x < b$. Thus letting $M(x,t) = 0$ for $x < b$ and $M(x,t) = K(x,t)$ for $x > b$ one finds that the Volterra equation becomes a Fredholm equation. If the unknown function $f(x)$ appears in the equations as linear function (without powers) then the integral equation is called linear integral equation.

For certain kinds of integral equations, there are exact methods of solution. They will be demonstrated briefly in the first section. However, it is well known that in most of the cases encountered in physics, the problem is ill-conditioned due to the form of the kernel operator and noisy observation, and the solutions obtained by applying exact approach are not practically reliable.

The recently developed direct and iterative inverse techniques as a way of solving integral equations have been applied as novel indirect methods of fish target strength estimation. Although these methods are more complex than conventional techniques, but by this cost they partly avoid the problems of ill-conditioned equations and related problems with a matrix inversion. For instance, to avoid ill conditioning a Singular Value Decomposition (SVD) method replaces inverse matrix by pseudoinverse, which eigenvalues, if too small, are replaced by zeroes. In addition, some of these methods, viz. a subclass of iterative techniques (EMS and MER) allow avoiding negative-valued solutions of a discrete form of an integral equation by superimposing proper constraints on solutions obtained by iterations. The most promising among these methods, which are subject of further analysis are Tikhonov and Maximum Entropy Regularization (MER), Windowed Singular Value Decomposition (WSVD), Wavelet Decomposition introduced to target strength estimation by Stepnowski and Moszyñski [154] and finally Expectation Maximization and Smoothing (EMS) method.

4.1. Exact solutions of integral equations

Integral equations may be solved directly only if they are separable. An integral kernel is said to be separable if

$$K(x,t) = \lambda \sum_{i=0}^{N} M_i(x)N_i(t) \tag{4.5}$$

This condition is satisfied by all polynomials; hence, the approximation of the kernel by a polynomial can lead to a fast solution.

In general, there are three well established in mathematics ways of indirect solutions of integral equations. First approach, transformation to equivalent differential equation, works well only for certain type of Volterra equations of the first kind. The differential equation can be obtained by differentiation with respect to upper limit x of integral Eq. (4.4).

The second method represents the form of iterative approach introduced by Picard in the solutions of differential equations. One of the methods in this group is based on the series expansion of Neumann type, for which the solution of integral equation can be expressed as:

$$f(x) = \lambda \int_a^b \Gamma(x,t,\lambda) z(t) dt + z(x) \tag{4.6}$$

where $\Gamma(x,t,\lambda) = \sum_{i=0}^{\infty} \lambda^i K_{i+1}(x,y,\lambda)$ is called resolvent of the integral equation kernel K and $K_n(x,t) = \int_a^b K(x,\tau) K_{n-1}(\tau,t) d\tau$ with $K_1(x,t) = K(x,t)$ is iterative kernel. The series converges to the exact solution, but practically very slowly.

The third method is based on the integral transforms theory, and is applicable only if the form of the integral equation kernel has its equivalent forward and inverse transform. In particular when the kernel is symmetrical $K(x,t) = K(t,x)$ the Hilbert-Schmidt orthogonalization process allows expressing the unknown function as an infinite series of orthogonal functions, which actually defines the transform. Then, the integral equation can be solved in transform domain algebraically and the solution is obtained by applying inverse transform to that solution. For example for difference kernel $K(x,t) = K(x-t)$, which constitutes convolution kernel, well-known Laplace transform (i.e. [7]) can be used and for division kernel $K(x,t) = K(x/t)/x$ (multiplicative convolution kernel), less-known Mellin transform defined by:

$$M[f;s] \equiv F(s) = \int_0^{\infty} f(t) t^{s-1} dt \tag{4.7}$$

can be adopted [123]. Application of Mellin transform to the problem of solving a single beam integral equation has been demonstrated in [105] along with its interpretation for PDF function as moments of random variable distribution.

4.2. Regularization methods

Linear inverse problems can be treated as a reconstruction of an unknown function $f(.)$ (target strength PDF) out of the observed function $z(.)$ (echo PDF). Thus, the single-beam integral equation can be presented as a linear operator equation:

$$z = K\, f + n \tag{4.8}$$

where K is the linear operator and n represents error or noise. To measure the ill-conditioning of an equation, the condition number defined by [124]:

$$\kappa = cond(K) = \|K\| \ \left\|K^{-1}\right\| \tag{4.9}$$

is used ($||.||$ is a matrix norm). An unstable or badly conditioned system has a large condition number. When using L_2 norm, condition number κ_2 is equal to the ratio of the largest and the smallest singular value of matrix K.

4.2.1. Tichonov regularization

One way to solve this problem is to apply square regularization introduced by Tichonov, Phillips and Twomey [158], according to which the solution estimate can be obtained as:

$$\hat{f}_\lambda = (\mathbf{K}^*\mathbf{K} + \lambda\,\mathbf{I})^{-1}\mathbf{K}^* z \tag{4.10}$$

where $\mathbf{I}$ is the identity matrix, $\mathbf{K}^*$ is a matrix conjugate to $\mathbf{K}$ and λ is a regularization parameter.

Alternatively, one can use iterative back-projection, which does not require matrices to be inverted that for ill-conditioned equations constitutes a major problem. The key issue is an optimal selection of regularization parameters in both methods.

A variation of this method introduces a tri-diagonal matrix as a $\lambda\mathbf{I}$ stabilizer. The advantage of this modification is the possibility of an additional regulation of the solution's behavior in boundary areas. The solution for the considered case is obtained as follows.

Regularization of the convolution integral equation of the first kind in TS domain leads to the integral equation of the second kind. It can be obtained by adding so called regulator to the right hand side of the equation. Tha regulator depends on the parameter λ, the unknown function f_x and its derivative. Introducing a functional that determines the error in space L_2 one should determine $f_x(x)$ by minimizing this functional that leads to Euler's equation.

The solution of this equation can be determined by substituting the integration with discrete summation and obtaining the following equation:

$$\mathbf{K}^*\mathbf{K}\,f_x - \mathbf{K}^* f_z = \lambda\,\mathbf{C}\,f_x \tag{4.11}$$

where K is the matrix of the transformation kernel formed from the convolution vector f_y and $\mathbf{C}$ stabilizer matrix in the form:

$$\begin{bmatrix} c_{11} & c_{12} & & & \mathbf{0} \\ c_{21} & c_{22} & c_{23} & & \\ & c_{32} & \ddots & \ddots & \\ & & \ddots & \ddots & \ddots \\ \mathbf{0} & & & \ddots & c_{nn} \end{bmatrix} \tag{4.12}$$

where coefficients on main diagonal $c_{i,i} = 1 + 2/h^2$ are calculated for $i = 2...n-1$, $c_{1,1} = c_{n,n} = 1+k/h^2$ with $k = 1$ for $f'_x(0) = f'_x(n) = 0$ and $k = 2$ for $f_x(0) = f_x(n)$ and coefficients on first diagonals $c_{i,i-1} = c_{i-1,i} = -1/h^2$ for $i = 2..n$ (h is sampling step). The matrix of stabilizer $\mathbf{C}$ is a tri-diagonal matrix because when computing the derivative the difference version was used which gives such relation between the following, current and previous index in vector f_x. At the same time, boundary conditions define the value of the first and last element on the main diagonal.

The PDF estimate of unknown target strength derived from Eq. (4.11) in explicit form can be written as:

$$\hat{\mathbf{p}}_{TS} = (\mathbf{P}_B^T \mathbf{P}_B + \lambda\ \mathbf{C})^{-1} \mathbf{P}_B^T \mathbf{p}_E \tag{4.13}$$

where $\hat{\mathbf{p}}_{TS}$ is vector of the estimate of target strength PDF, $\mathbf{P}_B$ is matrix of beam pattern PDF, $\mathbf{P}_B^T$ transpose of a matrix $\mathbf{P}_B$,λ is a regularization parameter, $\mathbf{C}$ matrix of regularization stabilizer and $\mathbf{p}_E$ vector of the echo PDF.

4.2.2. Maximum entropy regularization

The alternative regularization method Maximum Entropy Regularization (MER) falls into iterative techniques category. The method is often used in image reconstruction and other related problems where it is required to have only positive estimates. In the method the solution of inverse problem, in which observations are in the form of Eq. (4.8) are obtained by minimalization of the following expression [135]:

$$\|z - \mathbf{K}x\|^2 + \lambda \sum_{i=1}^{n} x_i \log(w_i x_i) \tag{4.14}$$

where x_i is a vector containing positive values and w_i are weighting coefficients. The summation part expresses entropy of x, hence the name of the method. The mathematical justification for the particular choice is that it yields a solution x which is most objective, or maximally uncommitted, with respect to the missing information in the right-hand side of Eq. (4.8)

The Maximum Entropy method obtains the regularized solution iteratively and for faster calculations, the nonlinear conjugate gradient algorithm can be used [139].

4.3. Decomposition methods

Singular value decomposition (SVD) that was introduced in spectral analysis has become a very useful method of solving ill-conditioned linear equations. The method was generalized by the usage of different orthonormal function basis than those, which arise from eigenanalysis of linear function operator. Wavelet-Vaguelette Decomposition method, which utilizes wavelet function basis was successfully applied into the problem as shown in next section.

4.3.1. Singular Value Decomposition method

The basic concept of using SVD to the solution of ill-posed problems is the substitution of a simple operator inversion $\mathbf{K}^{-1}$ by so called "pseudo-inverse" operator $(\mathbf{K}^T\mathbf{K})^{--1}\mathbf{K}^T$ [124]. It leads to obtaining a pseudo-inverse matrix, which guarantees a solution with a minimum mean-square error:

$$\begin{aligned} \mathbf{K} &= \mathbf{U}\mathbf{S}\mathbf{V}^T = [\mathbf{U}]\, diag(s_i)\, \left[\mathbf{V}^T\right] \\ \mathbf{K}^{\#} &= \mathbf{U}\mathbf{S}^{-1}\mathbf{V}^T = [\mathbf{U}]\, diag(1/s_i)\, \left[\mathbf{V}^T\right] \end{aligned} \tag{4.15}$$

where $\mathbf{K}^{\#}$ is a pseudo-inverse matrix computed numerically using the SVD algorithm, $\mathbf{U}, \mathbf{V}$ are orthonormal matrices and $\mathbf{S}$ is a diagonal matrix representing the singular

values of matrix $\mathbf{K}$.

If further assume that the product $K^T K$ is a linear operator, and if none of its singular values is a zero value then the unknown function f can be expanded in a series of the eigenfunctions of the self-adjoint operator $K^T K$ as:

$$f = \sum\nolimits_j \gamma_j^{-1} \left[\mathbf{K}f, h_j\right] e_j \tag{4.16}$$

where γ_j are singular values of $K^T K$, e_j are eigenfunctions of $K^T K$, h_j are normalized transforms defined as $h_j = K(e_j)/||K(e_j)||$, $\|.\|_2$ represents a norm in space L_2 and $[,]$ represents a scalar product.

In the case when singular values of the $K^T K$ operator approximate zero, it is necessary to introduce weights so that dividing by elements close to zero does not impact the stability of the solution. By adequate introduction of the weights, the so-called WSVD (Windowed SVD) is obtained which gives the reconstruction rule:

$$\hat{f}_w^{SVD} = \sum_j w_j \gamma_j^{-1} \left[z, h_j\right] e_j \tag{4.17}$$

where w_j are weights used for regularization of the solution and z are observations.

As an example, the simplest selection of weights is to assume $w_\nu = 1$ for small indexes ν and $w_\nu = 0$ for large ν, which reflects the name assigned to this method. Other approaches are possible as well. If one selects $w_\nu = k_\nu^2/(k_\nu^2 + \lambda)$, then the regularization method of the previous section is obtained in the direct form and when $w_\nu = (1 - (1 - \mu\, k_\nu^2)^m)$we obtain the method of iterative reconstruction ($m-$number of iteration).

By using the form of the Penrose-Moore pseudo-inverse matrix $\mathbf{K}^\#$ as an inverse matrix obtained in the SVD technique, a formula for target strength PDF estimate is obtained:

$$\hat{\mathbf{p}}_{TS} = \mathbf{P}_B^\# \mathbf{p}_E \tag{4.18}$$

4.3.2. Wavelet-Vaguelette Decomposition method

The imperfection of Singular Value Decomposition SVD arises from the fact that the eigenfuntions of linear operators represent *sine* and *cosine* functions (Fourier kernel), which induce oscillations in estimates [1]. In many cases, the better solution is obtained by use of other orthonormal function sets that guarantee better approximation with a smaller numbers of nonzero coefficients. Numerous classes of orthogonal functions represent so-called *wavelets* – functions being dilations and translations of certain function called mother wavelet [163]:

$$\psi_{j,k} = 2^{j/2}\psi(2^j t - k) \qquad j,\ \ k \in N \tag{4.19}$$

Wavelet expansion of Kf can be written as:

$$Kf = \sum_j \sum_k d_{j,k}\psi_{j,k} = \sum_j \sum_k [Kf, \psi_{j,k}]\psi_{j,k} \tag{4.20}$$

where $d_{j,k}$ represents wavelet coefficients.

Then the estimate of function f can be expressed as:

$$\hat{f} = \sum_j \sum_k \delta_\lambda([y, \psi_{j,k}]) K^{-1} \psi_{j,k} \tag{4.21}$$

where $\delta_\lambda(.)$ is a function removing noise effect by nonlinear thresholding, which level λ depends on number of samples and noise variance. The product $[y,\psi_{j,k}]$ has a sense of estimates $\hat{d}_{j,k}$ of coefficients $d_{j,k}$.

For discrete vector f with a length n, its discrete wavelet transform (DWT) could be also represented as a matrix operation:

$$w = W f \tag{4.22}$$

where W is orthogonal matrix of $n \times n$ elements being sampled values of wavelet functions $\psi_{j,k}(t)$ in discrete time moments t/n, t =0,1,...,$n-1$.

Application of a DWT to solving linear operator equation Eq. (4.8) in the context of decomposition Eq. (4.20) leads to calculation of wavelet coefficients as a matrix multiplication:

$$d = \mathbf{W} y \tag{4.23}$$

which after thresholding gives the solution:

$$f = (\mathbf{W} K)^{-1} \hat{d} \tag{4.24}$$

The inverse operator being used on a matrix $\boldsymbol{W}K$represents wavelet modified by operator K. This technique is called Vaguellete-Wavelet Decomposition (VWD), which has also reversed form called Wavelet-Vaguelette Decomposition (WVD).

The VWD technique was implemented in fish target strength PDF estimation from echo level PDF using matrix transforms. The inverse of beam pattern PDF was the kernel K of the operator equation in the considered case. The application of the method was presented in [97], where Symmlet wavelets were used in calculations.

4.4. Expectation Maximization methods

Expectation Maximization Smoothing (EMS) [136] is a modification of the EM method introduced by Dempster [20] as a maximum likelihood extension. The EMS smoothes or filters highly variable estimates from what should otherwise be a smooth result. In addition, the EMS method is useful with this type of problem because it constrains estimates to be positive and reduces the time needed to converge by smoothing groups of estimates per iteration. The method was further improved by the author by using adaptive approach.

4.4.1. Expectation Maximization and Smoothing method

The acoustic problem is discretized in order to deal with integer-valued observations. The EMS methodology a1so requires the expression of the echo voltage

observations in relation to two unobservable sets of discrete data. One of these unobservable sets of data are on-axis voltages. The other set of unobservables is termed the complete data, which is discussed below.

The EMS technique is applied to estimate the scaled PDF of the on-axis voltages, $f_x(x)$ in Eq. (4.8) from which fish backscattering length l_{bs} or backscattering cross-section σ_{bs} is determined. In addition, the method constrains estimates to be positive and reduces the time needed to converge by smoothing groups of estimates per iteration. To apply EMS method the single-beam integral is used as convolution integral in logarithmic domain.

With this logarithmic transformation, the "single beam integral equation" is less ill-conditioned than the Fredholm integral equation in the absolute variable (voltages), and is thus easier to solve. In addition, the convolution equation solution (in the logarithmic domain) involves uniform sampling of the histogram. For optimal solution in the absolute domain, in contrast, a non-uniform sampling is required, which is more difficult to achieve in practice. Furthermore, the logarithmic approach gives the estimates obtained directly as TS values, which are the most commonly used in fisheries practice.

Single beam integral equation can be approximated by the convolution sum to numerically obtain the solution:

$$f_E(j) = \sum_{i=1}^{n} f_{TS}(i)\, f_B(j-i)\, \Delta i \tag{4.25}$$

where the indices i and j correspond to bins in TS and B space respectively. Eq. (4.25) is a linear equation and can be presented in a matrix form:

$$\mathbf{z} = \mathbf{K}\,\mathbf{x} \tag{4.26}$$

where $\mathbf{K}$ is the kernel matrix of equation corresponding to B space, $\mathbf{z}$ is observed data matrix in E space, x is the unknown vector in TS space. Every iteration procedure performed during solution when using EMS method consists of three steps called respectively: expectation, maximization and smoothing.

First step estimates the statistics of $z(x)$ as a conditional expectation:

$$z^{(n)} = E\left(z | \sum_{i=1}^{N} z_{ij}, x_{ij}^{(n)} \right) \tag{4.27}$$

where $^{(n)}$ denotes n^{th} iteration.

The second step takes the estimated data to calculate maximum likelihood estimates as a solution of the following equation:

$$E\,(\,z_{ij}|\,x) = z^{(n)} \tag{4.28}$$

The last step in every iteration smoothes solution x using Gaussian kernel with locally weighted endpoints. The smoothing process centers the kernel at each data point:

$$x^{(n')} = \sum_j \mathbf{S}_{ij} x^{(n)} \tag{4.29}$$

where $\mathbf{S}$ is the smoothing matrix.

Finally, assuming that observations z result from a nonhomogeneous Poisson process we receive an equation describing the first two steps in a form:

$$x^{(n)} = \frac{x^{(n-1)}}{\sum_i K_{ij}} \left(\frac{z^t}{x^{(n-1)} \mathbf{K}^T} \mathbf{K} \right) \tag{4.30}$$

EMS method requires high experience in proper selection of variance for gaussian kernel, as there is a possibility of oversmoothing. It was firstly applied to fish target strength estimation by Hedgepeth [61].

4.4.2. Adaptive Expectation Maximization and Smoothing method

As stated before, SVD technique gives the solution with minimum squared error, which is typically used as a natural measure of global goodness-of-fit test for an estimate. However, due to sine-like nature of eigenfunctions of linear operator, SVD often leads to the artifacts when interpreting obtained estimate as a probability density function. On the other hand, the EMS estimate represents more smooth class of functions than those obtained by SVD and can be treated as a good estimate for a class of probability density functions, although resulting mean square error is much larger.

The root mean square error for EMS can be minimized and the smoothness of solution can be preserved by the changes introduced in the kernel K of integral equation Eq. (4.8). This is particularly relevant for the case of fish target strength estimation as the construction of the kernel is based on heuristic assumption made on angular distribution of fish in calculation of beam pattern PDF. Thus, the estimation algorithm may adaptively change kernel K by solving another inverse problem in which the beam pattern PDF p_B is reconstructed from echo level PDF p_E and target strength PDF p_{TS} estimated just before. New estimate of p_B PDF allows calculating a new kernel matrix K, which is used in the next step of such adaptive algorithm. The process can be terminated comparing the difference between two successive estimates. The concept of the Adaptive EMS (AEMS) methodology is presented in Fig. 4.1. The method constitutes at least three EMS inverse processes from which two represents one adaptive step.

The AEMS method has been applied to fish target strength estimation problem by the author [99]. The results contained in Tab. 4.1 show that only two adaptive steps are required to reduce rms error into the level comparable to SVD method with a still smooth solution.

Table 4.1

Root-mean-square error of WSVD estimate and succesive AEMS estimates

Method	WSVD	EMS	AEMS (n=1)	AEMS (n=2)	AEMS (n=3)
RMS error	0.0231	0.1288	0.0477	0.0426	0.0419

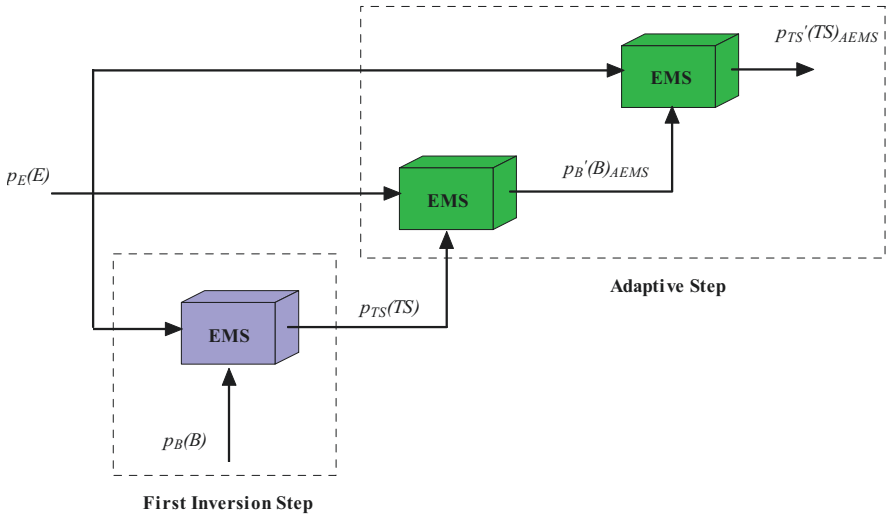

Fig. 4.1. The concept of AEMS method as applied in fish target strength estimation

Chapter 5

DETERMINATION OF THE KERNEL FOR INVERSE PROBLEMS IN FISHERY ACOUSTICS

It was shown in previous chapters that the inverse techniques may have its application in two problems related to fish abundance estimation. Firstly, in the problem of fish target strength estimation from single beam observation where unknown fish position in the beam may be removed by statistical processing of fish echo. Secondly, when transforming acoustic measure of fish scattering namely target strength into physical measure namely fish fork length where the effect of fish random orientation needs to be removed.

In case of fish target strength estimation from single beam data the so-called single beam integral equation needs to be solved for target strength probability distribution functions (PDFs). The integral equation may be formulated in so-called absolute (linear) domain where unknown PDF is represented by fish backscattering length or fish backscattering cross section, or in logarithmic domain where unknown function is target strength PDF. However, it was shown in [101] that in logarithmic domain the problem is less ill conditioned than in absolute domain, although it may lead to oversmoothing. In all this formulations the kernel of inverse problem is represented by the term, which in fishery acoustics is called beam pattern PDF. Actually, it is used to remove beam pattern effect from fish echo data. Although beam pattern is deterministic function, it is used in statistical sense as a function, which transforms random fish position into new random variable combining random fish position observed by beam pattern. Theoretically, unknown fish target strength does not depend on its position in the beam, so both distributions can be treated as random variables. Nevertheless, as the observed data are limited due to hydracoustic system threshold, they both became dependent.

In case of fish length estimation the inversion techniques may be used to convert fish target strength PDF into maximum fish target strength PDF by removal of fish directivity pattern effect. The term maximum fish target strength refers to the situation when the fish is insonified by the wave from the direction perpendicular to its maximum acoustic aperture, which for different species may not be perpendicular to its fish body or swimming direction. In this case, as the maximum fish target strength and fish directivity pattern both depend on fish length the problem requires processing PDFs of dependant random variables. As it will be shown in this chapter, the solution can be obtained by introducing conditional PDFs. Moreover, when the relation between maximum fish target strength and actual fish length (depends rather only on morphological parameters of the fish) is established, the PDF of fish length can be obtained.

In this chapter, several aspects related to determination of PDFs of transducer beam pattern and fish directivity pattern are considered, as both constitute the kernel used in inversion scheme.

5.1. Fish angular position in the transducer beam

Widely used assumption of uniform spatial distribution of fish in a water column, leads to *sine*-law distribution of the angular position of the fish in the beam [61, 94, 150]. This assumption is valid only for the case of the single (non-multiple) echoes received from individual fish in consecutive pings. However, when acquiring actual data from acoustic surveys, the multiple or correlated echoes may be collected from the same fish forming the fish traces.

Typically, calculation of PDF of fish angular position $p_\theta()$ is based on the assumption of uniform distribution of fish in a water column (cartesian coordinates). Let us then assume that a distribution of variable z representing depth on which fish appears in the conical area defined by observation angle $\theta_{\max}$ is uniform, i.e.

$$p_z(z) = \frac{1}{z_{\max}} \tag{5.1}$$

where $z_{\max}$ represents maximum depth. Due to linear relation between depth and radius of a circular slice $\underline{z} = \underline{R} \tan \theta_{\max}$, the distribution of random variable $\underline{R}$ become also uniform, i.e.

$$p_R(R) = \frac{1}{R_{\max}} \tag{5.2}$$

where $R_{\max} = z_{\max} / \sin \theta_{\max}$ is maximum possible radius of the slice. Substituting $\underline{\theta} = \operatorname{acos}(\underline{z}/\underline{r})$ and making simple calculations as presented in [151] the distribution of angular position θ has *sine* like law:

$$p_\theta(\theta) = \frac{1}{1 - \cos \theta_{\max}} \sin \theta \tag{5.3}$$

where $\theta_{\max}$ is maximum angle of beam pattern involved in calculation.

However, in most cases in acoustics surveys the same fish is observed in several contiguous pings so the set of echoes does not represent independent statistics. That is why it is more proper to include the effect of multiple echoes in the set. Theoretically, it is possible to consider two models of fish traces statistics: (1) assuming the vessel movement with stationary fish, and (2) assuming stationary vessel and moving fish. Both models were described by Moszynski in [100]. In the first model the uniform vessel movement with stationary fish is assumed. The second model assumes fish movement along arbitrary path in the transducer beam pattern cross-section. Actually, both models differ in a distribution of the crossing angle (the angle in which a fish enters the beam), which has *sine*-law PDF in the first model and uniform distribution in the second one. Although the behaviour of fish crossing the transducer beam is unpredictable [118], the distrubution of number of echoes in the trace obtained theoretically using the same assumptions, are in agreement with those observed in the data acquired during acoustic surveys [98].

Let us now consider the distribution of angular position of fish $\underline{\theta}$ that is necessary for calculation of beam pattern PDF. From the geometrical relations we have:

$$\underline{\theta} = a\cos\frac{\underline{z}}{\underline{r}} = a\cos\frac{1}{\sqrt{1+\left(\underline{\rho}/z\right)^2}} \tag{5.4}$$

where random variables $\underline{r}$, $\underline{\rho}$, $\underline{z}$ represent coordinates of fish position related by equation: $\underline{r}^2 = \underline{\rho}^2 + \underline{z}^2$. Let us also consider the random variable $\underline{t}$ called trace distance, which represents distance of the fish from the crossing point of circular slice. If fish swims on the chord and is "sampled" uniformly in the consecutive pings, we may treat its distribution as uniform in a range $(0,2\underline{r}\ sin\ \underline{\alpha})$. Thus, the trace distance random variable may be expressed as $\underline{t} = 2\underline{r}\ sin\underline{\alpha}\ \underline{u}$, where $\underline{u}$ has again normalised uniform distribution. Taking into account the cosine law in the non-right angled triangle we obtain:

$$\underline{\rho}^2 = \underline{r}^2 + \underline{t}^2 - 2\,\underline{r}\,\underline{t}\,\sin\underline{\alpha} = \underline{r}^2\left(1-(2\sin\underline{\alpha})^2(\underline{u}-\underline{u}^2)\right) \tag{5.5}$$

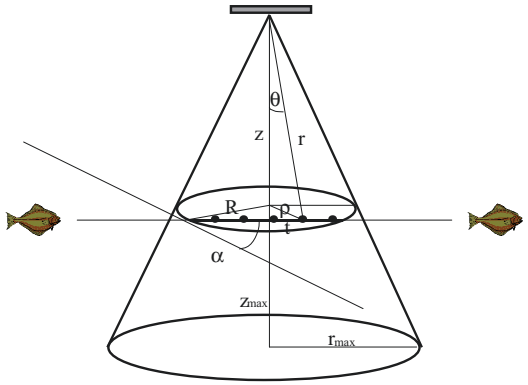

Fig. 5.1. Geometry of multiple echoes from a fish trace

Using the formulae for PDF of the product of random variables and substituting $\underline{z} = \underline{r}\tan\theta_{\max}$ which removes $\underline{z}$ dependence from Eq. (5.4) and $\underline{r}$ dependence in Eq. (5.5), we receive the PDF of angular position for the moving vessel model in the following form:

$$p_\theta(\theta) = \frac{1}{\tan^2\theta_{\max}} K\left(\frac{\tan\theta}{\tan\theta_{\max}}\right)\frac{\sin\theta}{\cos^3\theta} \tag{5.6}$$

where $K(x) = \int_0^{\pi/2}(1-x^2\sin^2\varphi)^{-1/2}d\varphi$ represents here complete elliptic integral of the first kind. It is worth to note that as one could expect there are more echoes received from off-axis angles, which results in increased distribution at this range of angles as compared to *sine*-like distribution known for the case of non-multiple echoes statistics.

Practically, the statistics of actual angular position of fish in the beam may be calculated using echo trace algorithm, which for split-beam system observations allows determing fish trace for each fish.

5.2. Transducer beam pattern PDF

In general, transducer beam pattern is deterministic quantity but in the context of unknown position of fish in the beam it can acquire nondeterministic meaning. For beam pattern PDF calculation let us consider first the ideal circular piston in a infinite baffle. Its one-way intensity domain beam pattern function $b(\cdot)$ (or two-way pressure domain) is:

$$b(\theta) = \left(\frac{2J_1(x)}{x}\right)^2 \tag{5.7}$$

where x is defined by $x = x(\theta) = ka \sin\theta$ (k – wave number, a – transducer radius) and $J_n(x) = \frac{1}{\pi}\int_0^\pi \cos(n\theta - x\sin\theta)d\theta$ is the Bessel function of first kind order n. It is worth to note that in the fishery acoustics and oceanography literature there are different definitions of beam pattern function. Defined here $b(\cdot)$ is equivalent to b^2 of MacLennan and Simmonds [87] and D^2 of Medwin and Clay [89], as they define its beam pattern function in pressure domain. The different definitions come from two facts: (1) the transmitting b_t (or D_t) and the receiving b_r (or D_r) patterns are theoretically the same due to reciprocity of a transducer $D_t = D_r$, (2) due to two-way transmission the net effect is multiplication of both patterns $b = D_r \cdot D_t = D^2$ (as in [149]), hence the square in Eq. (5.7) for the beam pattern of circular transducer, when interpreting this function in pressure domain.

The logarithmic version of two-way pattern is derived by transform:

$$B(\theta) = 10\log b^2(\theta) = 20\log b(\theta) \tag{5.8}$$

and is presented in Fig. 5.2.

The beam pattern PDF is defined using theory of function of random variable for b($\underline{\theta}$) [120]:

$$p_b(b) = \frac{p_\theta(\theta)}{\left|\frac{db}{d\theta}\right|} \tag{5.9}$$

This function for circular transducer may be expressed as a parametric function $p_b(b) = (b(\theta), p_b(\theta))$ with angle θ as a parameter [106]:

$$p_b(b) = \left(\left(\frac{2J_1(x)}{x}\right)^2, \frac{p_\theta(\theta)tg\theta}{\left|\frac{8J_1(x)J_2(x)}{x}\right|}\right) \tag{5.10}$$

where $p_\theta()$ is a probablity density function of random angular position of fish. Using logarithmic transform of variables $B(b) = 20\log b$ its PDF relation may be written as:

$$p_B(B) = \frac{\ln 10}{20}\left|10^{\frac{B}{20}}\right| p_b\left(10^{\frac{B}{20}}\right) \tag{5.11}$$

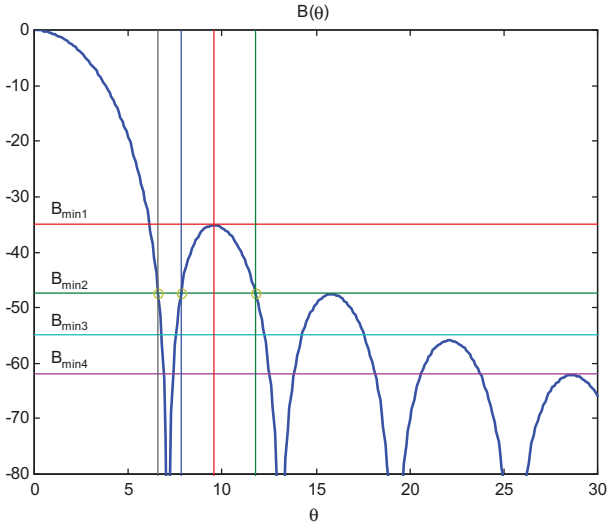

Fig. 5.2. Two-way beam pattern function for ideal circular piston in an infinite baffle

Practically, the beam pattern in commercially manufactured echo sounders may differ from theretically obtained for circular piston. The approximation used by Moszynski [95] is particularly useful for PDF calculation. As he showed the following approximation:

$$b(\theta) = \left(1 - (1 - 2^{-\gamma})\frac{1 - \cos\theta}{1 - \cos\theta_{3dB}}\right)^{\frac{2}{\gamma}} \tag{5.12}$$

allows fitting the slope to the actual pattern by the usage of the exponential coefficient γ. In case of angular distribution of fish position described by Eq. (5.3), it leads to simple formulae for beam pattern PDF:

$$p_b(b) = \frac{c_b}{b^{1-2/\gamma}} \tag{5.13}$$

with c_b as normalization constant. The logarithmic transform gives following equation:

$$p_B(B) = \frac{\ln 10}{20}\frac{\gamma}{1 - 2^{-\gamma}}\frac{1 - \cos\theta_{3dB}}{1 - \cos\theta_{\max}}10^{\frac{\gamma B}{20}} \tag{5.14}$$

where $\theta_{\max}$ is maximum angle considered in analysis. Taking into account multiple echo statistics described by Eq. (5.6), it results in a parametric equation (with angular position θ as a parameter):

$$p_B(B) = \left(20\log b(\theta)\ ,\ \frac{\ln 10}{20}\frac{\gamma}{1 - 2^{-\gamma}}\frac{1 - \cos\theta_{3dB}}{\tan^2\theta_{\max}}K\left(\frac{\tan\theta}{\tan\theta_{\max}}\right)\frac{b(\theta)^\gamma}{\cos^3\theta}\right) \tag{5.15}$$

Another practical note is worth to be mentioned. When only main lobe of beam pattern is used, the inverse of beam pattern function needed for $p_b()$ computation is single-valued. However, when side-lobes are involved the inverse function is non single-valued Fig. 5.2 and then its PDF calculation must be made for all angles θ having the same value B. This makes the equations for beam pattern PDF $p_B(B)$ still valid but inverse function $b^{-1}(\cdot)$ needs to be computed to find all occureances of θ for every b being now independent variable. The procedure must be followed by the sumation of PDF values for those angles. The inverse of beam pattern function now called $\theta(b)$ may be calculated iteratively using Newton iteration as showed in [104]. The final result of this approach is presented in Fig. 5.3, showing theoretical beam pattern PDF $p_B(\cdot)$ with inclusion of three side-lobes. The components from sidelobes are presented as dotted lines. Note the theoretical left-sided infinities in PDF where sidelobes reach its local maxima. Practically, it is recommended to operate without side-lobe, where beam pattern PDF has monotonic representation described by an approximation i.e. Eq. (5.14) or Eq. (5.15).

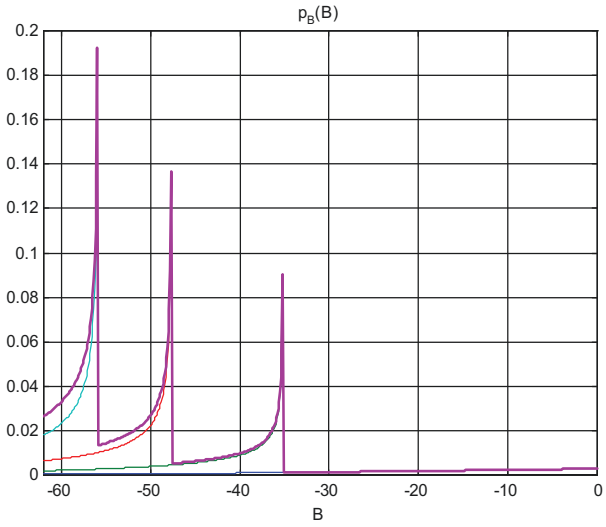

Fig. 5.3. Theoretical beam pattern probability density function (PDF) for ideal circular piston when three sidelobes are included

To construct the kernel of inverse problem, the beam pattern PDF needs to be discretized. In most cases this leads to simple sampling of theoretical PDF, however in this case due to infinities and histogram nature of observed echo level PDF $p_E()$ it must be done carefully. To check the behaviour of discretized version of PDF another method of its determination is suggested. The proposed method is based on random generation of assumed angular position. The distribution described by PDF function can be generated using inverse of cumulative distribution function (CDF) method. Note that the discrete approximation depends not only on bin size but also on bins positions, especially when the bin contains theoretical infinity and low

values alltogether. Additionally, the values in border bins may be inaccurate. Sample simulations and the analysis of actual data from the acoustic survey assuming side-lobe acquisition were presented in [104].

5.3. Influence of threshold on the beam pattern kernel

In the acoustic surveying of fish stocks and subsequent estimation of biomass, the sampling volume of the acoustic instruments is of great importance, as for randomly distributed targets the received echo energy is linearly related to this volume. As a signal threshold is applied in order to eliminate contribution from noise the effective sampling volume is always less than the full volume of the acoustic beam. The problem was treated in several papers. Kalikhman [70] combined the beam pattern of the transducer with scattering characteristics of the fish averaged over azimuth. Their conclusion is that, for a single fish, the effective equivalent beam angle depends not only on the threshold but also on the angle of insonification. Foote [39] developed an expression for the effective equivalent beam angle in terms of the directivity of the transducer, the backscattering cross-section of the fish as function of tilt angle and the signal threshold. Detailed literature survey on the problem can be found in papers of Reynisson [126] and Fleischman [31]. The problem of bias introduced by threshold will be described here by statistical analysis of the target strength and beam pattern distributions.

In simplified and often used case, the random variables $\underline{TS}$ and $\underline{B}$ are treated as independent random variables, which allows expressing their probability density functions (PDFs) in the form of convolution integral equation. However, although from dual-beam systems we have exact TS for each detected fish echo $\underline{E}$, when applying threshold to obtained echoes it restricts not only the dynamic range of the data but also introduces dependence on $\underline{TS}$ and $\underline{B}$ random variables. Thus, statistically, we can write the equivalent equation for dual beam case:

$$\underline{E'} = \underline{TS'} + \underline{B'} \tag{5.16}$$

where primes denote that we operate on conditinal variables. As the consequence, the PDFs of these variables should be expresses by a conditional PDF as follows:

$$p_{E'}(E') = p_E(E|E > E_{\min}) \tag{5.17}$$

$$p_{TS'}(TS') = p_{TS}(TS|E > E_{\min}) \tag{5.18}$$

$$p_{TS'}(TS') = p_{TS}(TS|E > E_{\min}) \tag{5.19}$$

where $E_{\min}$ is the echo level threshold value.

The net effect is that the mean value of backscattering cross-section $\bar{\sigma}'$evaluated from transformed distribution of conditional random variable $\underline{TS}$' is biased as compared to actual mean value $\bar{\sigma}$evaluated from variable $\underline{TS}$. It is noteworthy that in the single beam case the fact of introducing the threshold modifies only the range of integration in convolution-like integral:

$$p_E(E|E > E_{\min}) = \int_{E_{\min}-B}^{0} p_{TS}(E-B)p_B(B)dB \tag{5.20}$$

and the reconstructed $p_{TS}(TS)$ is unconditional if properly assumed $p_B(B)$ is used.

Statistical removal of the bias introduced by the threshold in dual beam processing requires calculation of $p_{TS}(TS)$ from conditional $p_{TS}(TS|E > E_{\min})$. The latter distribution, which is *de facto* observed, can be expressed as:

$$p_{TS}(TS|E > E_{\min}) = p_{TS}(TS|TS + B > E_{\min}) \tag{5.21}$$

which may be evaluated by integration of joint distribution of independent random variables $\underline{TS}$ and $\underline{B}$:

$$p_{TS}(TS|E > E_{\min}) = \frac{\int_{E_{\min}-TS}^{\infty} p_{TS,B}(TS,B)dB}{\int_{-\infty}^{+\infty}\int_{E_{\min}-TS}^{\infty} p_{TS,B}(TS,B)dBdTS} \tag{5.22}$$

As the denominator evaluate to the constant value (normalization constant) and independency of variables $\underline{TS}$ and $\underline{B}$ allows replacing joint PDF by multiplication of its PDFs, it results in:

$$p_{TS}(TS|E > E_{\min}) = c_1 p_{TS}(TS) \int_{E_{\min}-TS}^{\infty} p_B(B)dB \tag{5.23}$$

The integral in above equation can be expressed using cumulative distribution function (CDF) $F_B()$ of beam pattern random variable $\underline{B}$, which finally gives:

$$p_{TS}(TS|E > E_{\min}) = c_1\ p_{TS}(TS)\ [1 - F_B(E_{\min} - TS)] \tag{5.24}$$

which describes the connection between conditional distribution of observed target strength and required unconditional distribution. Note that, it requires the knowledge of unconditional distribution of beam pattern CDF.

The same approach applied to conditional distribution of beam pattern function $p_B(B|E > E_{\min})$ gives the following equation:

$$p_B(B|E > E_{\min}) = c_2\ p_B(B)\ [1 - F_{TS}(E_{\min} - B)] \tag{5.25}$$

In both cases, the expression in brackets represents CDF of the second function scaled to domain of first function. Thus, dependence introduced by threshold is observed as a multiplication of unconditional PDF of one function by scaled CDF of the second one. The constants c_1 and c_2 normalize equivalent distributions. The removal of threshold effect on measured distribution of target strength requires solution of equations (5.24) and (5.25), which represents a set of integral equations.

5.4. Fish directivity pattern PDF

From among several fish backscattering models presented in Chapter 2, it is not necessary for statistical processing to use high resolusion model that would reflect precisely fish scattering properties. For that pupose it is reasonable to use a simple tilted cylinder model that allows fish target strength to be rewritten in the logarithmic form. It more clearly shows dependence on angular position of the fish expressed by fish body tilt angle χ and swimbladder tilt angle χ_0:

$$TS = TS_0(l_{ecb}, a_{ecb}) + B_f(\chi, \chi_0, l_{ecb}) \tag{5.26}$$

where $TS_0 = 20\log l_{bs0}$ is maximum target strength of the fish and B_f is the fish angular directivity pattern in dorsal aspect expressed in logarithmic domain:

$$B_f(\chi, \chi_0, l_{ecb}) = 20\log\left(\frac{\sin\left(kl_{ecb}\sin(\chi+\chi_0)\right)}{kl_{ecb}\sin(\chi+\chi_0)}\sqrt{\cos(\chi+\chi_0)}\right) \tag{5.27}$$

When the echoes are acquired from fish population having random orientation the Eq. (5.26) can be interpreted as the sum of random variables. However, in this case the variables are not independent due to dependence of both variables $\underline{TS}_0$ and $\underline{B}_f$ on equivalent cylinder length l_{ecb}.

In general case, the PDF of sum of two random variables $\underline{z} = \underline{x}+\underline{y}$ can be expressed by integral [120]:

$$p_z(z) = \int p_{x,y}(x, z-x)dx \tag{5.28}$$

where $p_{x,y}(x, y)$ is joint PDF of two random variables $\underline{x}$ and $\underline{y}$. If $\underline{x}$ and $\underline{y}$ are dependent variables then using Bayesian theory the joint PDF can be replaced by the product of PDF of one variable $p_x(x)$ and appropriate conditional PDF of the second variable:

$$p_z(z) = \int p_x(x)\, p_{y|x}(z-x, x)dx \tag{5.29}$$

For considered TS_0 and B_f random variables it means:

$$p_{TS}(TS) = \int p_{TS_0}(TS_0)p_{B_f|TS_0}(TS-TS_0, TS_0)dTS_0 \tag{5.30}$$

Eq. (5.30) represents integral equation for reconstructing the distribution of maximum target strength of the fish TS_0 from the observation of fish with random orientation. Conditional fish pattern PDF $p_{B_f|TS_0}(B_f, TS_0)$ represents kernel of this equation. To calculate this function it is required to establish the value of maximum target strength TS_0 of the fish and then calculate its directivity pattern B_f. When fish is observed from dorsal aspect, its directivity pattern depends mainly on orientation expressed by the sum of fish body tilt angle χ and swimbladder tilt angle χ_0. Thus, additionally, the distribution of both random variables influencing the angle in which fish is observed should be known. Finally, it is recomended to construct fish directivity pattern PDF by random generation of such distribution and transforming obtained PDF by fish directivity pattern function.

Sample randomly generated fish conditional directivity pattern PDF at 120 kHz is presented in Fig. 5.4. During PDF calculation, it was assumed that the fish body tilt angle has normal distribution with a mean value of 8° and the variance 3°. The mean value can be interpreted as a swimbladder tilt angle χ_0 and variance is a measure of changes in fish body orientation. Note, however, that the swimbladder tilt angle may be treated only as a mean value for particular species as it may change during fish grow history. In other words, it means that the different size fish may have different swimbladder tilt angle. Additiononally, the changes in fish orientation observed by the acoustic system are also related to fish movement in the beam and are limited due to transducer beam pattern.

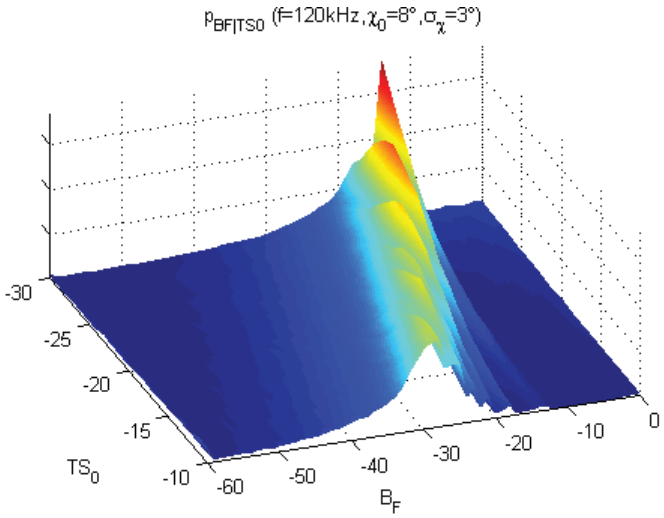

Fig. 5.4. Sample randomly generated fish conditional directivity pattern PDF at 120 kHz assuming normal distribution of tilt angle ($\chi_0 = 8°$, $\sigma_\chi = 3°$)

Theoretically, when only fish straight movement in the beam is considered, the tilt angle statistics would be the same as fish angular position in the beam presented before. Hence, to calculate conditional fish directivity pattern it is possible to use fish angle statistics from echo tracing algorithm. However, true tilt angle statistics needs to reflect fish behaviour, which may be registered only by video observations or additional knowledgde on its migrations.

As the fish scattering model is used to calculate the fish directivity pattern PDF, it is obvious that not only distribution of maximum target strength could be calculated from inverse processing but also fish length distribution. This is true, if for observed fish its equivalent parameters for scattering model are known, what is possible if fish species are identified. Species identification is well-recognized problem in fishery acoustics and for some cases of commercial fishes it is well worked out [74].

Chapter 6

STATISTICAL ANALYSIS OF ACOUSTIC SURVEY DATA

In order to justify the correctness of inversion approach and validate its results two case studies will be presented. In following two sections, the data that comes from two acoustic surveys will be statistically analysed. The first dataset were collected with a dual-beam system and the analysis is aimed to compare the target strength estimates obtained from direct and indirect processing. The second dataset collected with a dual frequency split-beam system and containing echoes from known species will show the results of inverse processing in reconstruction of fish length distribution from target strength distribution.

6.1. Targets strength single beam estimation vs dual beam estimation

This section presents the analysis of data derived from an acoustic survey on pelagic fish populations (mostly salmon and trout) in Coeur d'Alene Lake, Idaho using dual-beam digital echosounder with 6° narrow beam and 15° wide beam transducers operated at 420 kHz. It were provided by J.B. Hedgepeth, Biosonics Inc., Seattle and E. Parkinson, University of Vancouver, Canada. Over 6500 pings were processed from which over 10000 fish echoes were extracted for analysis. Using fish tracing algorithm 2009 fish was counted.

The distribution of the number of multiple echoes in fish trace are shown in Fig. 6.1, in a form of histogram. Note, that due to border effect in obtaining PDF estimate by histogram technique the range between $N = 0$ and $N = 1$ cumulates as only $N = 1$ has physical sense. The shape of the histogram curve agrees with theoretical models [100].

6.1.1. Direct dual beam estimation

When using a dual beam system the PDF estimates can be obtained directly. They are presented here in the form of histograms, which can be treated as an estimate of probability density function [135]. The echo PDF $p_E(E)$ obtained from narrow beam channel is presented in Fig. 6.2. The data were thresholded with $E_{\min} = -70$ dB and covers 40 dB range up to around –30 dB. Target strength PDF $p_{TS}(TS)$ obtained by processing of narrow and wide channel data is shown in Fig. 6.3. Similarly, beam pattern PDF for narrow beam channel is presented in Fig. 6.4. Note, that due to thresholding there are less echoes from off-axis angles as only large fish located off-axis can be observed. Hence, the TS estimate is conditional estimate due to threshold.

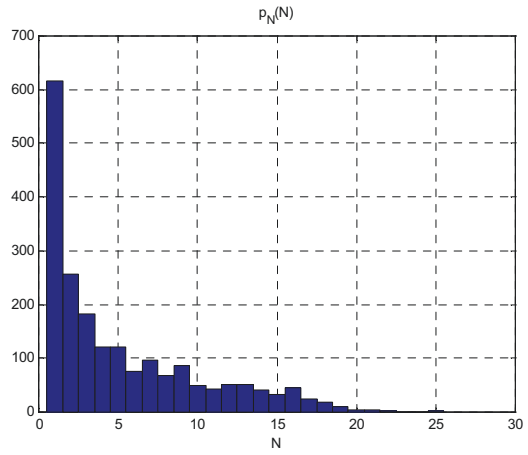

Fig. 6.1. Sample distribution of the number of multiple echoes in fish traces from survey

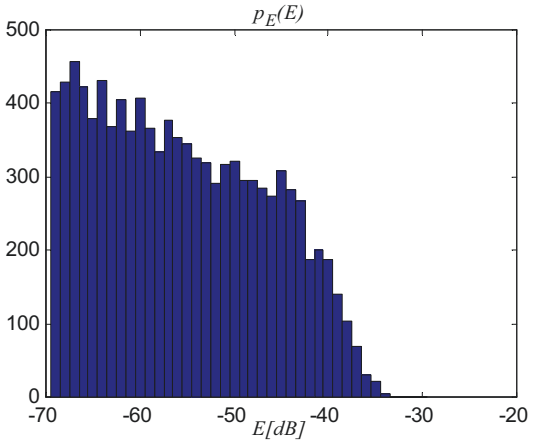

Fig. 6.2. Echo PDF from narrow beam channel

The same data were used to calculate the distribution of angular position of the fish from distribution of beam pattern. Assuming beam pattern of narrow beam channel to be close to ideal circular piston placed in the infinite buffle, the unknown distribution of angular position θ was calculated using two channel data and Newton iteration was used for evaluation of inverse of beam pattern function. The results of numerical calculation for actual dataset are presented in Fig. 6.5. Both numerical experiments conducted on survey data show good agreement with presented models of fish statistical behaviour during measurements.

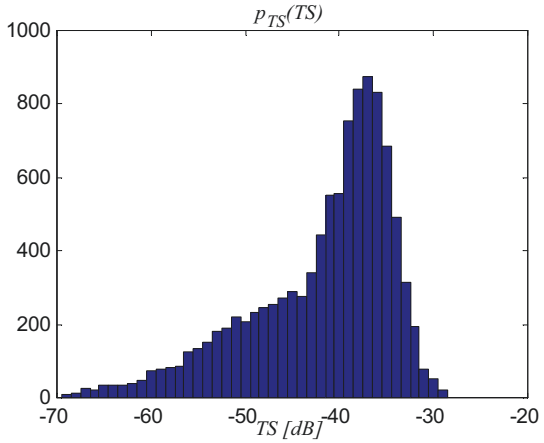

Fig. 6.3. Target strength estimate obtained from the dual-beam processing

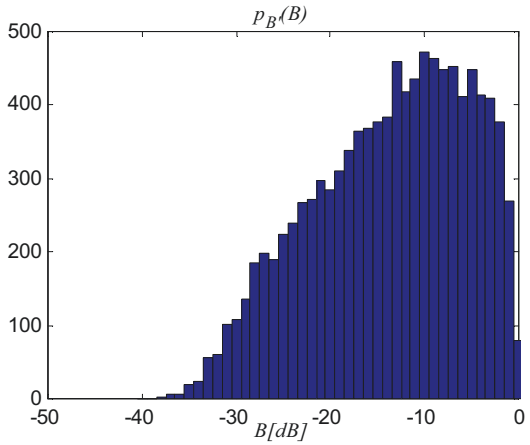

Fig. 6.4. Beam pattern PDF from dual-beam processing

6.1.2. Indirect single beam estimation

The analysis using inverse procesing requires fitting the approximation of beam pattern function into actual system beam pattern function. Using approximation presented in Chapter 5 the slope coefficient of beam pattern approximation γ = -0.1 was fitted. Beam pattern PDF calculation assumes multiple fish echoes statistics. Resulting beam pattern PDF used as kernel function for inversion is presented in Fig. 6.6. The influence of larger number of echoes from off-axis positions can be observed in the form of higer density at lower beam pattern values. Note also the difference between conditional beam pattern PDF obtained by direct processing of dual-beam data (Fig. 6.4) and assumed one which is unconditional.

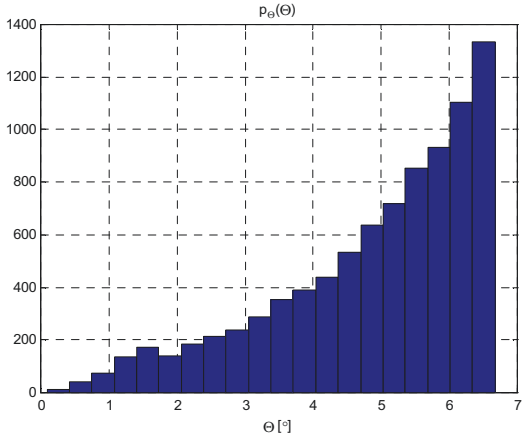

Fig. 6.5. Sample distribution of angular position of fish in the dataset

The samples of echo PDF derived directly from histogram (Fig. 6.2) were used as observed data, and processed by Adaptive Expectation Maximization and Smoothing inversion technique. The resulting target strength PDF estimate is presented in Fig. 6.7, along with the estimate from dual-beam processing for comparison. Transformed PDFs from logarithmic domain into backscattering strength l_{bs} domain are also presented in Fig. 6.8. Note the shift between the modal values of both PDFs, which originate from thresholding the echo data.

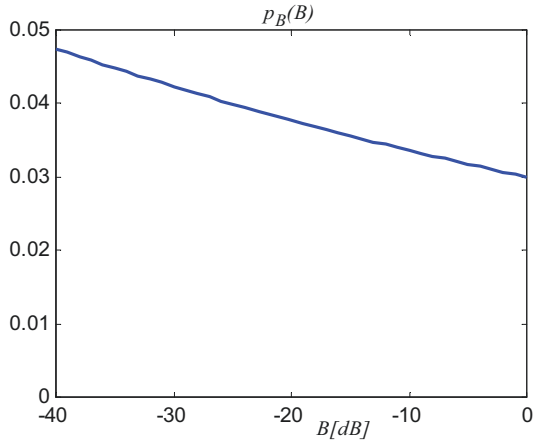

Fig. 6.6. Beam pattern PDF – kernel of inversion scheme

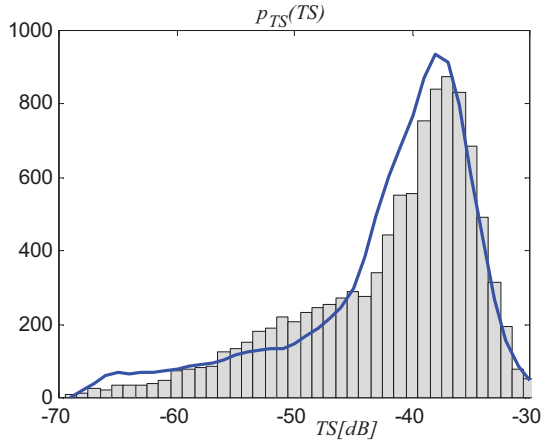

Fig. 6.7. Reconstructed target strength PDF by EMS inversion and compared to histogram obtained from dual-beam estimate

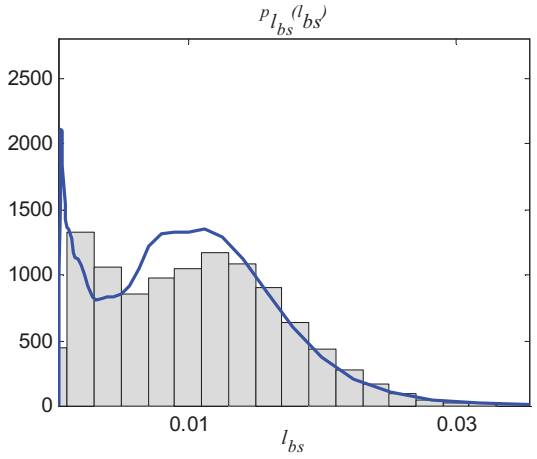

Fig. 6.8. Backscattering length PDF estimate obtained by logarithmic transform of target strength PDF estimate along with histogram estimate from dual-beam calculations

6.1.3. Comparison of inverse techniques

Modern digital data processing techniques of inverse problem solution have been successfully applied to indirect *in situ* estimation of fish target strength. The results obtained by the techniques introduced in Chapter 4 demonstrate their usefulness to the problem in question, as they constitute the tools of reliable and much more accurate TS-estimation than other state-of-the art methods.

The comparison of the performance of the introduced and analyzed inverse tech-

niques for fish target strength estimation is presented in Fig. 6.9 and Fig. 6.10 in the form of TS-PDF's and l_{bs}-PDF's estimates plots respectively. The first TS-density estimate plot (a) was obtained from the dual-beam method and is used as a reference for investigated estimates derived from the indirect techniques. The second plot (b) shows the estimate calculated by "conventional" Craig and Forbes method for comparison purposes. The plots (c) throughout (g) illustrate the estimates obtained by newly developed indirect techniques. As it is easily seen, these estimates, as compared to plot (b), demonstrate significantly improved results when comparing the shape (smoothness) and the accuracy (mean value) of the TS-PDF's estimates. For instance, the bias introduced by Craig and Forbes method (calculated as a difference of its mean value referenced to dual-beam mean value) is equal 1.4 dB, while the bias introduced by the newly developed methods never exceeds 0.6 dB, and in the best case (EMS estimate) the bias is only 0.2 dB.

Among the introduced methods two iterative techniques EMS and MER seem to be superior to other methods as they give smoothed (by iterations) estimates mostly similar to the dual-beam reference. WSVD and Wavelet methods produce slight artefactual modes and oscillations, which appeared for the small TS-estimate values region, but on the other hand they give much faster numerical solutions, and also correctly locate the main modal value of the estimated PDF's. The Tichonov Regularization – plot (c) seems to appear the poorest of the analyzed estimates probably due to its oversmoothing which results from not well defined value of the regularization parameter.

The $l_{bs}-$PDF's estimate plots shown in Fig. 6.10 demonstrate practically similar features and performance as their analogs in logarithmic domain presented in Fig. 6.9.

The absolute domain estimates are superior to their logarithmic domain counterparts as they more clearly reveal the bimodality of PDF plots, which is easily seen from comparison of the dual-beam PDF estimates represented by curve a) in Fig. 6.9 and Fig. 6.10.

However, in general, the $l_{bs}-$PDF's estimate performance is poorer than TS-PDF's estimates as the latter are "less ill conditioned". This is due to the fact that estimates in absolute domain are derived from the single beam integral equation, which kernel argument and differential have both the rational form.

6.2. Fish length estimation

The data analysed in the section were collected on Bering Sea by Alaska Fisheries Science Center (NOAA) during summer 2002 survey using dual frequency Simrad EK500 split beam echosounder. The author would like to thank Neil Williamson and John Horne for providing the sample data.

The anaylsis is aimed to test the application of inverse methods to the problem of reconstructing fish length distribution. To do this, near two thousands traces of walleye pollock (*Theragra chalcogramma*) were extracted from over 6000 of pings (Fig. 6.11). The catch data acquired before and after the survey are presented in Fig. 6.12.

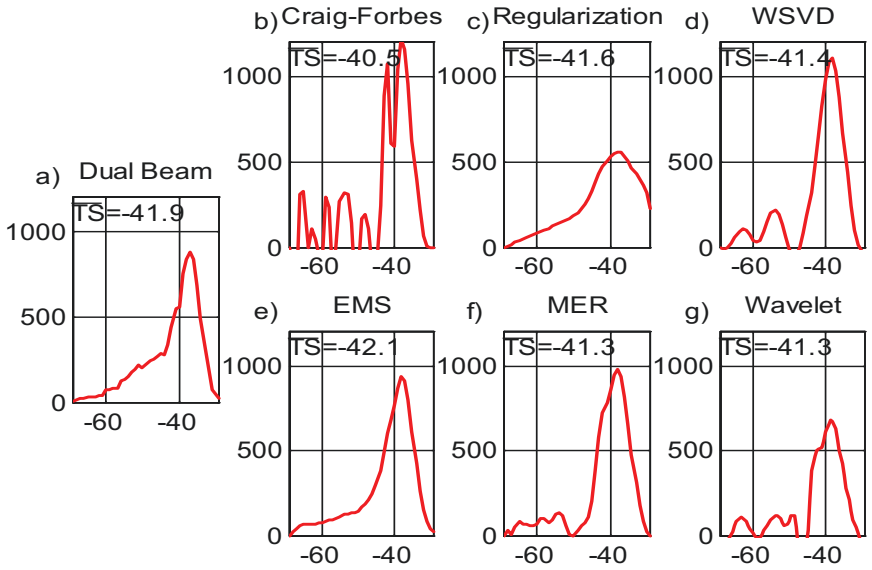

Fig. 6.9. Comparison of the target strength PDF's estimates obtained by different indirect methods with dual-beam method reference

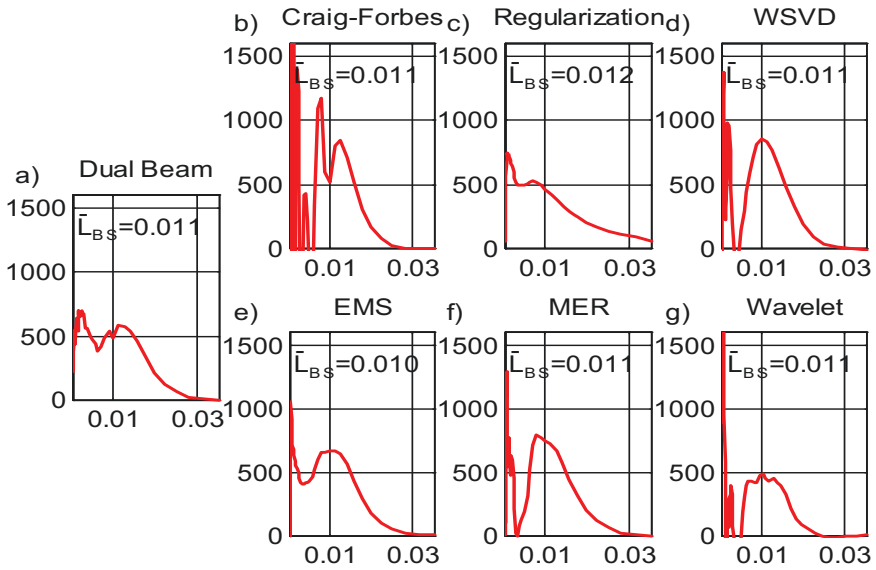

Fig. 6.10. Comparison of the backscattering length PDF's estimates obtained by different indirect methods with dual-beam method reference

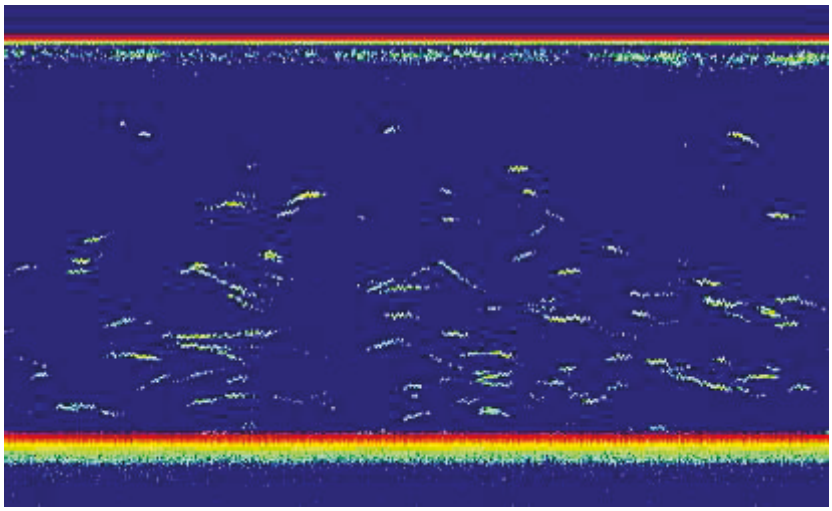

Fig. 6.11. Sample echogram from summer 2002 survey on Bering Sea containing walleye pollock echoes (fragment of around 800 registered pings)

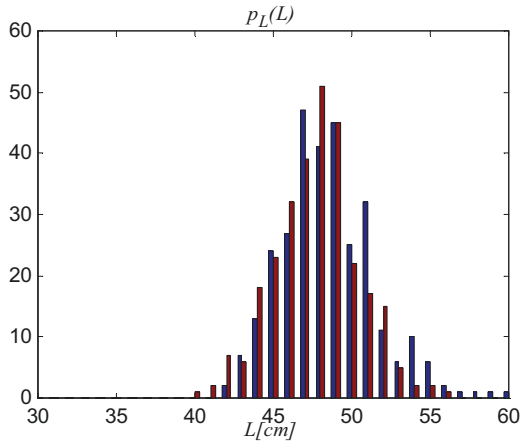

Fig. 6.12. Catch data representing walleye pollock length distribution before and after acoustic survey

6.2.1. Single frequency approach

The analysis presented in this section will be performed on data collected at 38 kHz only. To do the inversion the fish directivity pattern conditional PDF is calculated by random generation technique. It assumes normal distribution of fish tilt angle χ with variance equal 3°, which seems to be the reasonable value approximating a

half of beamwidth of the transducer beam pattern [106]. The mean swimbladder tilt angle of walleye pollock is assumed to be $\chi_0 = 8°$, which is derived from its morphological studies by X-ray radiography (Fig. 6.13). The equivalent parameters of walleye pollock swimbladder were assumed to be similar as in Haslet tilted cylinder model $l_{ecb} = L/4$ and $a_{ecb} = L/40$. Obtained fish directivity pattern conditional PDF is presented in Fig. 6.14. The distribution of target strength obtained by echosounder's firmware processing is presented in Fig. 6.15 in the form of histogram, whereas the results of inverse processing in the form of length estimate in Fig. 6.16, along with catch result for comparison. Note that althought *TS* distribution is multimodal the length distribution is unimodal. This result can be easily clarified by multimodal structure of fish directivity pattern conditional PDF.

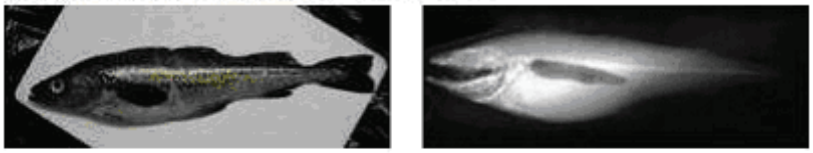

Fig. 6.13. Walleye pollock and its X-ray radiograph from dorsal aspect

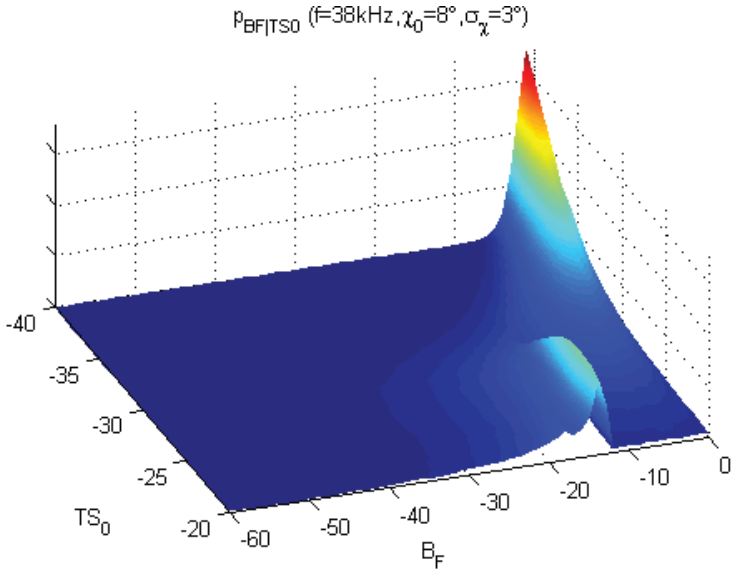

Fig. 6.14. Fish directivity pattern conditional PDF

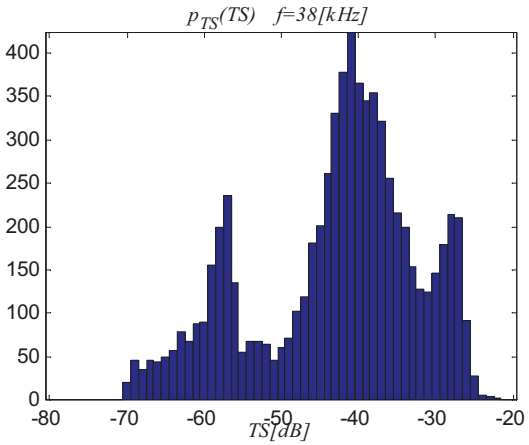

Fig. 6.15. Target strength PDF obtained from 38 kHz split-beam system

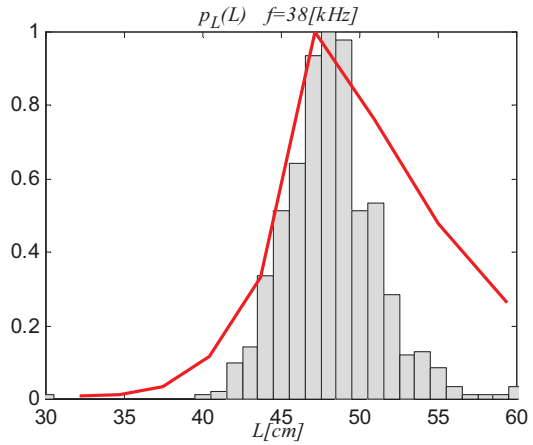

Fig. 6.16. Walleye pollock length distribution as results of inverse processing along with mean histogram from both catches

6.2.2. Dual frequency approach

Now, the processing was carried out using data acquired on two frequencies, namely 38 kHz and 120 kHz. For each frequency the inverse processing using EMS technique was performed using randomly generated conditional PDF of fish directivity pattern as before. Reconstructed fish length PDF for different mean swimbladder tilt angle χ_0 – along with estimate from trawl data for comparison purpose – are presented in Fig. 6.17. As for both frequencies the results should be the same, minimum of RMS error for estimates obtained from these two frequencies allows for estimation of mean swimbladder tilt angle χ_0. Function shown in Fig. 6.18 demonstrates the minimum

for χ_0=7°, which is in good agreement with morphological value of this parameter for walleye pollock [60]. However, the mean value of the estimate is biased (Fig. 6.19) as compared with catch histogram. This effect may result from the assumption made for the values of fish swimbladder equivalent parameters in tilted cylinder model as they determine the shift between target strength PDF and fish length PDF.

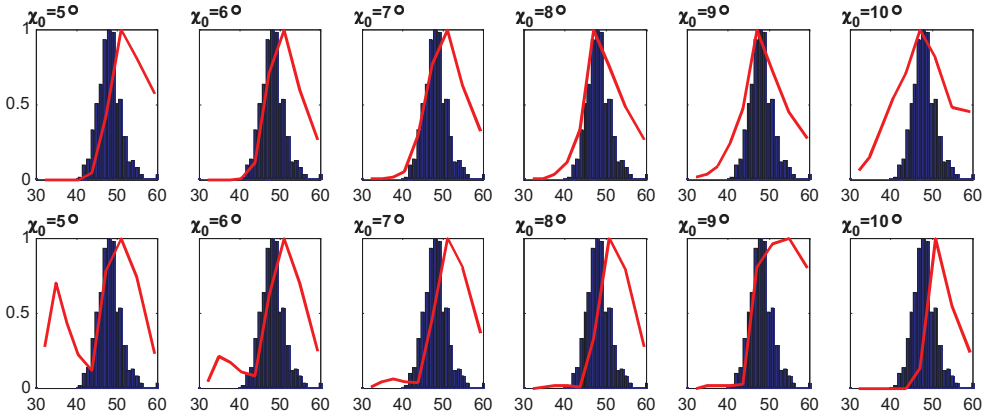

Fig. 6.17. Reconstruction of fish length PDF for different mean swimbladder tilt angle χ_0 along with estimate from catch data; upper sequence for 38 kHz and lower for 120 kHz (x-axis represents fish length in cm)

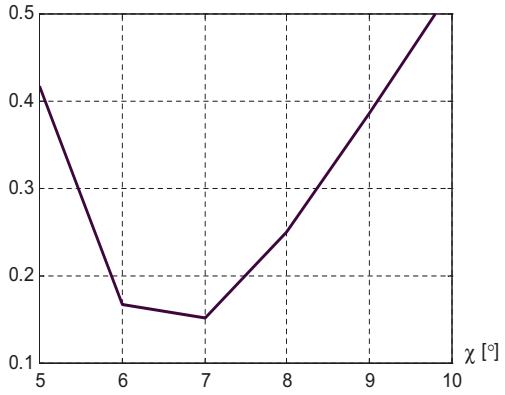

Fig. 6.18. Root-mean-square error function obtained from 38 kHz and 120 kHz estimates (x-axis tilt angle in degrees)

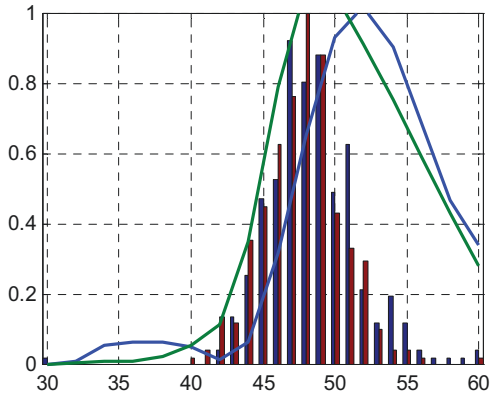

Fig. 6.19. Estimates of length PDF for mean swimbladder tilt angle χ_0=7° along with catch data

6.3. Conclusions

Presented analysis confirms that inversion techniques seem to be very useful in statistical processing of fish echoes. Firstly, they can be used to estimate fish target strength distribution from data collected with not specialized single beam systems and secondly they can be used even to estimate physical measures of fish in the form of fish length distribution.

In first case however, as a remedy for unknown fish position in the beam, the acoustic researches have invented multichannel echosounders, which more precisely locate insonfied objects in space coordinates. Nevertheless, the estimates obtained from dual- and split-beam systems are biased due to limited dynamic range of acoustic systems. The weak point of statistical approach comes rather from initial assumption for construction of kernel of integral equation, which mathematically describes the observation phenomena. However, as it was shown, this limitation can be alleviated when adaptive approach is applied.

The second considered problem, the estimation of physical measures from acoustical measures requires besides that an applicable model of fish scattering properties and its behaviour. Acoustically, for the downlooking observation, the variability of fish tilt angle becomes the fundamental reason for observed variations in acquired echo amplitudes and calculated fish target strength. As it was shown, by proper assumptions, the reconstruction of fish length distribution is possible, but only when a known species are surveyed. Although most of real factors related to wide range of behavioural, physical and physiological factors [118] influencing acoustical measures are neglected, the proposed method is suited especially to single species case with known fish morphology. However, due to identification algorithms, which can help in selecting the echoes originated from different groups of fish, it can be generalized. Additional improvements can be attained by multifrequency analysis. In the example

shown in this chapter, the analysis of data acquired at two frequencies allowed for indirect estimation of mean swimbladder tilt angle. This parameter appeared to be one of the crucial for fish angular statistics.

The last comment refers to the inverse methods applied to both problems. The well-known methods derived from various regularization and decomposition (SVD, WVD) approaches are in general more reliable than those based on deconvolution principle. They provide a minimax linear estimator or near-minimax estimators that are optimal (or near-optimal) over classes of functions of given regularity. However, they do not work sufficiently well in case of statistical inverse problems. The main reason of observed oscillations in estimates lies in the globalized Fourier-like eigenfunctions of linear operator representing kernel of inversion. These oscillations can be easily misinterpreted. In the author's opinion, the methods derived from expectation-maximization approach (EM, EMS, AEMS) certainly outperform the previous ones. They represent maximum likelihood extension, which filters highly variable estimates due to smoothing procedure. Definitely, they are superior for the class of probability density functions, which more often demonstrate rather smooth regularity. In fact, algorithmically, they are based on statistical assumptions, which are actually adequate for statistical linear inverse problems. Additionally, adaptive approach introduced by the author in the way similar to the adaptive filtering technique is especially relevant for the cases when the kernel of inversion are only heuristically determined.

Chapter 7

NON-SIGNAL METHODS IN FISHERY RESEARCH

The nature of scientific computing has changed dramatically over the past couple of decades. The appearance of the personal computer in the early 1980s changed forever the landscape of computing. Fisheries science as a discipline was slow to adopt personal computers on a wide-scale basis, being well behind use in the business world [90]. However, already the decade earlier the one of the very first computerized system for fish stock assessment was set up on Polish ship R.V. Profesor Siedlecki [152]. The authors of that pioneered system have managed to run it on the machine Elliott 905 equipped with only 8 kB of operational memory.

Since that time, during over thirty years of development of sonar systems, signal processing techniques applied in fish echo analysis became a standard processing algorithms. Echo sounding became a powerful and widely used technique for remote sensing of the marine environment. However, even modern digital signal and data processing techniques successively introduced recently do not constitute the final stage of development in acoustic methods of exploration and monitoring of marine living resources. Real time processing as a great advantage of digital signal processing in the context of fish resources management allows only for indirect reasoning on fish abundance and its behavior.

In order to enhance the power of sonar systems, a couple of post-processing systems have been designed (i.e. [91]). Some of them are part of the standard software that is essentially machine independent [44]. This could been done by adhering to the following international standards: the UNIX operating system, the C programming language, the X Window Systems, the Structured-Query Language (SQL) for communication with a relational database, and Transport Control Protocol/Internet Protocol (TCP/IP). Preprocessed data are transferred nowadays from the echo sounder to the post-processing system by means of a local-area network (LAN), viz. Ethernet.

Development of the postprocessing system, for analysis of such diverse scatterers as plankton, pelagic, and bottom fish, and the bottom itself, requires careful analysis of user requirements and computing environment, including hardware, software, and external communications. The typical system design of post-processing system for research vessels includes specific data flow and dedicated graphical user interfaces as shown in Fig. 7.1. Moreover, design philosophy and the method of implementation may have broader applications in acoustics than that ostensibly concerned only with the quantitative estimation of fish abundance [44].

Concurrently, in the last decade it appeared that the visual output of preprocessed data drawn in the form of classical echogram could be extended to the form of so-called 3D scenes. This could be achieved by complementary non-signal methods, namely by application of modern techniques of Information Technology (IT). The

main advantage of the approach is that 3D visualization allows for direct realistic imaging of fish data including fish tracing and remote sensing of entire populations and individuals as well. The echo data for such dynamic echograms could be delivered by the modern split–beam echo sounders as they allow for unambiguous localization of targets in the water column, and also provide tracking capabilities of individual fish's echo in the successive pings.

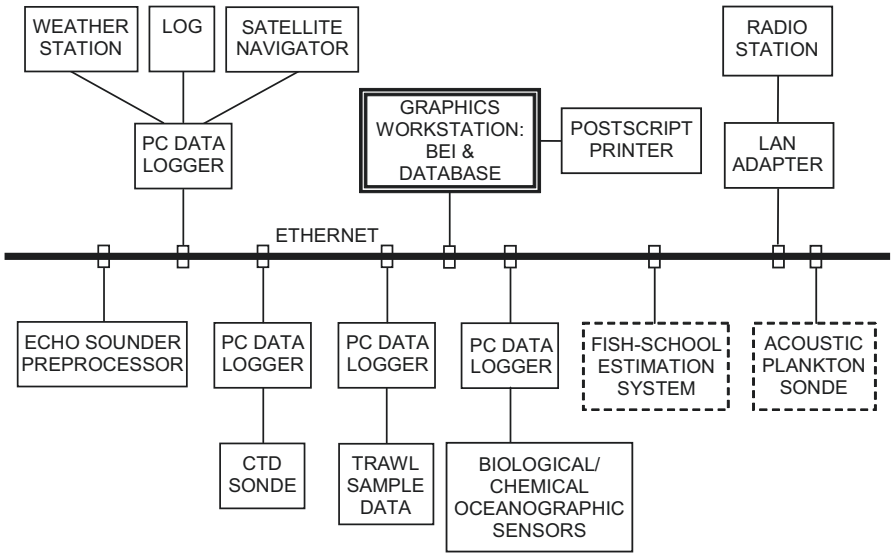

Fig. 7.1. A sample data network for research vessels

7.1. 2D visualization techniques in fishery acoustics

Advanced systems for acquisition (including preprocessing) and postprocessing of the hydroacoustic fishing survey data have been extensively used for the past three decades. The most popular echo sounders are often supported by dedicated software used for data storage as well as for its analysis, processing and visualization. Because of the extremely large amount of collected data, their visualization is performed using 2D graphics including classical imaging types like A and M [110] on an oscilloscope or a color computer screen. Such visualization, used mostly for echo analysis is usually supported by a color echogram, which displays echo sequences in successive transmissions. Both kinds of visualization have the time domain rescaled into distance and expressed in meter resolution. This type of visualization is typically used in all kinds of echo sounders. Newer systems, used for searching pelagic fish and estimating their target strength, are equipped with two transducers i.e. dual-beam systems or four transducers called split-beam echo sounders. The split-beam method uses a special configuration of the echo sounder's transducer as described in Chapter 3. The transducer is split into four sectors (quadrants), which in the transmitting phase are

working parallel with the same amplitude and phase, forming together one full beam. In the receiving mode, an echo signal reflected from a singular target is received by each sector separately. Then two pairs of segments, which are in perpendicular planes (parallel and perpendicular to ship axis), acquire the amplitude and echo phases what allows estimating the target location as shown in Fig. 7.2.

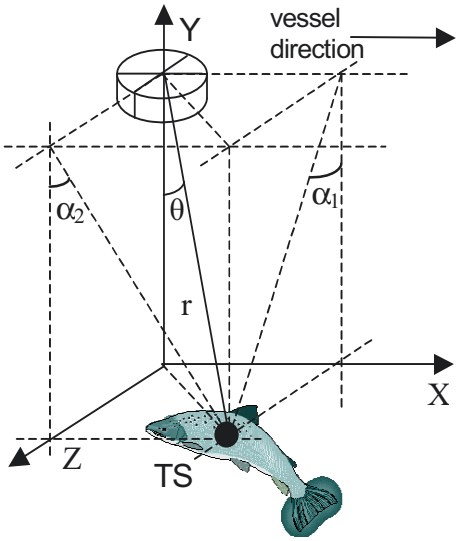

Fig. 7.2. Split-beam echo sounder coordinate system

In the Cartesian coordinate system the target's location is received by a simple transformation of the spherical coordinates [151]:

$$\begin{cases} y = r\cos\theta \\ x = y\tan\alpha_1 \\ z = y\tan\alpha_2 \end{cases} \tag{7.1}$$

where $\theta = \arctan\sqrt{\tan^2\alpha_1 + \tan^2\alpha_2}$, r is the distance from the target and angles α_1 and α_2 are displayed in Fig. 7.2. Note that the coordinate system is rather typical for graphics processors as it is different from those used typically in underwater applications, in which z coordinate defines the depth. The split-beam system guarantees accurate target localization and by adding GPS data with latitude and longitude information it is possible to achieve geographical coordinates of every detected object in every transmission. An example of a typical visualization of the split-beam echo sounder output is shown in Fig. 7.3. Along with classical echogram and oscilloscope displays, it shows the target position versus the angle (*bulls-eye* display). Such visualization is available only with a split-beam system.

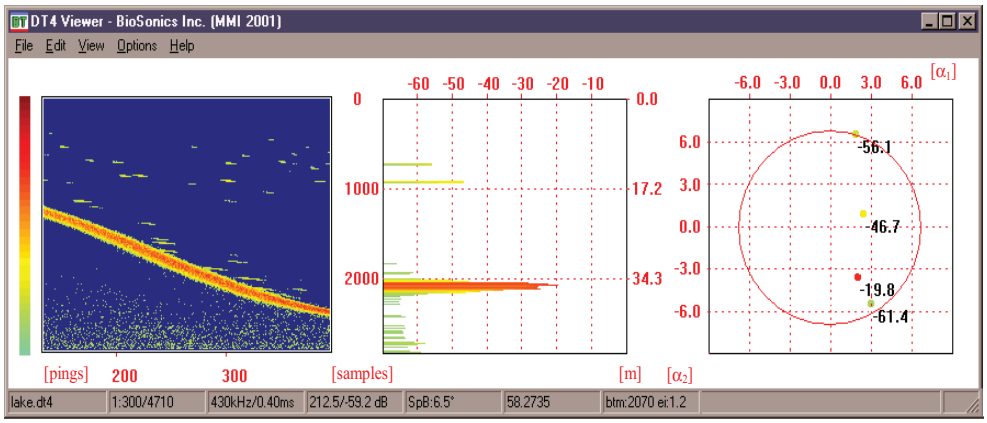

Fig. 7.3. 2D fish data visualization in DTX Biosonics Inc. system as implemented by the author

7.2. Modern hydroacoustic data processing

Hydroacoustic data processing block diagram for a three-dimensional visualization is shown in Fig. 7.4. The data, as records of envelope samples of the successive echosounder transmissions, are analyzed and recorded as a separate echo of a fish. Than, the match is made between the echo and echoes from the previous transmissions. A single moving fish in a beam gives a single echo (*fish tracking*). The algorithm requires a precise bottom detection algorithm, as the evaluated depth introduces limit in the fish counting algorithm. The data enriched with the angle data of the split-beam can be transformed to the relative Cartesian coordinates and then transformed to the absolute Cartesian coordinates, after matching them with the current geographical coordinates. Then transformed data are converted to the form which is in compliance with the VRML language. The obtained 3D scene could be extended by embedding electronic chart data.

As an example, Fig. 7.5 shows results of fish tracking algorithm in the form of simple 3D visualization [71] attached to the 2D multiresolution echogram. Subfigure A represents an echogram from a hull-mounted 120 kHz submersible transducer. The area bounded by horizontal lines shows the depth range covered by the printouts and the scattering layer with greater resolution are presented in Fig. 7.5B in 10 m range. Tracking and smoothing performed on targets found within circle in B are shown in subfigure C. The target was tracked for 135 echoes, average smoothed speed was ~8 cm/s, and average TS –74.1 dB. Horizontal plane in figure corresponds to the real horizontal plane. Subfigure D shows the track recorded simultaneously with track in subfigure C, where totally 125 echoes with average smoothed speed ~3 cm/s and average TS –68.2 dB were presented.

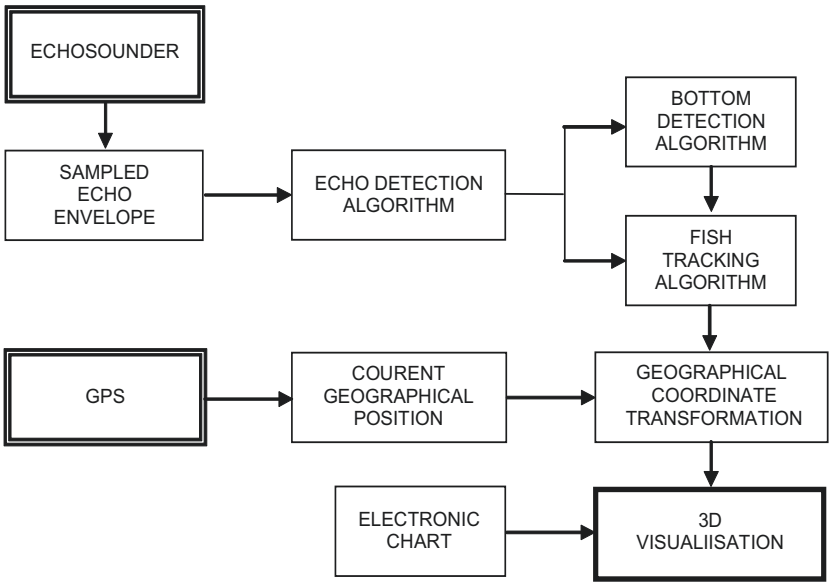

Fig. 7.4. Modern hydroacoustic fish data processing chain

7.3. Virtual reality modeling

Virtual Reality Modeling Language VRML is a popular language used in modeling of 3D static and animated scenes. Using its built-in properties, it is relatively easy to visualize movement of fish treated as an object in any coordinate system. VRML despite the typical application in computer graphics is also used in other various fields. For instance, in chemistry it is used for visualization of atom particles, in medicine for modeling of human organs, in astronomy for visualization of trajectories of the stars and in geography and navigation for creation of 3D maps. Hence, in this paper we describe its application in fisheries. Additionally, as any WWW browser can be equipped with a VRML plugin, 3D fish visualization can be redistributed on the Internet.

The Virtual Reality Modeling Language (VRML) was established in 1994, when the WWW enrichment by virtual reality was discussed during WWW Convention in Geneva. As a current standard version, we consider now VRML 97 (VRML 2.0), which was announced an international standard by International Standard Organization (ISO) in December 1997. VRML was developed in a natural process as the Internet evolved, moving from the text to the WWW era. This evolution was inspired by a demand of graphical presentation of the Internet data. VRML is a language of multi-factorial interactive simulations. The simulations are provided to a user over Internet and they are mutually connected through WWW. The simulations consist of predefined simple 3D objects, compounding of the complicated virtual world scenes. VRML is characterized by three features, which make it very attractive as compared to other 3D graphic applications. The first one is accessibility – it allows to see the

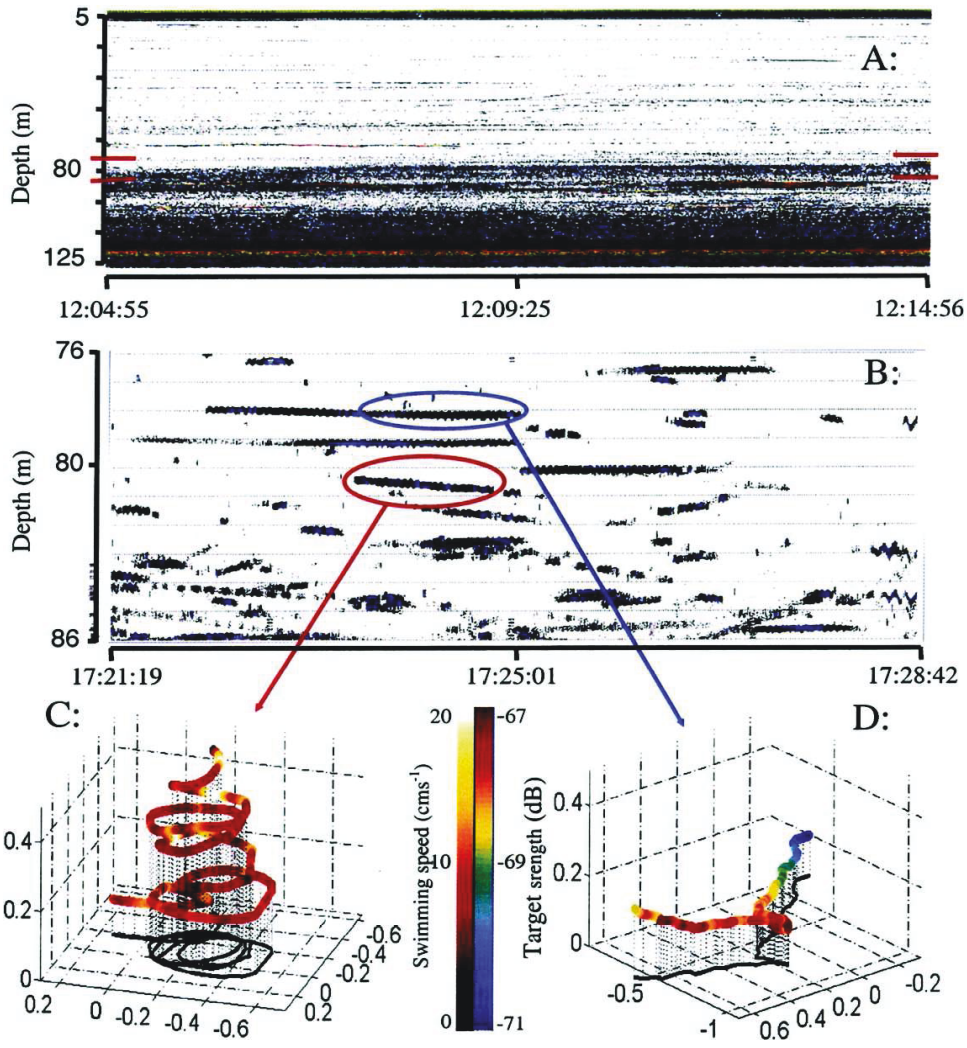

Fig. 7.5. An example of 3D visualization of echo trace from split beam data [71], XYZ-scales in meters

simulation over Internet even from a distance. The second is mobility – it allows a user to walk around the scene and to move objects (it is not possible in traditional 3D applications like AutoCad, 3DStudio). The third advantage is interactivity, which allows a user to have an influence on a behavior of objects by implementation of different kinds of sensors. The access to the simulation over Internet can be achieved by embedding VRML file into HTML code. The VRML has been successfully used by the author in visualization of multibeam sonar bathymetric data, especially in presentation of wrecks lying on the sea bottom [6].

The code defining 3D models is prepared as ASCII files. As an illustration let's consider a part of sample VRML source code presented in Fig. 7.6. It contains the definition of the fish model, as implemented by a Japanese company Toucan Corp. (http://www.toucan.co.jp). It makes use of some basic VRML nodes like Viewpoint, Background and Shape [12]. The crucial element of the model definition are x, y, z coordinates of the points for the fish body. It is achieved by IndexedFaceSet node, which contains coordinates of the model in Coordinate node and its indices of the body facets in coordIndex field. The look of the fish is defined by the 2D texture contained in ImageTexture node included in Appearance node. The indices of texture coordinates, which select proper fragments of the texture for every defined facet of the fish model, are defined in TextureCoordinate node. The result of modeling can be viewed in a WWW browser window.

```
#VRML V2.0 utf8

Viewpoint {
 description "Side"
 position -0.4 0.24 1
 orientation 0.2 0.3 0 -0.4
}
Background {
 skyColor [ 1  1  1 ]
}
Shape {
  appearance Appearance {
   material Material {diffuseColor 1  1  1}
   texture ImageTexture {url "PacifiT.gif"}
  }
  geometry IndexedFaceSet {
   coord DEF FishBody Coordinate { point [
    -0.3809437  5.339676E-02 -4.185965E-03 ,
    -0.4046955  4.374583E-02 -2.986661E-03 ,
    ... # x,y,z coordinates of an object
    -0.4450082 -5.569656E-02 -3.193669E-02 ,
    -0.4450365 -5.567609E-02 -3.193422E-02 ,
   ]}
   coordIndex [
     10  9  0 -1
     0  1  10 -1
     ... # indices of point coordinates
     1484  1489  1486 -1
     1489  1484  1487 -1
   ]
   texCoord TextureCoordinate { point [
     7.9845E-02  0.283,
     5.4412E-02  0.266,
     ...  # s,t coordinates of the texture
     0.3554  0.7716 ,
     0.3553  0.7716 ,
   ]}
   creaseAngle 1.5
  }
}
```

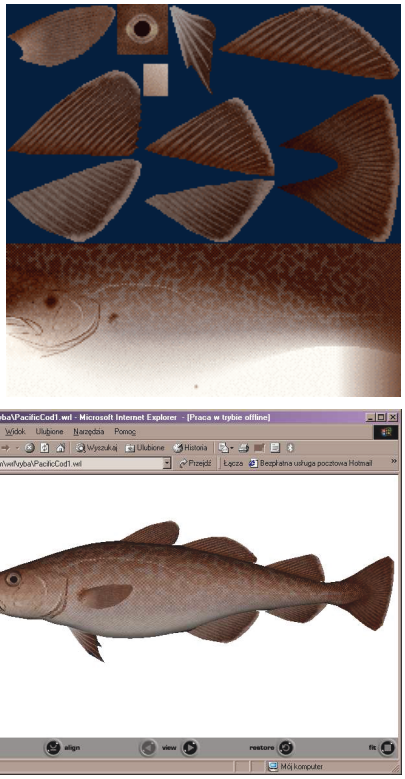

Fig. 7.6. The part of a sample VRML source code defining the fish model of pacific cod along with 2D texture and 3D result embedded in WWW browser (based on http://www.toucan.co.jp)

7.4. 3D fish data visualization in VRML

The sample VRML scene has been constructed from the measured data and presented in [103]. It consists of following elements: a sea area model, a ship model with an echo sounder, and a target model (fish). The model of the sea is made with the ElevationGrid node for a representation of the bottom and the Box node for a representation of the sea surface. The ship model was developed with the VRCreator 2.0 support using elements included in the program resources. The fish was generated with IndexedFaceSet node, and the rear fin of the fish was implemented with a CoordinateInterpolator node. The input data for the fish description consist of: the target number (fish), the target echo start time, the target location in the echo sounder beam in the 3D Cartesian coordinate system (x, y, z), the target size, the target strength and the location of target in the $y0z$plane. The target echo time is based on its sample number and the sounder transmitting rate. The target is located according to the Eq. (7.1) and the target size L is determined using empirical dependency between target strength (*TS)* and the fish length [19]:

$$\overline{TS} = 20 \log L - 29,2 \tag{7.2}$$

The fish is presented with a color according to the false color scale, which depends on the target strength. The target direction on the $y0z$ plane is determined from two successive location of the target in the echo sounder beam. It is possible to freely move over the scene and defined cameras allow observation of the simulation process. To improve the observation comfort, a LOD (*Level of Detail*) node was used, which sets the minimum distance, when the individual elements of the scene are visible [12].

An example of dynamic visualization was developed from the actual data, collected during the acoustic survey on Lake Washington; the data were acquired by the digital echo sounder DT6000 operated at 420 kHz. There are 4710 pings each having 2825 samples. Data processing module detected 8000 fish echoes and the number of fish extracted by fish tracking module was around 1000. As the data were collected with a rate of five pings per second, the acquisition time was about 17 minutes. In the scene description, the time is kept by the simulation through internal mechanisms of VRML. Fig. 7.7 presents an overview of the scene, and Fig. 7.8 presents a side of the beam. Fig. 7.9 is a top view and in the same moment, the profile of the beam is displayed. Note the 3D side view can be treated as 3D equivalent of classical echogram and top view as a 3D equivalent of bulls-eye display.

The software which converts the binary records from an acquisition system to the VRML scripting language was developed in C and Matlab languages. The Matlab allowed for a simultaneous control of data correctness and their transformation. As it turned out an interpretation of the scene (scene rendering) requires much computing power for fluent display. However, it should be noted, that although a user can easily and freely move around the entire virtual scene, only the fishes registered by the echo sounder can be visible. Their size is estimated by an approximate regression formula as presented in Chapter 3, and a move, a direction and an orientation are approximated using interpolation based on the data from the echo sounder.

It is author's hope that the concept of virtual 3D echogram as presented in this last chapter may replace traditionally used echogram in near future. Although the

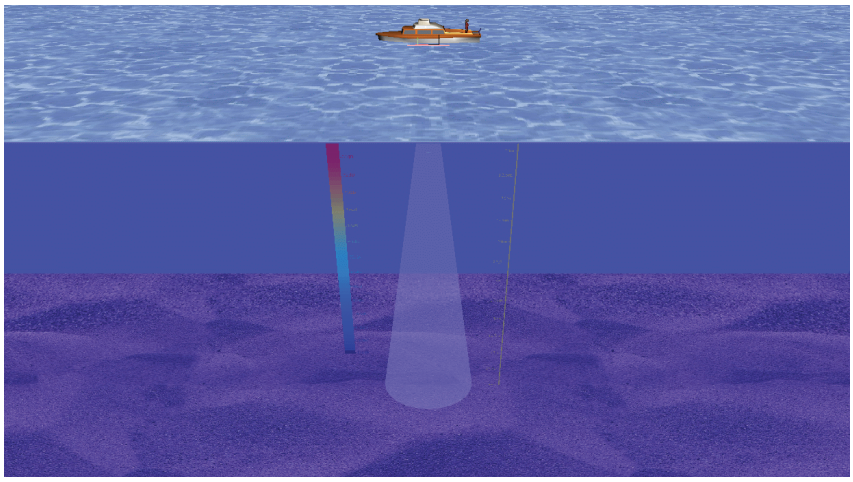

Fig. 7.7. General view of the scene containing fish in aquatic environment

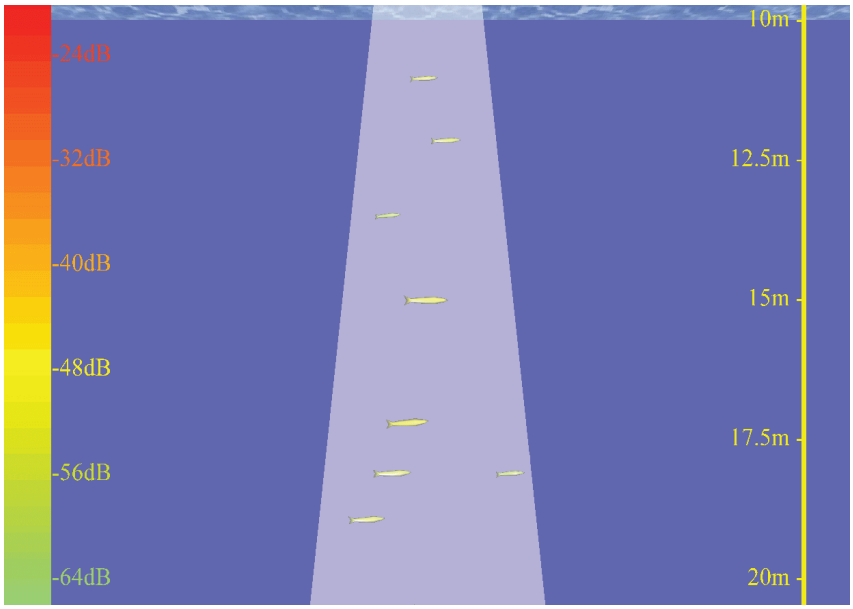

Fig. 7.8. Side of the beam – 3D equivalent of the echogram

recent developments in information technology has made revolutionary progress, the visualization of the data collected by sonar systems is still a challenging problem. Nevertheless, we can expect new ideas very soon.

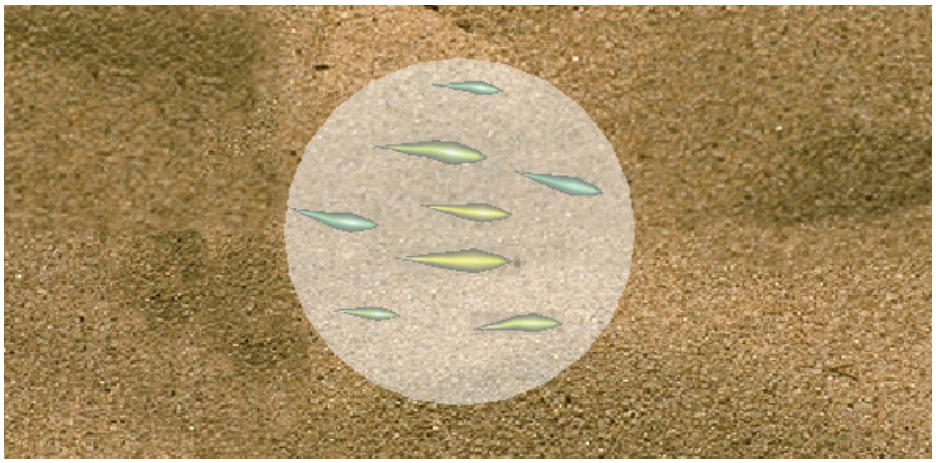

Fig. 7.9. Top view – equivalent of the bulls-eye display

BIBLIOGRAPHY

[1] Abramovich F., Silverman B.W.: The vaguelette-Wavelet Decomposition approach to Statistical inverse problems. *Biometrika*, 1998, 85(1), 115–129.

[2] Ainslie M.A.: The sonar equation and the definition of propagation loss. *J. Acous. Soc. Am.*, 2004, 115(1), 131–134.

[3] Albers V.M., editor: *Underwater Acoustics*, volume 2. New York: Plenum, 55–88.

[4] Andreeva I.B.: Scattering of sound by air bladders of fish in deep sound scattering ocean layers. *Sov. Phys. Acoust*, 1964, 10, 17–20.

[5] Baar R., Coombs R.F.: Target phase: An extra dimension for fish and plakton target identification. *J. Acous. Soc. Am.*, 2005, 118(3), 1358–1371.

[6] Bikonis K., Moszyński M., Stepnowski A.: Submerged Object Imaging Using Virtual Reality Modeling Language. In: *Underwater archeology – Bodrum*.

[7] Bracewell R.: *The Fourier Transform and Its Application*. Mc Graw-Hill, Inc., 1965.

[8] Brekhovskikh L.M., Godin O.A.: *Acoustics of Layered Media*. Berlin Heidelberg: Springer-Verlag, 1990.

[9] Burczynski J.: Introduction to the use of sonar systems for estimating fish biomass. *FAO Fish. Tech. Paper No. 191*, 1979.

[10] Burdic R.J.: *Underwater Acoustics System Analysis*. Englewood Cliffs, Prentice-Hall Inc., 1985.

[11] Burton A.J., Miller G.F.: The application of the integral equation method to the numerical solution of some exterior boundary values problems. *Proc. of Royal Soc. London. Series A*, 1971, 323, 201–210.

[12] Carey R., Bell G., Marrin C.: *The Virtual Reality Modeling Language*. The VRML Consortium Inc., 1997.

[13] Chivers R.C., Anson L.W.: Calculation of the backscattering and radiation force functions of spherical targets for use in ultrasonic beam assessment. *Ultrasonics*, 1981, 20, 25–34.

[14] Clay C.S.: Deconvolution of the fish scattering PDF from the echo PDF for a single transducer sonar. *J. Acous. Soc. Am.*, 1983, 73(6), 1989–1994.

[15] Clay C.S.: Low-resolution acoustic scattering models: fluid-filled cylinders and fish with swimbladders. *J. Acous. Soc. Am.*, 1991, 89, 2168–2179.

[16] Clay C.S., Heist B.G.: Acoustic scattering by fish – acoustic models and a two-parameter fit. *J. Acous. Soc. Am.*, 1984, 75, 1077–1083.

[17] Clay C.S., Horne J.K.: Acoustic models of the fish: The Atlantic cod (*Gadus morhua*). *J. Acous. Soc. Am.*, 1994, 96, 1661–1668.

[18] Craig R.E., Forbes S.T.: Design of a sonar for fish counting. *FiskDir. Ser. Haveunders.*, 1969, 15, 210–219.

[19] Crocker M.J., editor: *Encyclopedia of Acoustics*. John Wiley & Sons, Inc., 493–500.

[20] Dempster A.P., Laird N.M., Rubin D.B.: Maximum likelihood from incomplete data via the EM algorithm (with discussion). *J. R. Statist. Soc. B.*, 1977, 39, 1–38.

[21] Do M.A., Surti A.N.: Estimation of dorsal aspect target strength of deep-water fish using a simple model of swimbladder backscattering. *J. Acous. Soc. Am.*, 1990, 87(4), 1588–1596.

[22] Döring R.: Concepts of Sustainable Fisheries. In: *The Tenth Biennial Conference of*

the International Institute of Fisheries Economics and Trade.

[23] Edwards J.I., Armstrong F.: Measurements of the target strength of live herring and mackerel. In: *FAO Fisheries Report*, volume 300. 69–77.

[24] Ehrenberg J.E.: Estimation of the intensity of a filtered Poisson process and its application to acoustic assessment of matine organisms. In: *Univ. Wash. Sea Grant Publ. WSG 73-2*.

[25] Ehrenberg J.E.: New methods for indirectly measuring the mean acoustic backscattering cross section of fish. In: *ICES/FAO Symposium on Fisheries Acoustics, Bergen*.

[26] Ehrenberg J.E.: A review of *in situ* target strenfth estimation techniques. In: *ICES/FAO Symposium on Fisheries Acoustics, Bergen*. 85–90.

[27] Ehrenberg J.E., Carlson T.J., Traynor J.J., Williamson N.: Indirect measurement of mean acoustic backscattering cross section of fish. *J. Acous. Soc. Am.*, 1981, 69, 955–962.

[28] FAO: *The State of World Fisheries and Aquaculture*. FAO, Rome, 2000.

[29] Faran J.J.: Sound scattering by Solid Cylinders and Spheres. *J. Acous. Soc. Am.*, 1951, 23, 405–418.

[30] Feuillade C., Nero R.W.: A viscous-elastic swimbladder model for describing enhanced-frequency resononce from fish. *J. Acous. Soc. Am.*, 1998, 103, 3245–3255.

[31] Fleischman S.J., Burwen D.L.: Correcting for position-related bias in estimates of the acoustic backscattering cross-section. *Aquatic Living Resources*, 2000, 13, 283–290.

[32] Foote K.G.: Angular measures of dorsal aspect target strength functions of fish. *Fiskeridirektoratets Skrifter Serie Havundersokelser*, 1980, 17, 49–70.

[33] Foote K.G.: Averaging of fish target strength functions. *J. Acous. Soc. Am.*, 1980, 67(2), 504–515.

[34] Foote K.G.: Importance of the swimbladder in acoustic scattering from fish: A comparison of gadoid and mackerel target strengths. *J. Acous. Soc. Am.*, 1980, 67, 2084–2089.

[35] Foote K.G.: Optimising copper spheres for precision calibration of hydroacoustic equipment. *J. Acous. Soc. Am.*, 1982, 71, 742–747.

[36] Foote K.G.: Rather-high-frequency sound scattering by swimbladdered fish. *J. Acous. Soc. Am.*, 1985, 78, 688–700.

[37] Foote K.G.: A critique of Goddard and Welsby's paper 'The acoustic target strength of live fish'. *J. Cons. Int. Explor. Mer.*, 1986, 42, 212–220.

[38] Foote K.G.: Fish target strength for use in echo integrator surveys. *J. Acous. Soc. Am.*, 1987, 82(3), 981–987.

[39] Foote K.G.: Acoustic sampling volume. *J. Acous. Soc. Am.*, 1991, 90, 959–964.

[40] Foote K.G.: Summary if methods for determining fish target strength at ultrasonics frequencies. *ICES J. Mar. Sci.*, 1991, 48, 211–221.

[41] Foote K.G.: Coincidence echo statistics. *J. Acous. Soc. Am.*, 1996, 99(1), 266–271.

[42] Foote K.G., Aglen A., Nakken O.: Measurement of fish target strength with a split-beam echo sounder. *J. Acous. Soc. Am.*, 1986, 80(2), 612–621.

[43] Foote K.G., Francis D.T.I.: Comparing Kirchhoff-approximation and boundary-element models for computing gadoid target strengths. *J. Acous. Soc. Am.*, 2002, 111, 1644–1654.

[44] Foote K.G., Knudsen H.P., Korneliussen R.J., Nordbö P.E., Röang K.: Postprocessing system for echo sounder data. *J. Acous. Soc. Am.*, 1991, 90(1), 37–47.

[45] Foote K.G., MacLennan D.N.: Comparison of copper and tungsten carbide calibration spheres. *J. Acous. Soc. Am.*, 1982, 71, 742–747.

[46] Foote K.G., Traynor J.J.: Comparisons of walleye pollock target strength estimates determined from *in situ* measurements and calculations based on swimbladder form. *J. Acous. Soc. Am.*, 1988, 83, 9–17.

[47] Francis D.T.I.: A gradient formulation of the Helmholtz integral equation for acoustic radiation and scattering. *J. Acous. Soc. Am.*, 1993, 93, 1700–1709.
[48] Francis D.T.I., Foote K.G.: Depth-dependent target strength of gadoids by the boundary-element method. *J. Acous. Soc. Am.*, 2003, 114, 3136–3146.
[49] Furusawa M.: Prolate Spheroidal Models for Predicting General Trends of Fish Target Strength. *J. Acous. Soc. Jpn. (E)*, 1988, 9, 13–24.
[50] Furusawa M., Sawada K.: Effects of transducer motion on quantifying single fish echoes. *Nippon Suisan Gakkaishi*, 1991, 57, 857–864.
[51] Gauthier S., Horne J.K.: Acoustic characteristics of forage fish species in the Gulf of Alaska and Bering Sea based on Kirchhoff-approximation models. *Can. J. Fish. Aquat. Sci.*, 2004, 61, 1839Ũ–1850.
[52] Gerlotto F., Georgakarakos S., Eriksen P.K.: The application of multibeam sonar technology for quantitive estimates of fish density in shallow water acoustic surveys. *Aquatic Living Resources*, 2000, 13, 385–393.
[53] Gerlotto F., Soria M., Freon P.: From two dimensions to three: the use of multibeam sonar for a new approach in fisheries acoustics. *Can. J. Fish. Aquat. Sci.*, 1999, 56, 6–12.
[54] Glasko V.B.: *Inverse Problems of Mathematical Physics*. New York: American Institute of Physics, 1988.
[55] Gordon H.S.: The Economic Theory of a Common-Property-Resource: The Fishery. *Journal of Political Economy*, 1954, 62, 124–142.
[56] Gorska N., Ona E.: Modelling the acoustic effect of swimbladder compression in herring. In: *Proc. of ICES Symposium on Fisheries and Aquatic Ecology – Montpellier*.
[57] Haddon M.: *Modelling and quantitative methods in fisheries*. Chapman and Hall/CRC, 2001.
[58] Hasegawa T.: Comparison of two solutions for acoustic radiation pressure on a sphere. *J. Acous. Soc. Am.*, 1977, 61, 1445–1448.
[59] Haslett R.W.G.: Measurements of the dimensions of fish to facilitate calculation of echo strength in acoustic fish detection. *J. Cons. Int. Explor. Mer.*, 1962, 27, 261–269.
[60] Hazen E.L., Horne J.K.: A method for evaluating effects of biological factors on fish target strength. *ICES Journal of Marine Science*, 2003, 60, 555–562.
[61] Hedgepeth J.B.: *Stock assessment with hydroacoustic estimates of abundance via tuning and smoothed EM estimation*. Ph.d. diss., University of Washington, Seattle WA., 1994.
[62] Hedgepeth J.B., Gallucci V.F., O'Sullivan F., Thorne R.E.: An expectation maximization and smoothing approach for indirect acoustic estimation of fish size and density. *ICES J. Mar. Sci.*, 1989, 56, 36–50.
[63] Hickling R.: Analysis of Echoes from a Solid Elastic Sphere in Water. *J. Acous. Soc. Am.*, 1962, 34, 1582–1592.
[64] Hochstadt H.: *Integral Equations*. New York: John Wiley & Sons, 1973.
[65] Horton J.W.: *Fundamentals of Sonar, 2nd ed.*. United States Naval Institute, Annapolis, 1959.
[66] Hwang W.S.: Boundary spectral method for acoustic scattering and radiation problems. *J. Acous. Soc. Am.*, 1997, 102, 96–101.
[67] Jech J.M., Schael D.M., Clay C.S.: Application of three sound scattering models to threadfin shad (*dorosoma petenense*). *J. Acous. Soc. Am.*, 1995, 98(4), 2262–2269.
[68] Jensen F.B., Kuperman W.A., Porter M.B., Schmidt H.: *Computational Ocean Acoustics*. American Institute of Physics, Woodbury, NY, 1994.
[69] Johannesson K.A., Mitson R.B.: Fisheries acoustics: a practical manual for biomass estimation. *FAO Fish. Tech. Paper No. 240*, 1983.

[70] Kalikhman I.L., Tessler W.D.: The effective parameters of the real acoustic beam. In: *FAO Fisheries Report*, volume 300. 9–17.

[71] Klevjer T.A., Kaartvedt S.: Split-beam target tracking can be used to study the swimming behaviour of deep-living plankton *in situ*. *Aquatic Living Resources*, 2003, 16, 293–298.

[72] Kloser R.J., Williams A., Koslow J.A.: Problems with acoustic target strenght measurements of deepwater fish, orange roughy (*Hoplostethus atlanticus*, Collett). *ICES Journal of Marine Science*, 1997, 54, 60–71.

[73] Knight W.C., Pridham R.G., Kay S.M.: Digital Signal Processing for Sonar. *IEEE Proc.*, 2000, 69, 1451–2562.

[74] Korneliussen R.J., Ona E.: Synthetic echograms generated from the relative frequency response. In: *Proc. of ICES Symposium on Fisheries and Aquatic Ecology – Montpellier*.

[75] Lasota H.: Mechanism of acoustic wave propagation: A real role of virtual sources. *Journal of Computational Acoustics*, 2001, 9(7), 719–730.

[76] Love R.H.: Target strength of an individual fish at any aspect. *J. Acous. Soc. Am.*, 1977, 62(6), 1397–1403.

[77] Love R.H.: Resonant acoustic scattering by swimbladder-bearing fish. *J. Acous. Soc. Am.*, 1978, 64, 571–580.

[78] Lurton X.: *An Introduction to Underwater Acoustics*. Springer, 2002.

[79] MacLennan D.N.: Time varied gain functions for pulsed sonars. *J. of Sound. and. Vibration*, 1986, 110(3), 511–522.

[80] MacLennan D.N.: Acoustical measurement of fish abundance. *J. Acous. Soc. Am.*, 1990, 87(1), 1–15.

[81] MacLennan D.N.: Fishing gear selectivity: an overview. *Fisheries Research*, 1992, 13, 201–204.

[82] MacLennan D.N., Dunn J.R.: Estimation of sound velocities from resonance measurements on tungsten carbide calibration spheres. *J. of Sound. and. Vibration*, 1984, 97(2), 321–331.

[83] MacLennan D.N., Fernandes P.G., Dalen J.: A consistent approach to definitions and symbols in fisheries acoustics. *ICES J. Mar. Sci.*, 2002, 59, 365–369.

[84] MacLennan D.N., Fernandes P.G., Dalen J.: A consistent approach to definitions and symbols in fisheries acoustics. *ICES J. Mar. Sci.*, 2002, 59, 365–369.

[85] MacLennan D.N., Forbes S.T.: Acoustic methods of fish stock estimation. *Rapp. P.-v. Reun. Cons. Int. Explor. Mer.*, 1984, 184, 7–18.

[86] MacLennan D.N., Menz A.: Interpretation of *in situ* target strength data. *ICES J. Mar. Sci.*, 1996, 53, 233–236.

[87] MacLennan D.N., Simmonds E.J.: *Fisheries Acoustics*. London: Chapman and Hall, 1992.

[88] Marple S.L.: *Digital Spectral Analysis*. Prentice-Hall Inc., 1987.

[89] Medwin H., Clay C.S.: *Fundamentals of Acoustical Oceanography*. Academic Press, 1998.

[90] Megrey B.A., Moksness E.: *Computers in Fishery Research*. Chapman & Hall, 1996.

[91] Midson B.: Acoustic systems for the assessment of fisheries. *FAO Fish. Circ.*, 1984, 778, 1–132.

[92] Midttun L.: Fish and other organisms as acoustic targets. *Rapp. P.-v. Reun. Cons. Int. Explor. Mer.*, 1984, 184, 25–33.

[93] Morfey C.L.: *Dictionary of Acoustics*. Academic, San Diego, 2001.

[94] Moszyński M.: *Metody rozwiązania zagadnienia odwrotnego estymacji siły celu ryb*. Ph.d. diss., Gdansk University of Technology, Faculty of Electronics, Telecommunica-

tion and Informatics, 1997.
[95] Moszyński M.: Main lobe approximation for the target strength inverse problem. In: *Proc. of 4th European Conference on Underwater Acoustics, Rome*.
[96] Moszyński M.: Wavelet Decomposition In Target Strength Estimation. In: *Proc. of 4th European Conference on Underwater Acoustics, Rome*.
[97] Moszyński M.: Wavelet decomposition versus singular value decomposition (SVD) in fish target strength estimation. In: *Forum Acousticum, Berlin*.
[98] Moszyński M.: Inverse Methods of Indirect Fish Target Strength Estimation Combined with Fish Counting Statistics. In: *Proc. of 5th European Conference on Underwater Acoustics, Lyon*. 1533–1538.
[99] Moszyński M.: Adaptive Expectation Maximization Smoothing (AEMS) inverse technique for indirect fish target strength estimation. In: *Proc. of ICES Symposium on Fisheries and Aquatic Ecology – Montpellier*.
[100] Moszyński M.: Fish Target Strength Estimation Using Multiple Echo Statistics. *Acoustical Physics*, 2002, 48(2), 201–208.
[101] Moszyński M.: Fish Target Strength Estimation Versus Fish Backscattering Cross-section Estimation. In: *Proc. of 6th European Conference on Underwater Acoustics, Gdansk*.
[102] Moszyński M.: Indirect Methods of Fish Target Strenght Estimation in Absolute and Logarithmic Domain. *Acta Acustica united with Acustica*, 2002, 88(5), 726–729.
[103] Moszyński M., Bikonis K., Demkowicz J.: VRML visualization of pelagic fish movement in the echosounder beam. In: *Hydroacoustics*. 53–58.
[104] Moszyński M., Hedgepeth J.B.: Using single-beam side-lobe observation of fish echoes for fish target strength and abundance estimation in shallow water. *Aquatic Living Resources*, 2000, 13, 379–383.
[105] Moszyński M., Stepnowski A.: Using the Discrete Mellin Transform (DMT) and singular value decomposition (SVD) for estimation of fish target strength from acoustics echoes. In: *Proc of 3rd European Conference On Underwater Acoustics, Heraclion, Kreta*.
[106] Moszyński M., Stepnowski A.: The Statistics of Fish Echo Traces for Beam Pattern PDF Calculation. In: *Proc. of 5th European Conference on Underwater Acoustics, Lyon*. 1437–1442.
[107] Moszyński M., Stepnowski A.: Increasing the Accuracy of Time-varied-gain in Digital Echosounders. *Acta Acustica united with Acustica*, 2002, 88(5), 814–817.
[108] Moszyński M., Stepnowski A.: The Estimation Of Fish Length Distribution From Its Acoustical Estimates. In: *Proc. of Sixth European Conference on Underwater Acoustics*.
[109] Nakken O., Olsen K.: Target strength measurements of fish. *Rapp. P.-v. Reun. Cons. Int. Explor. Mer.*, 1977, 170, 52–69.
[110] Nowicki A.: *Diagnostyka ultradźwiękowa*. Wydawnictwo Medyczne MAKmed, Gdańsk, 2000.
[111] Olsen K.: Fish behaviour ad acoustic sampling. *Rapp. P.-v. Reun. Cons. Int. Explor. Mer.*, 1990, 189, 147–158.
[112] Ona E.: Target tracking with a split-beam echo sounder. In: *International Symposium on Fishery Acoustics – Seattle*.
[113] Ona E.: Physiological factors causing natural variations in acoustic target strength of fish. *J. Marine Biological Association of the United Kingdom*, 1990, 70, 107–127.
[114] Ona E.: An expanded target strength relation for herring. In: *Proc. of ICES Symposium on Fisheres and Aquatic Ecology – Montpellier*.
[115] Orfanidis S.J.: *Optimum signal processing: An Introduction*. New York: Macmillan

Publishing Company, 1985.
[116] Orłowski A.: Hydroacoustic characteristics of scattering layers in the Northeastern Atlantic Ocean. *J. Acous. Soc. Am.*, 1990, 88(1), 298–309.
[117] Orłowski A.: Acoustic methods applied to fish environmental studies in the Baltic Sea. *Fisheries Research*, 1998, 34, 227–237.
[118] Orłowski A.: Behavioural and physial effect on acoustic measurements of Baltic fish within diel cycle. *ICES J. Of Marine Science*, 2001, 58, 1174–1183.
[119] Ostrovsky L.A., Klusek Z., Sutin A.M., Soustova I.A., Matveyev A.I., Potapov A.I.: Observation of nonlinear scattering of acoustical waves at a subsurface bubble layer. In: *The 130th Meeting of the Acoustical Society of America.*
[120] Papoulis A.: *Probability, Random Variables, and Stochastic Processes.* Mc Graw-Hill, Inc., 1965.
[121] Petersen M.L., Clay C.S., Brandt S.B.: Acoustic estimates of fish density and scattering function. *J. Acous. Soc. Am.*, 1976, 60, 618–622.
[122] Polyanin A.D., Manzhirov A.V.: *Handbook of Integral Equations.* Boca Raton: CRC Press, 1998.
[123] Poularikas A.D.: *The transforms and applications handbook.* IEEE Press, 1996.
[124] Press W.H., Flannery B.P., Teukolsky S.A., Vetterling W.T.: *Numerical Recipes in C.* Cambridge University Press, 1988.
[125] Reeder D.B., Jech J.M., Stanton T.K.: Broadband acoustic backscatter and high-resolution morphology of fish: Measurement and modeling. *J. Acous. Soc. Am.*, 2004, 116(2), 747–761.
[126] Reynisson P.: Evaluation of threshold-induced bias in the integration of single-fish echoes. *ICES J. Mar. Sci.*, 1996, 53, 345–350.
[127] Robinson B.J.: *In situ* measurements of the target strength of the pelagic fish. *FAO Fish. Rep.*, 1983, 300, 99–103.
[128] Rose G.A.: A review of problems and new directions in the application of fisheries acoustics on the Canadian east Coast. *Fisheries Research*, 1992, 14, 105–128.
[129] Rose G.A., Porter D.R.: Target strength studies on Atlantic cod (*Gadus morhua*) in Newfoundland waters. *ICES J. Mar. Sci.*, 1996, 53, 259–265.
[130] Rudstam L.G., Clay C.S., Magnuson J.J.: Density and size estimates of cisco (*coregonus artedii*) using analysis of echo peak PDF. *Can. J. Fish. Aquat. Sci.*, 1987, 44, 811–821.
[131] Saenger R.A.: Swimbladder size variability in mesopelagic fish and bioacoustic modeling. *J. Acous. Soc. Am.*, 1988, 84(3), 1007–1017.
[132] Sawada K., Furusawa M., Williamson N.J.: Conditions for the precise measurement of fish target strength *in situ*. *Fisheries Research*, 1993, 20, 139–144.
[133] Schenk H.A.: Improved integral formulation for acoustic radiation problem. *J. Acous. Soc. Am.*, 1968, 44, 41–58.
[134] Schmidt C.C.: Fish crisis: A problem of scale. *OECD Observer*, 2002, August.
[135] Silverman B.W.: *Density Estimation for Statistics and Data Analysis.* London: Chapman and Hall, 1996.
[136] Silverman B.W., Jones M.C., Nychka D.W., Wilson J.D.: Smoothed EM approach to indirect estimation problems with particular reference to stereology and emission tomography. *J. R. Statist. Soc. B.*, 1990, 52(2), 271–324.
[137] Simpson P.K., Denny G.F.: Scifish 2000: A Broadband Sonar Fish Identification System. In: *Proc. of ICES Symposium on Fisheries and Aquatic Ecology – Montpellier.*
[138] Skudrzyk E.: *The Foundations of Acoustics.* Springer-Verlag, 1971.
[139] Smith C.R., Grandy W.T.: *Maximum-Entropy and Bayesian Methods in Inverse Problems.* Boston: Reidel, 1985.

[140] Soule M.A., Barange M., Hampton I.: Evidence of bias in estimates of target strength obtained with split-beam echo-sounder. *ICES J. Mar. Sci.*, 1995, 52, 139–144.
[141] Soule M.A., Hampton I.: Use of multi beam echo sounders for estimation of target strength of fish *in situ*. In: *Proc. of ICES Symposium on Fisheries and Aquatic Ecology – Montpellier*.
[142] Spindel R.C., McElroy P.T.: Level and zero crossing in volume reverberation signals. *J. Acous. Soc. Am.*, 1973, 53, 1417–1426.
[143] Stanton T.K.: Density estimate of biological sound scatterers using sonar echo peak PDFs. *J. Acous. Soc. Am.*, 1985, 78, 1868–1873.
[144] Stanton T.K.: Volume scattering: echo peak PDF. *J. Acous. Soc. Am.*, 1985, 77, 1358–1366.
[145] Stanton T.K.: Sound scattering by cylinders of finite length. I. Fluid cylinders. *J. Acous. Soc. Am.*, 1988, 83, 55–63.
[146] Stanton T.K.: Sound scattering by cylinders of finite length. II. Elastic cylinders. *J. Acous. Soc. Am.*, 1988, 83, 64–67.
[147] Stanton T.K.: Simple appoximate formulas for backscattering of sound by spherical and elongated objects. *J. Acous. Soc. Am.*, 1989, 86, 1499–1510.
[148] Stanton T.K.: Sound scattered by cylinders of finite length. III. Deformed cylinders. *J. Acous. Soc. Am.*, 1989, 86, 691–705.
[149] Stanton T.K., Clay C.S.: Sonar Echo Statistics as a Remote-Sensing Tool: Volume and Seafloor. *IEEE Journal of Ocean Engineering*, 1986, OE-11(1), 79–96.
[150] Stepnowski A.: *Zarys teorii i technika hydroakustycznych metod oceny siły celu i populacji ryb*. Hab. diss., Akademia Marynarki Wojennej 111C, Gdynia, 1991.
[151] Stepnowski A.: *Systemy Akustycznego Monitoringu Środowiska Morskiego*. Gdańsk: Gdańskie Towarzystwo Naukowe, 2001.
[152] Stepnowski A., Martin W., Salamon R., Burczyński J.: The computerized system for estimating spatial distribution of fish stock used on R.V. Profesor Siedlecki. In: *Proc. 8th International Congress on Acoustics (ICA)*, volume 2.
[153] Stepnowski A., Mitchell R.S.: ECOLOG II: a real-time acoustic signal processing system for fish stock assessment. *Ultrasonics*, 1990, 28, 256–265.
[154] Stepnowski A., Moszyński M.: Inverse problem solution techniques as applied to indirect *in situ* estimation of fish target strength. *J. Acous. Soc. Am.*, 2000, 107, 2554–2562.
[155] Sund O.: Echo sounding in fisheries research. *Nature*, 1935, 135, 953–955.
[156] Szczucka J.: *Akustyczne badania biologicznych warstw rozpraszających w Południowym Bałtyku*. Hab. diss., Inst. Oceanol. PAN, Sopot, 2003.
[157] Taroudakis M.I., Makrakis G.N.: *Inverse Problems in Underwater Acoustics*. New York: Springer-Verlag, 2001.
[158] Tikhonov A.N., Arsenin V.Y.: *Solution of ill-posed problems*. New York: Wiley, 1977.
[159] Tollefsen C.S., Zedel L.: Evaluation of a Doppler Sonar System for Fisheries Applications. In: *Proc. of ICES Symposium on Fisheries and Aquatic Ecology – Montpellier*.
[160] Traynor J.J.: Target strength measurement of walleye pollock (*Theragra chacogramma*) and Pacific whiting (*Merluccius productus*). *ICES J. Mar. Sci.*, 1996, 53, 253–258.
[161] Traynor J.J., Ehrenberg J.E.: Fish and standard sphere target strength measurements obtained with dual-beam and split-beam echosounding system. *Rapp. P.-v. Reun. Cons. Int. Explor. Mer.*, 1990, 189, 325–335.
[162] Trevorrow M.V., Mackas D.L., Benfield M.C.: Comparison of multifrequency acoustic and *in situ* measurements of zooplankton abundances in Knight Inlet, British Columbia. *J. Acous. Soc. Am.*, 2005, 117(6), 3574–3588.
[163] Unser M., Blu T.: Wavelet Theory Demystified. *IEEE Transactions on Signal Processing*, 2003, 51, 2, 470–483.

[164] Urick R.J.: *Principles of Underwater Sound*. New York: Mc Graw Hill, 1983.
[165] Vath M.: *Volterra and integral equations of vector functions*. New York: Marcel Dekker Inc., 2000.
[166] Waite A.D.: *Sonar for Practising Engineers*. John Wiley & Sons, Ltd, 2002.
[167] Wang W., Atalla N., Nicols J.: A boundary integral approach for acoustic radiation of axisymmetric bodies with arbitrary boundary conditions valid for all wave numbers. *J. Acous. Soc. Am.*, 1997, 101, 1468–1478.
[168] Yang S.A.: Acoustic scattering by a hard and soft body across a wide frequency range by the Helmholtz integral equation method. *J. Acous. Soc. Am.*, 1997, 102(5), 2511–2520.
[169] Yang S.A.: An investigation into integral equation methods involving nearly singular kernels for acoustic scattering. *J. of Sound and Vibration*, 2000, 234(2), 225–239.
[170] Zienkiewicz O.C., Taylor R.L.: *The Finite Element Method*. London: McGraw-Hill, 1989.

STATISTICAL ANALYSIS FOR DIGITAL PROCESSING OF PELAGIC FISH ECHOES

The dissertation presents the application of inverse methods in fishery acoustics in the problems of fish target strength estimation and fish length estimation. After introductory part, which constitutes the first chapter of the book, in the second chapter the scattering from underwater objects is described. In particular, the aspects related to theory of scattering by a sphere and a cylinder, which are used in modeling of a scattering properties of a fish are considered. To measure reflecting properties of the fish terms like backscattering cross section, backscattering length and target strength are defined, which are commonly used for monostatic systems used in fisheries. Some experimentally obtained formulae for target strength to length relationship are presented along with acoustic models of the fish.

It is shown in chapter 3, that among the methods used in these days for remote classification of fish populations the only reasonable ones are in situ acoustic methods. The hydroacoustic systems used in fisheries until eighties equipped with classical single beam systems allowed for fish abundance estimation using so called echo integration approach. The unknown fish position in the transducer beam push forward the development of specialized system for fishery application like dual- beam systems and split-beam systems. Nevertheless, as the fish echoes were resolved, the fish target strength estimates could be calculated from single-beam systems by statistical removal of unknown fish position, which were though at that time as a very modern method. The detailed analysis of echo formation process presented in the chapter and formulated in the form of stochastic process allows solving the problem of fish target strength estimation by applying the concept of beam pattern probability density function (PDF) as a kernel function of integral equations. The effective solution of such equations leads to application of inverse techniques.

Hence, in chapter 4 the inverse methods as applied to fish target strength estimation are presented. It is well known that in most practical cases found in physics, the inverse approach results in numerically ill conditioned and unstable solution, so exact methods of solution simply fail. However, as it was shown in the chapter the modern methods based on regularization and iterative approaches give quite reliable solutions particularly useful for probability density estimates.

In chapter 5, transducer beam pattern PDF and fish directivity pattern PDF and the ways of their determination are presented. Both PDFs represent kernel functions of integral equation required for solving the inverse problem. The former is used in fish target strength estimation, the latter – in fish length estimation.

Chapter 6 contains examples of data acquired in acoustic surveys and the results of its statistical processing using methods presented in previous chapters.

The last chapter is slightly different from the main stream of the book. It introduces the modern Information Technology techniques in the field of fishery acoustics. The results of signal processing and specialized algorithms as used by the author allow for 3D visualization of fish echo data.

ANALIZA STATYSTYCZNA W CYFROWYM PRZETWARZANIU ECH OD RYB PELAGICZNYCH

Praca poświęcona jest zastosowaniu metod odwrotnych w akustyce rybackiej, a w szczególności ich adaptacji do estymacji rozkładu siły celu ryb (ang. *fish target strength – TS*), która to wielkość jest akustycznym parametrem charakteryzującym zdolność rozpraszania ryb oraz rozkładu ich długości (ang. *fish fork length*), będącym ich fizycznym parametrem.

Po wprowadzeniu, które stanowi rozdział pierwszy rozprawy, w rozdziale drugim przedstawiono zagadnienia rozpraszania dźwięku na obiektach podwodnych. Omówiono wybrane aspekty związane z teorią rozpraszania fal na kuli i cylindrze, jako że obiekty te są często wykorzystywane w modelowaniu właściwości odbijających organizmów morskich. Przedstawiono definicje typowych parametrów używanych w monostatycznych pomiarach hydroakustycznych, a mianowicie: przekroju rozproszenia wstecznego σ_{bs}, długości rozpraszania wstecznego l_{bs} oraz siły celu *TS*. Podano również wyznaczone empirycznie relacje, określające związek pomiędzy wspomnianymi parametrami akustycznymi a fizyczną długością ryby.

W rozdziale trzecim omówiono walory metod akustycznych używanych w szacowaniu zasobów wodnych, zwracając szczególną uwagę na te metody, które realizowane są w naturalnym środowisku (*in situ*) występowania ryb. Omówiono także typowe systemy przetwarzania sygnałów hydroakustycznych, używane w akustyce rybackiej, a w szczególności te systemy, które są specyficzne dla zastosowań rybackich tj. system z podwójną wiązką (ang. *dual beam system*) i rozszczepioną wiązką (ang. *split beam system*), pozwalające oszacować nieznane położenie kątowe wykrytych obiektów poprzez specjalne konfiguracje przetworników echosondy.

Dla typowych systemów jednowiązkowych przedstawiono najczęściej stosowaną metodę kwantyfikacji wielkości zasobów, polegającą na tzw. integracji echa. Pokazano, że wynik całkowania echa jest proporcjonalny do gęstości ryb z współczynnikiem proporcjonalności równym średniej wartości przekroju rozproszenia wstecznego. Dla szeroko stosowanych systemów jednowiązkowych, w których położenie kątowe celu nie jest znane, pokazano, że stosując przetwarzanie rozkładu prawdopodobieństwa amplitudy echa, można usunąć efekt nieznanego położenia ryby w wiązce echosondy. Stanowi to podstawę tzw. pośrednich metod estymacji siły celu. Szczegółowa analiza procesu formowania się echa pokazuje, że do tego celu wymagane jest wprowadzenie szczególnej wielkości, jaką jest funkcja rozkładu prawdopodobieństwa charakterystyki kierunkowej. Funkcja ta reprezentuje jądro równania całkowego Fredholma, które, jak się okazuje, można efektywnie rozwiązać, stosując metody odwrotne.

Dlatego też, w kolejnym rozdziale – czwartym, omówiono techniki stosowane w rozwiązywaniu równań całkowych występujących w zagadnieniu estymacji parametrów rozpraszania ryb. Wykazano, że w większości przypadków występujących w zagadnieniach praktycznych, rozwiązanie zagadnienia odwrotnego prowadzi do źle uwarunkowanych (ang. *ill-conditioned*) i niestabilnych rozwiązań, dla których zastosowanie rozwiązań analitycznych prowadzi do znacznych błędów, gdy próbuje się im nadać sens fizyczny. Pokazano również nowoczesne podejście, wykorzystujące tzw. regularyzację równania całkowego, które prowadzi

do rozwiązań szczególnie użytecznych, gdy interpretowane są one w terminach funkcji rozkładu prawdopodobieństwa.

W rozdziale piątym zarysowano problematykę związaną ze sposobem wyznaczania funkcji rozkładu prawdopodobieństwa charakterystyki kierunkowej przetwornika oraz wprowadzono jej oryginalne rozwinięcie na funkcję opisującą charakterystykę kierunkową rozpraszania celu (ryby). Obie te funkcje stanowią jądra równań całkowych: pierwsza – w estymacji rozkładu siły celu ryb na podstawie rozkładu amplitudy echa, druga – w estymacji rozkładu długości ryb z estymaty rozkładu siły celu.

Rozdział szósty zawiera przykłady analizy danych pochodzących z przeszukiwań akustycznych, przeprowadzonych na różnych akwenach i dla różnych gatunków ryb pelagicznych. Pokazano tu też wyniki statystycznego przetwarzania, stosując różne metody, a zwłaszcza wprowadzoną przez autora do omawianej dziedziny adaptacyjną metodą uśredniania, maksymalizacji i wygładzania, nazwaną AEMS (ang. *Adaptive Expectation Maximization and Smoothing*).

Ostatni, siódmy rozdział, różni się od poprzednich, gdyż dotyczy „niesygnałowych" – w nomenklaturze autora – metod monitorowania i wizualizacji populacji ryb. Pokazuje on możliwości wykorzystania nowoczesnych metod grafiki komputerowej w zastosowaniu do wizualizacji danych z przeszukiwań akustycznych. Zastosowane przez autora języki opisu wirtualnej rzeczywistości do danych zawierających echa od ryb pozwoliły na stworzenie nowej trójwymiarowej techniki dynamicznej wizualizacji, będącej propozycją zastępującą tradycyjnie używany od lat echogram.

Appendix A

ACOUSTIC SCATTERING PARAMETERS

In fisheries acoustics there has been a long-standing problem of naming conventions mainly due to confusing descriptions of the various scattering measures that are central to biological observations using sonar and echo integrators. To incorporate common practice in fisheries acoustics terminology and the related fields, the scheme developed by MacLennan [83] and commended by the ICES Fisheries Acoustics and Technology Working Group (WGFAST) is cited here.

Acoustical quantities such as the target strength TS are not measured directly. They are determined by numerical evaluation of the defining equation $X = f(Q_p)$, where Q_p is a set of a primary quantities as presented in the form of the following table.

Table A.1

Primary acoustical measurement parameters

Symbol	Description	Units
r	distance of the measurement position from the target	[m]
θ, φ	spherical polar angle coordinates of measurement position	[rad]
I_{inc}	intensity of the transmitted wave at the target	[Watts/m^2]
$I_{scat}(r,\theta,\varphi)$	intensity of scattered wave at the measurement position	[Watts/m^2]
$I_{bs}(r)$	intensity of backscattered wave equal to $I_{scat}(r,-?,0)$	[Watts/m^2]
z	distance along the propagation path of a plane wave	[m]
$I(z)$	intensity of a plane wave as a function of distance along the propagation path	[Watts/m^2]
n	number of targets per unit volume	[m^{-3}]
V	Volume occupied by a scattering medium	[m^3]

Table A.2 shows a list of derived quantities relevant to scattering by one or more insonified targets. The emphasis is on scattering phenomena starting with the scattering equations for a small target, the volume and area coefficients relevant to multiple and distributed targets. Some quantities have equivalent logarithmic version. Many are in regular use, especially target strength $TS = 10\log\sigma_{bs}$. As to the volume and area, the log name is simply the linear name with "strength" substituted for "coefficient". The expression like "mean target strength" imply the logarithm of the averaged linear quantity, not the average of the logarithm. An important example is the "mean volume backscattering strength", which is well known as $10\log\overline{s}_v$. Logarithmic measures have symbols beginning with capital Roman letters.

Table A.2

Acoustic scattering parameters

Symbol	Description	Formulae	Units
α	acoustic absorption coefficient	α=10log$_{10}$ {$I(z)/I(z+\Delta z)$}/Δz	[dB/m]
$\sigma(\theta,\varphi)$	acoustic cross-section	$\sigma(\theta,\varphi)$=[$r^2 I_{scat}(r,\theta,\varphi)10^{ar/10}$]/$I_{inc}$	[m^2]
σ_{bs}	backscattering acoustic cross-section	σ_{bs} =[$r^2 I_{bs}(r)10^{ar/10}$]/I_{inc}	[m^2]
σ_{sp}	spherical cross-section	σ_{sp}=[$4\pi r^2 I_{bs}(r)10^{ar/10}$]/$I_{inc}$	[m^2]
σ_s	total scattering cross-section	$\int_0^{2\pi}\int_0^{\pi} s(\theta,\varphi)\sin(\theta)d\theta d\varphi$	[m^2]
σ_e	extinction cross-section	σ_e={ΔIo(z)/Δz-ln10/10}/{$nl(z)$}	[m^2]
σ_a	absorption cross-section	σ_a=σ_e-σ_s	[m^2]
σ_{ag}	aggregate backscattering cross-section	$\sigma_{ag} = \sum \sigma_{bs}$	[m^2]
s_V	volume backscattering coefficient	$s_V = \sum \sigma_{bs}/V$	[m^{-1}]
s_a	area backscattering coefficient	$s_a = \int_{z_1}^{z_2} s_V dz$	[m^2/m^2]
s_A	nautical area backscattering coefficient	s_A =4π(1852)$^2 s_a$	[m^2/nmi^2]
TS	target strength	TS=10log$_{10}$(σ_{bs})	[dB re 1m^2]
S_V	mean volume backscattering strength	S_V=10log$_{10}$(s_V)	[dB re 1m^{-1}]
S_a	area backscattering strength	S_a=10log$_{10}$(s_a)	[dB re 1m^2/1m^2]
S_A	nautical area backscattering strength	S_A=10log$_{10}$(s_A)	[dB re 1m^2/1nmi^2]

The most important application of acoustics in fisheries research is the estimation of the density or abundance of biological targets. Thus, the density of the targets expressed as the number per unit surface area of the layer between depths z_1 and z_2 may be written in equivalent formulations in terms of s_a or s_A:

$$\rho_a = \frac{s_a}{\langle\sigma_{bs}\rangle} \ [\mathrm{m}^{-2}] = \frac{s_A}{4\pi\langle\sigma_{bs}\rangle} \ [\mathrm{nmi}^{-2}]$$

where $\langle\sigma_{bs}\rangle$ denotes an expected value rather than mean value, since it is determined indirectly from the size distribution of fish samples and empirical equations relating the target strength to fish length.

Appendix B

SONAR EQUATION PARAMETERS

The relationship between the target and the received echo may be expressed simply by the so-called sonar equation [164]. The sonar equation is a useful tool for quantifying the signal to noise for the purpose of sonar performance prediction, usually either for analysis or design. The equation can take on different forms depending on the nature of the sonar and details of the processing such as a narrow band or broadband [2]. The traditional definitions can be found in many references as for example in [164, 65, 68]. Rigorous definitions of some relevant terms can also be found in [93].

Consider an isolated target that is insonified by a pulsed sonar. The echo level EL in logarithmic units depends on the source level SL, the one-way transmission loss TL, the receiver sensitivity RS, and the value of beam pattern function B:

$$EL = SL + RS + TS - TL + B$$

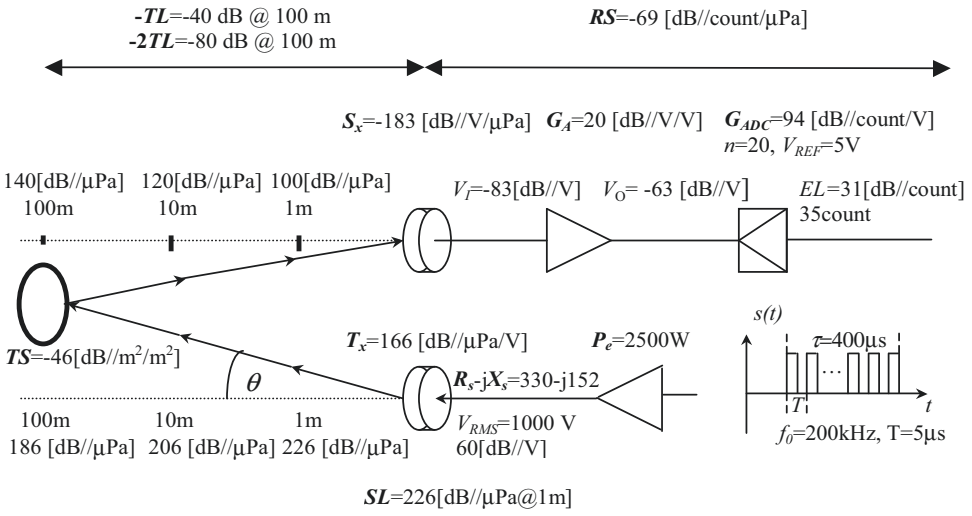

Fig. B.1. Sample parameters of single beam sonar system; the pressure values as if the target was located on transducer axis ($\theta = 0^\circ$) in fresh water ($\alpha = 0^\circ$)

This equation shows how the transmitted pulse is modified successively by the target, the transmission medium and the receiver. Changes in target strength TS give rise to corresponding changes in echo level EL. The calibration coefficient K_x, which is not explicitly written here ($K_x = SL + RS$), includes transmit power level, transducer sensitivity, fixed amplifier gain and A/D conversion factors.

Table shows sonar equation parameters as used in fishery acoustics in target strength calculations. Note, however, that in fishery acoustics for quantitative purposes, the raw echo sounder amplitude is often converted to volumetric backscattering strength S_V, defined as the decibel equivalent of the backscatter cross section per unit volume. This conversion is accomplished through another form of standard sonar equation [89]:

$$EL = SL + RS + S_V - TL + 20 \log V$$

where depth dependent insonified volume V replaces beam pattern factor for volume backscattering and can be expressed in terms of equivalent solid angle of transducer Ψ and pulse duration τ [162, 156].

Fig. B.1 shows sample parameters of a single beam sonar system. Their meaning and the way of determination are presented in Tab. B.1.

Table B.1

Sonar equation parameters

Symbol	Description	Formulae
EL	echo level [dB re μPa^2/μPa^2]	$EL = SL + RS + TS - TL + B$
SL	source level[dB re 1μPa @ 1m] p_1– pressure at 1m from source I_1 – intensity at 1m from source	$SL = 20 \log (p_1/p_0) = 10 \log (I_1/I_0)$ $SL = 170.8 + 10 \log P_e + 10 \log \eta + DI$ $SL = T_x + 20 \log V_{RMS}$
p_0,I_0	reference pressure and intensity	p_0=1[μPa], $I_0 = p_0^2/\rho c$ [Watts/m^2]
c	sound velocity in water [m/s] T-temperature [°C], S-salinity [psu]	$c \approx 1410 + 4.21T - 0.037T^2 + 1.1S$ i.e. T =14, S =35, c ≈1500
η	electroacoustic efficiency of transmitter	
P_e	sonar transmitter electric power [Watts]	$P_e = V_{RMS}^2/R_P$
T_x	transducer transmit voltage response [dB re 1V/μPa]	
V_{RMS}	voltage amplitude on xducer terminals	$V_{RMS}^2 = V_{PP}^2/8$
R_P	transducer paralell resistance [Ω] R_S+jX_S –transducer serial imp.	$R_P = R_S(1+X_S^2/R_S^2)$
DI	transducer directivity index [dB] circular transducer: diameter d =2a, aperture A=πa^2	$DI = 10 \log (4\pi/\Psi) \approx 10 \log \left(4\pi A/\lambda^2\right)$ $DI \approx 20 \log \pi d_\lambda = 45.5 - 20 \log \theta_w$
Ψ	equivalent integrated beam width	$\Psi = \int_0^{2\pi} \int_0^{\pi/2} b^2(\theta, \varphi) \sin\theta d\theta d\varphi$
θ_w	beam width circular transducer: $d_\lambda = d/\lambda = df/c$ –diameter in wavelengths	θ_w =2θ_{3dB}, $b(\theta_{3dB},\varphi)$=b(0,0)/2 $\theta_w[^\circ] \approx 60/d_\lambda$ i.e. d_λ=10, θ_w=6, *DI*=30
$b(\theta,\varphi)$	intensity domain transducer beam pattern circular transducer $x = \pi d_\lambda \sin\theta$:	$b(\theta,\varphi)$=$I_1(\theta,\varphi)/I_1$(0,0) $b(\theta, \varphi) = (2J_1(x)/x)^2$, πd_λ=1.61/sinθ_{zdB}

continued from prevoius page

1	2	3
B	logarithmic two-way beam pattern	B=10log$b^2(\theta,\varphi)$=20log$b(\theta,\varphi)$
TL	one-way transmisson loss [dB re 1 m] spherical spreading:	$TL = 10\log\left(I(r)/I(r_1)\right), r_1$=1[m] $2TL = 40\log(r/r_1) + 2\alpha r$
r	distance from source to target $\tau_s = 1/f_s$ – sampling period, n - sample τ_d– receiver delay, τ– pulse duration	$r = ct/2$ $r = c(n\tau_s - \tau_d)/2 = nc/2f_s - c\tau_d/2$ $\tau_d \geq \tau/2$
α	absorption coefficient [dB/m] in sea water: f_r[kHz]=21.9 $10^{6-1520/(T+273)}$	$\alpha \approx 2Sf_r f^2/\left(f_r^2 + f^2\right) + 2.9f^2/f_r$ $[10^{-5}]$ i.e. f = 200[kHz],T = 14,S = 35,$\alpha \approx$ 0.07
RS	receive sensitivity [dB re 1V/1μPa]	$RS = VR + G$
VR	transducer receive voltage response [dB]	$VR \leq S_x$
S_x	open circuit voltage response [dB]	$S_x = T_x$ + 10log$(R_s^2 + X_s^2) + J$
J	spherical reciprocity parameter [dB]	$J = -354 - 20\log f$[kHz]
G	receiver gain [dB]	$G = G_A + G_{ADC}$
G_A	analog receiver gain [dB re V/V] V_I,V_O – input and output valtages (Fig.1)	G_A = 20log(V_O/V_I)
G_{ADC}	analog-to-digital conversion gain n-number of ADC useful bits V_{REF}–ADC reference voltage	G_{ADC} =20log$2^n/V_{REF}$ =6n−20logV_{REF}

Appendix C

FISH X-RAY PHOTOGRAPHS

The pictures presented in the appendix were prepared by John Horne from Fishery Acoustic Research department of the University of Washington, Seattle. Enabling rough estimation of equivalent parameters of tilted cylinder model of fish swimbladder, they are very useful for modeling fish backscattering properties. They are presented as classical picture along with lateral and dorsal X-ray photographs. At the moment of writing they were available at the official site of Fishery Acoustic Research department on http://acoustics.washington.edu.

Marine Species

Atlantic cod (*Gadus morhua*)

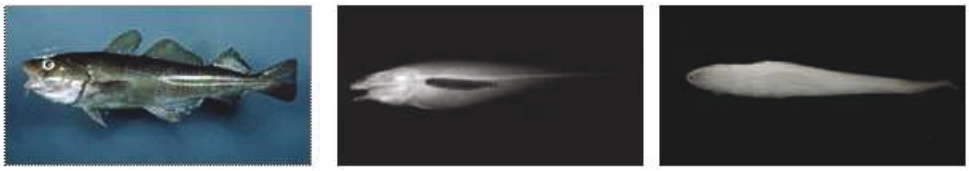

Horse Mackerel (*Trachurus symmetricus*)

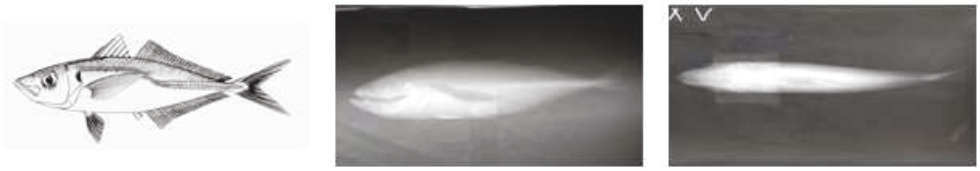

Namibian pilchard (*Sardinops ocellatus*)

Striped Bass (*Morone saxatillis*)

Walleye pollock (*Theragra chalcogramma*)

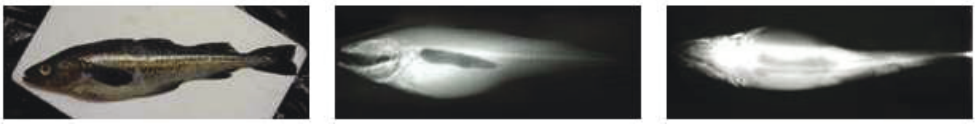

Freshwater species

Alewife (*Alosa pseudoharengus*)

Brook trout (*Salvelinus fontinalis)*

Lavnun (*Mirogrex terraesanctae = Ancanthobrama terraesanctae)*

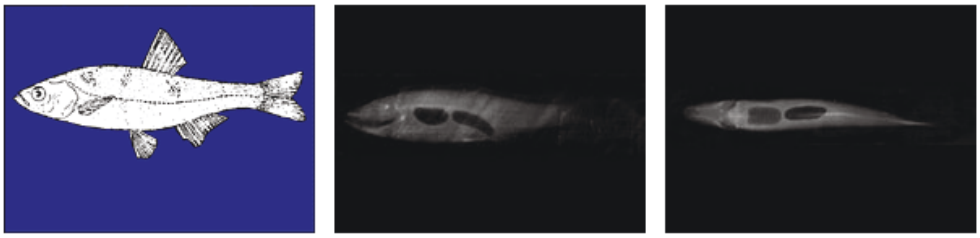

Paddlefish (*Polydon spathula*)

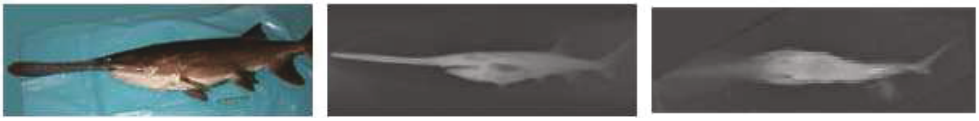

Rainbow smelt (*Osmerus mordax*)

Anadromous Species

Chinook Salmon (*Oncorhynchus tshawytscha*)

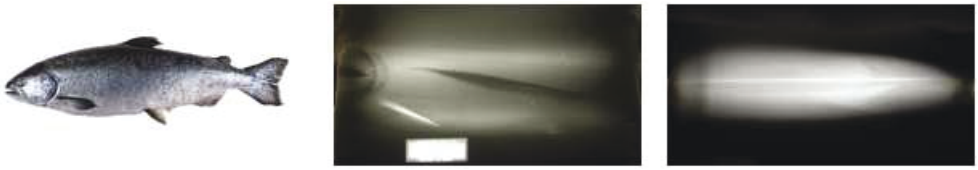

Sockeye Salmon (*Oncorhynchus nerka*)

ACKNOWLEDGEMENTS

Traditionally in the end, there is a need to share the final thoughts related to some aspects of the book with the reader. There is no hesitation that my primary thanks will go to my scientific supervisor, Andrzej Stepnowski, who pushed me into the field of fishery acoustics, whom I shared all my ideas with and who sacrificed a lot of his valuable time for stimulating discussions on the subject. My scientific interest would not be so fruitful without Janusz Burczyński, who, together with Andrzej Stepnowski, introduced me to the community of fishery acousticians and has given me a chance to cooperate with many well-known scientists in the field, including Kenneth G. Foote, Timothy K. Stanton, John K. Horne, Bill Acker and John Hedgepeth. Many informal discussions held with my fellow-workers at the Gdańsk University of Technology viz. Roman Salamon, Henryk Lasota, and Waldemar Lis, have given to me broader glimpse into underwater acoustics. My deep thanks need to go to unforgettable Tadeusz Bartkowski, who, as my first supervisor at the university, fired up my interest in computer sciences. The last but not the least thanks go to Krzysztof Bikonis, who recently managed to alter my virtual ideas into reality.

A fish plays a very important role in modern commercialized society. Throughout the ages it was not only the source of food for the body but for some people it was a nourishment for their soul. You may come across a fish symbol in many places on your way and read several beautiful biblical and apocryphal stories about, as it became a symbol of sharing. That is why I dedicate the book to the memory of John Paul II, the greatest fisherman in the world, who has just left his barque closing his last doors on the Earth and happily observes us from his heavenly window how we share with what was given to us. He has left but is still ... *catching*.

December, 2005

Ayios Nikolaos, Crete (photo by K. Bikonis)